EVALUATION OF THE PERFORMANCE OF A HOUSEHOLD REFRIGERATOR USING A VARIABLE SPEED COMPRESSOR WITH 1D SIMULATIONS

A Thesis Submitted to
the Graduate School of Engineering and Science of
İzmir Institute of Technology
in Partial Fulfillment of the Requirements for the Degree of

MASTER OF SCIENCE

in Mechanical Engineering

by
Ömer Buğra KANARGI

July, 2013
İZMİR

We approve the thesis of **Ömer Buğra KANARGI**.

Examining Committee Members:

Assist. Prof. Dr. Ünver ÖZKOL
Department of Mechanical Engineering
İzmir Institute of Technology

Assoc. Prof. Dr. Moghtada MOBEDİ
Department of Mechanical Engineering
İzmir Institute of Technology

Assoc. Prof. Dr. Tahsin BAŞARAN
Department of Architecture
İzmir Institute of Technology

4 July 2013

Assist. Prof. Dr. Ünver ÖZKOL
Supervisor, Department of Mechanical Engineering
İzmir Institute of Technology

Prof. Dr. Metin TANOĞLU
Head of the Department of
Mechanical Engineering

Prof. Dr. R. Tuğrul SENGER
Dean of the Graduate School of
Engineering and Sciences

ACKNOWLEDGMENTS

This thesis is dedicated to the most precious people in my life: my parents Nuray and Halil KANARGI, and my brother Boran, who have always supported me and my decisions, helped and believed me throughout my life.

I want to express my gratitude towards my professors from the Mechanical Engineering Department of the Izmir Institute of Technology, not only for their endless effort to teach all their knowledge to their students, but also for leading and supporting me on my way to realize my future plans and my higher education.

I would very much like to thank my supervisor Dr. Ünver ÖZKOL for providing me a chance to study on a subject directly related to my research interests.

I would like to thank my colleague Mr. Egemen AĞAKAY, who was conducting the experimental part of the same study with me, for his great help and support throughout my studies.

It is impossible not to mention the Fluid Mechanics Lab members here, who were always there, whenever something went wrong or something disappointing occurred. With an ability to maintain an enthusiastic atmosphere, they always made me feel like home.

Last but not the least, I am most grateful to my best friend Miss Gamze YILMAZ for her endless care and support not only for my studies but for me, as well. May happiness and success be with us during our journey of life that we are about to start together.

I also gratefully acknowledge the Scientific and Technological Research Council of Turkey (TUBITAK) for their support throughout my studies.

ABSTRACT

EVALUATION OF THE PERFORMANCE OF A HOUSEHOLD REFRIGERATOR USING A VARIABLE SPEED COMPRESSOR WITH 1D SIMULATIONS

Inefficient use of electricity is considered as an indirect contributor to the emission of greenhouse gases into the atmosphere. One way to reduce these emissions is to improve the energy conversion efficiencies of the electric equipment. The household refrigerators are designed to satisfy the maximum cooling load to which they are exposed. However, they operate under part load conditions for most of their lifetime. In the literature, some refrigeration capacity control methods are presented such as on/off control, hot gas bypass, evaporator temperature control, clearance volume control, multiple compressor control, cylinder unloading and the variable speed compressor (VSC) control. VSC control has been reported to be the most useful refrigeration capacity modulation method in many studies in terms of its ability to match the refrigeration capacity to the instantaneous cooling load while at the same time decreasing the average and instantaneous power requirements, therefore the total energy consumption (EC) of a refrigerator. In this thesis, three different VSC control algorithms are studied utilizing the 1D model of a commercial household refrigerator. The ECs and the cooling performances are compared with those of the standard on/off compressor control algorithm at the nominal frequency of 50 Hertz (Hz). Temperature management of the cold store and the freezer compartments are investigated in detail, considering the regulations on household refrigerating appliances, characteristics and test methods declared by the British Standards Institute. In addition to the standard EC calculations during the steady state operating conditions, the performances of the VSC control algorithms are evaluated under transient cooling load conditions, as well. It is shown that using a VSC control algorithm to modulate the refrigeration capacity of a refrigerator, when the refrigerator operates under part load conditions, could provide considerable energy savings.

ÖZET

DEĞİŞKEN DEVİRLİ KOMPRESÖRLÜ EV TİPİ BİR BUZDOLABI PERFORMASININ 1B SİMÜLASYONLARLA DEĞERLENDİRİLMESİ

Elektrik enerjisinin verimsiz kullanımı, atmosfere salınan sera gazı miktarına dolaylı olarak katkıda bulunmaktadır. Sera gazı salınımını azaltmanın yöntemlerinden biri elektrikli aletlerin enerji dönüşüm verimliliklerini arttırmaktır. Ev tipi buzdolapları, maruz kalabilecekleri en yüksek soğutma yükünü karşılayabilecek şekilde tasarlanırlar ancak çalışma hayatlarının çok büyük bir kısmını kısmi soğutma yüklerinin etkisi altında geçirirler. Literatürde çeşitli soğutma kapasitesi kontrol yöntemlerinden bahsedilmiştir. Dur/kalk kontrol, sıcak gaz baypas kontrol, evaporatör sıcaklığı ile kontrol, piston ölü hacmi ile kontrol, çoklu kompresör ile kontrol, silindir boşaltma ve değişken devirli kompresör ile kontrol bunlardan bazılarıdır. Değişken devirli kompresör ile kontrol edildiğinde, buzdolabının soğutma kapasitesi anlık soğutma yüküne göre ayarlanabildiği ve kompresörün enerji tüketimi azaltılabildiği için bu yöntemin en başarılı yöntemlerden biri olduğu belirtilmiştir. Bu tezde, ev tipi bir buzdolabının 1B modelinden yararlanılarak üç farklı değişken devirli kompresör kontrol algoritması üzerinde çalışılmıştır. Bu algoritmaların enerji tüketim ve soğutma performansları, kompresörün 50 Hz frekansta dur/kalk şeklinde çalıştığı zaman elde edilen verilerle karşılaştırılmıştır. Soğutucu bölme ve derin dondurucu bölmelerinin sıcaklık yönetimleri detaylı olarak incelenmiş, bu süreçte İngiliz Standartlar Enstitüsü'nün ev tipi soğutma uygulamaları için belirlediği karakteristik özellikler ve test yöntemleri dikkate alınmıştır. Karalı durumdaki standart enerji tüketimi hesaplarının yanı sıra, değişken devirli kompresör kontrol algoritmalarının performansları zamana bağlı soğutma yüklerinin etkisi altında incelenmiştir. Bir buzdolabının soğutma kapasitesini kontrol etmek için değişken devirli kompresör kontrol algoritması kullanmanın önemli derecede enerji tasarrufu sağlayabildiği kanıtlanmıştır.

TABLE OF CONTENTS

LIST OF FIGURES

Figure **Page**

LIST OF TABLES

LIST OF SYMBOLS

P	Pressure	Bar
h	Specific enthalpy	kJ/kg
s	Specific entropy	kJ/kg K
c_p	Specific heat	kJ/kg K
$\dot{Q}$	Heat transfer per unit time	W
$\dot{W}$	Work input per unit time	W
m	Mass	kg
$\dot{m}$	Mass flow rate	kg/sec
r	Compressor compression ratio	-
e	Absolute surface roughness	m
g	Gravity	m/sec^2
t	Time	sec
k	Gain	-
x	Vapor quality	-
D	Diameter	m
L	Length	m
N	Compressor rotary speed	RPM
V_A	Actual piston displacement	m^3/sec
V_P	Piston displacement	m^3/sec
T_{cs}	Average cold store air temperature	°C
$T_{cs\ out}$	Air temperature at the exit of the cold store compartment	°C
T_f	Average freezer air temperature	°C
$T_{f\ out}$	Air temperature at the exit of the freezer compartment	°C
$T_{f\ out\ desired}$	Desired air temperature at the exit of the freezer compartment	°C
$T_{th\ mass}$	Highest thermal mass temperature in the freezer compartment	°C
AH	Absolute humidity	-
EC	Average energy consumption over a 24-hour period	kWh/24h

EC_{total}	Average energy consumption over a 24-hour period	kWh

Greek Symbols

η	Efficiency	-
ρ	Density	kg/m^3
μ	Dynamic viscosity	kg/m sec
υ	Kinematic viscosity	m^2/sec
λ	Thermal conductivity	W/m K
α	Convective heat transfer coefficient	W/m^2 K

Subscripts

avg	Average
cnd	Conduction
comp	Compressor
cond	Condenser
conv	Convection
cr	Cross sectional
dis	Discharge
evap	Evaporator
inc	Increase
inst	Instantaneous
isen	Isentropic
LO	Liquid only
sat	Saturation
suc	Suction
TP	Two-phase
VO	Vapor only
vol	Volumetric

Dimensionless numbers

Re	Reynolds Number	-
Gr	Grashof Number	-
Pr	Prandtl Number	-
Nu	Nusselt Number	-

CHAPTER 1

INTRODUCTION

The change which the Great Britain underwent between the middle 18th to middle 19th century was named as “The Industrial Revolution” by the German author Friedrich Engels in 1844 (Lerner & Lerner, 2004). This time period was the time when the Great Britain transformed from a large agrarian society to a new one dominated by industry. It is an unquestionable fact that the Industrial Revolution had made the most profound changes not only on the British society but on the history of the mankind as well. The world has become a brand new place in just about a hundred years.

Historians have argued about the real insight of the changes that occurred during the revolution and the ultimate effects of the revolution on the Great Britain and the world. It was definite that some major economic sectors such as textiles, iron and steel had grown up, creating a great employment and making the life of the human race much easier than ever before thanks to the availability of the manufacturing of cheaper and higher quality end products. All this development was made possible with the invention of the steam engine in 1763. Inventing the steam engine, James Watt replaced the human power with that of the machines, making it possible to increase the productivity. However, all this development was made possible with the abundant use of a non-renewable energy resource. The most commonly used biofuel, wood, was substituted with coal, which had a higher energy density, extracted out of the soil, powered the steam engines for decades while at the same time no one had paid attention to the danger of pollution resulting from its abusive use. It was until 1979 when it was scientifically declared that there was a problem. In a paper published by the National Academy of Sciences (Charney et al., 1979), the problem was explained in a sentence:

“If carbon dioxide continues to increase, the study group finds no reason to doubt that climate changes will result and no reason to believe that these changes will be negligible.”

The increase in the average temperature of the Earth had proved itself to be a real and formidable problem, which was thereafter known as “The Global Warming”.

At the beginning of the 19th century, another breakthrough invention has come up out of Nicola Tesla: the alternating current (AC) electricity generator. The AC was a more beneficial substitute for the direct current (DC), which was already known and being used at the time, however the DC was not capable of being transmitted over long distances due to the resulting power loss. Solving the transmission problem of electricity using high voltage AC current, Tesla has brought in a new energy source. The steam engines were modified to run AC generators to convert mechanical energy into electrical energy, which is a secondary source of energy and could be used practically in all kinds of devices. As the technology developed, the efficiency of the steam engines and the AC generators increased considerably. Today, electric energy is created using both renewable and non-renewable energy sources using steam and water turbines.

Since the renewable energy resources cannot be stored for later use, they are not as dependable as the non-renewable resources of energy such as fossil fuels (Twidell & Weir, 2006). For this reason, to supply the world's energy demand, it is inevitable to use the non-renewable energy resources along with the renewable energy resources. Due of the fact that the electricity generation process necessarily requires the use of carbon dioxide emitting fossil fuels, the inefficient use of electricity to supply the industrial and household devices is considered to be an indirect contributor to the emission of greenhouse gases emitted in the atmosphere. The only way to eliminate the undesirable consequences of this is to increase the energy conversion efficiencies of the electrically operated equipment.

Energy savings has become of great importance during the last few decades and the improvement of the energy conversion efficiencies of the electrically operated equipment has made itself quite an obligation that some standards were created to ensure its continuity all over the world. As for the continent of Europe, for instance, the European Union has adopted the Directive 2010/30/EU energy labels on May 19th, 2010 (European Commission, 2010). These labels help the customers choose the products that will save energy, therefore their money. This organization also provides incentives to the industry to make investments in energy efficient products.

The aim of the present study is to increase the energy conversion efficiency of very well-known equipment: a household refrigerator. In this thesis, first, the refrigeration process is briefly explained. Next, the components of the refrigeration cycle are introduced. The compressor efficiency and the factors affecting the efficiency

are discussed. The refrigeration capacity control methods from the literature are presented and one of these methods, variable speed control of the compressor, is studied in detail. A 1D model of a certain household refrigerator, prepared on 1D Modeling and Analysis Software: LMS Amesim, is utilized to perform simulations for variable speed compressor operation. The results of the simulations are compared with the experimental results.

1.1. The Vapor Compression Refrigeration Cycle

Refrigeration is the transfer of heat from a place where it is not wanted to another place where it is unobjectionable. In other and more technical words, refrigeration is the process of heat removal to keep the temperature of an enclosed space lower than the temperature of the surroundings (Dossat, 1961). Refrigeration is a cyclic process and in the most traditional form it consists of a minimum number of four components: a compressor, a condenser, an expansion valve and an evaporator. In terms of the level of development and efficiency, the number of the components may increase. The refrigeration cycle is schematically shown in Figure 1.1.

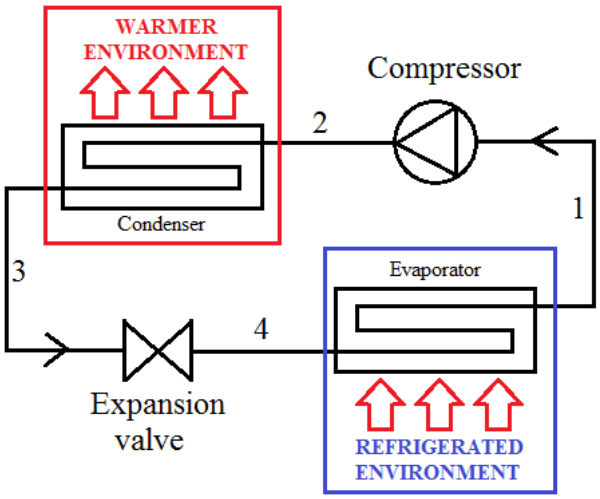

Figure 1.1. The schematic representation of the simple refrigeration cycle

For a better understanding, it would be much useful to study Figure 1.1 on a T-s (temperature vs. entropy) diagram of an ideal vapor compression refrigeration cycle, which is presented in Figure 1.2.

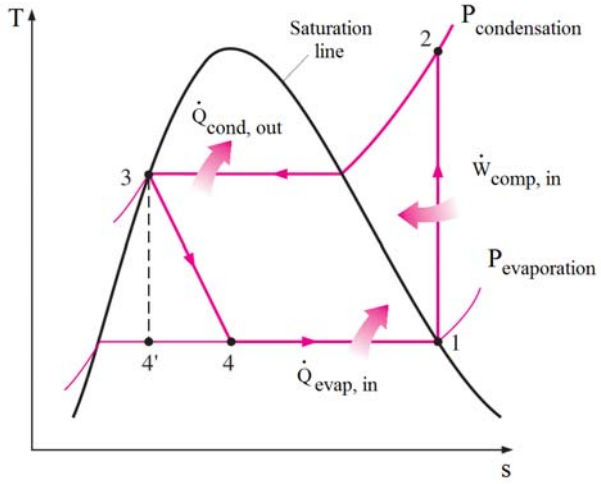

Figure 1.2. T-s diagram of an ideal refrigeration cycle
(Source: Çengel & Boles, 2007)

In the figures above, the stage 1 refers to the outlet of the evaporator. At this stage, the refrigerant is supposed to be on the saturation line, having % 100-vapor content. The compressor compresses the saturated vapor at low pressure ($P_{evaporation}$) to superheated vapor at high pressure ($P_{condensation}$), indicated with stage 2. Entering the condenser, the superheated refrigerant starts dissipating heat to the surroundings, which have a lower temperature than the refrigerant. In the condenser, first, the temperature of the refrigerant decreases until it reaches the saturation point and the condensing temperature. Second, heat dissipation continuous with an accompanied phase change at constant temperature and pressure. Upon reaching the stage 3, the refrigerant has completely changed its phase from superheated vapor to saturated liquid. At this point, the refrigerant pressure and temperature needs to decrease so that it becomes available to absorb heat from the refrigerated environment. This task is accomplished by the use of an expansion valve. An expansion valve is a flow-restricting device and the process occurring in such devices is known as “wire-drawing”. When this process occurs adiabatically, the enthalpy of the refrigerant does not change since there is no heat transfer between the refrigerant and the surroundings. However, flowing through a restricted area, the fluid is exposed to a great amount of friction, which changes the pressure and the temperature of the fluid very fast and this results in a heat transfer within the fluid, resulting in an increase in the entropy (Dossat, 1961). Briefly, when the high-pressure liquid refrigerant flows through an expansion valve, its pressure decreases to $P_{evaporation}$, its temperature decreases to $T_{evaporation}$ and it expands, changing its phase into a saturated mixture at $T_{evaporation}$ (stage 4). Since $T_{evaporation}$ is less than the

temperature of the refrigerated environment, heat is absorbed by the refrigerant and the vapor content of the two-phase refrigerant mixture increases until it leaves the evaporator. The cycle is completed at this point when the refrigerant enters the compressor as saturated vapor at stage 1.

There are some basic terms and definitions that will be used in this thesis to perform the performance analysis of the refrigeration cycle (Çengel & Boles, 2007). First, the measure of the effective cooling power of a refrigerator is known as the refrigeration capacity. This is equal to the rate of heat absorption by the refrigerant in the evaporator and it is defined as

$$\dot{Q}_{evap,\,in} = \dot{m}_{refrigerant}\left(h_1 - h_4\right) \tag{1.1}$$

For the refrigeration cycle to operate, there is a constant power input requirement to the compressor. Assuming that the electric motor and the compressor have % 100 efficiencies –no loss and no irreversibility– the power input to the compressor is calculated as

$$\dot{W}_{comp,\,in} = \dot{m}_{refrigerant}\left(h_2 - h_1\right) \tag{1.2}$$

The calculation of the compressor power will be mentioned in detail in the following chapters, including the compressor and electric motor efficiency aspects.

The superheated refrigerant dissipates the heat energy to the environment until it enters to the expansion valve as a saturated liquid at $P_{condensation}$. The rate of heat dissipation from the condenser is calculated as

$$\dot{Q}_{cond,\,out} = \dot{m}_{refrigerant}\left(h_2 - h_3\right) \tag{1.3}$$

In an ideal vapor compression refrigeration cycle, the conservation of energy could be written as

$$\dot{Q}_{cond,\,out} = \dot{Q}_{evap,\,in} + \dot{W}_{comp,\,in} \tag{1.4}$$

The performance of a refrigerator is best expressed in terms of the coefficient of performance (COP). It is defined as

$$\text{COP}=\frac{\text{Desired output}}{\text{Required input}} \tag{1.5}$$

In the refrigeration cycle, the desired output is the rate of heat absorption of the evaporator, $\dot{Q}_{evap,\,in}$, whereas the required input is the compressor inlet power, $\dot{W}_{comp,\,in}$.

$$COP_{Refrigeration} = \frac{\dot{Q}_{evap,\,in}}{\dot{W}_{comp,\,in}} \tag{1.6}$$

There is another definition used to evaluate the performance of a refrigerator which is the specific power consumption (Tassou & Qureshi, 1994). It is defined as the power input in kW per unit cooling capacity. Even though it is not formally acknowledged, it is the inverse of the COP, therefore a dimensionless ratio.

1.2. Refrigeration Compressors and Compressor Efficiencies

There are many types of compressors used in industrial and household applications (HVAC: Systems and Equipment, 2000) and they are mainly divided into two groups: “dynamic compressors” and “positive displacement compressors”.

The dynamic compressors have specifically designed rotating blades, turning at high speeds, which force the compressible fluid to flow through a contracting flow area at very high speeds. The centrifugal and the axial compressors are the examples of the dynamic compressors, the examples of which can be seen in Figure 1.3.

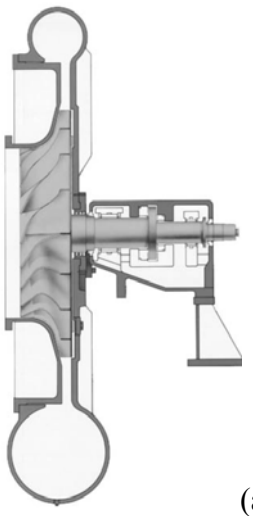

(a)

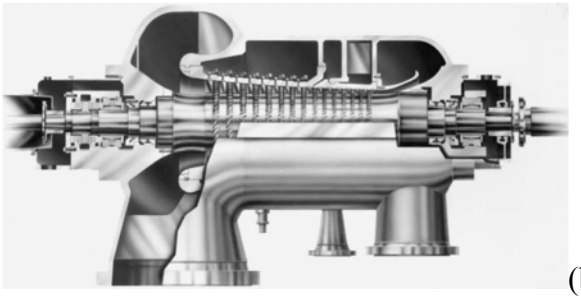

(b)

Figure 1.3. (a) Centrifugal compressor (b) Axial compressor
(Source: Hanlon, 2001)

Centrifugal and axial compressors are preferred when the application requires very high mass flow rates.

The positive displacement compressors, on the other hand, have enclosed volumes inside their bodies to increase the pressure of a compressible gas and they can be classified as in Figure 1.4.

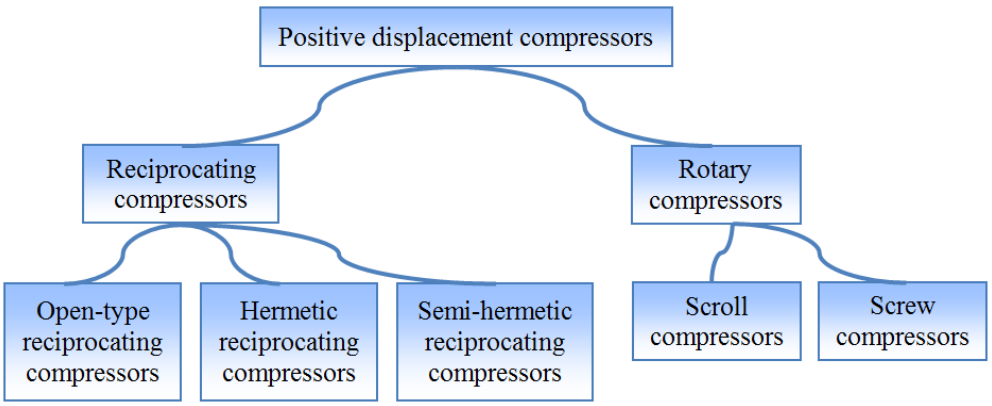

Figure 1.4. Classification of the positive displacement compressors

Rotary compressors are used for small capacity systems such as household refrigeration and small commercial applications. In some certain applications, they can also be used as booster compressors. They are divided into two groups: scroll or screw compressors.

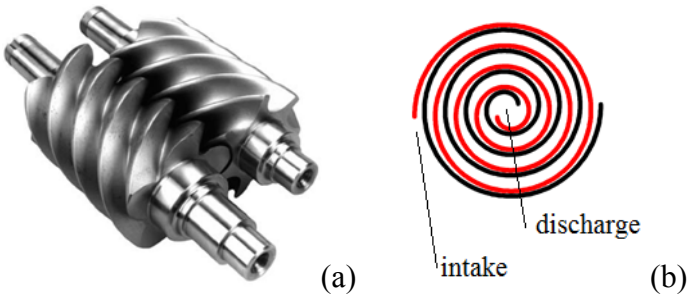

Figure 1.5. (a) Screw compressor (b) Scroll compressor
(Source (a): Giampaolo, 2010)

Reciprocating compressors are very suitable for medium size refrigeration applications and today they are the most frequently used type of compressor in the refrigeration industry. They consist of a cylinder, a piston and a crankshaft. The main difference among the reciprocating compressors is the design of the compressor body.

The semi-hermetic reciprocating type compressors are also known as “bolted”, “accessible” or “serviceable” compressors. The reason for being known with such names is that the electric motor of the compressor is assembled into the compressor in such a way that when a problem occurs in the electric motor, the compressor body could be easily disassembled and the electric motor could be fixed or replaced with a new one. “Serviceability” is the main consideration in naming the reciprocating type of compressors. In Figure 1.6, the side view of a semi-hermetic type of compressor could be seen.

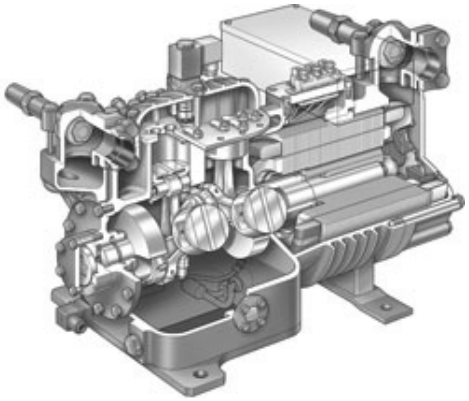
Figure 1.6. Side view of a semi-hermetic type compressor
(Source: Aircon, 2013)

In the open-type reciprocating compressors, the pistons are placed in a separate housing and the rotary movement from the electric motor is transmitted to the shaft of the compressor pistons via a coupling or a belt. This makes both parts of the compressor

serviceable: both the piston-crank mechanism and the electric motor. An example of a semi-hermetic type compressor is presented in Figure 1.7.

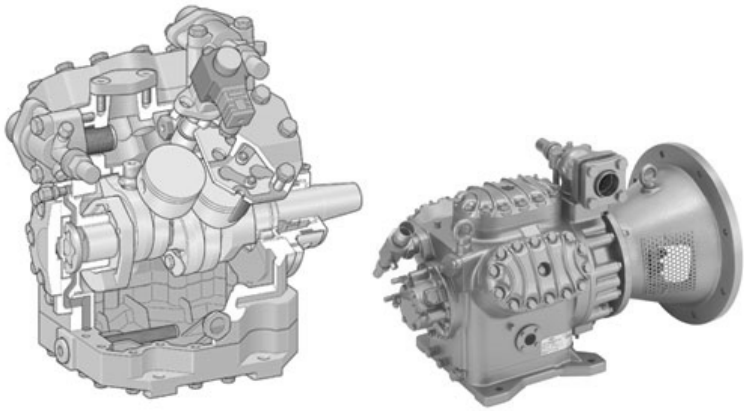

Figure 1.7. Open type compressor
(Source: Aircon, 2013)

In the semi-hermetic compressors, the electric motor of the compressor is cooled by the suction refrigerant gas, which flows over the compressor windings. This results in a temperature increase in the refrigerant before entering the compressor. Since the compressor inlet temperature is increased, the superheating of the refrigerant at the compressor outlet is increased, too. However, in the open type reciprocating compressors, the electric motor is not cooled by the refrigerant suction line, but by the windings of the electric motor itself. Therefore such a superheating does not occur in the open type compressors.

Figure 1.8. Hermetic reciprocating compressor
(Source: Liyang, 2013)

In the hermetic reciprocating compressors (Figure 1.8), on the other hand, the electric motor and the pistons are enclosed in a steel box. Welding is the most usual method used for the sealing purpose instead of bolts. From this aspect, hermetic compressors are very compact devices; therefore they are the most frequently used ones

in household refrigerators. However, their assembly makes it difficult to replace a broken electric motor or a discharge or an intake valve. In the case of a breakdown of one of the components of the hermetic compressors, it is completely replaced with a new one. In hermetic compressors, the crankshaft of the pistons and the shaft of the rotor of the electric motor are the same. They have an inbuilt lubrication system for the lubrication of the pistons, cylinders and the crankshaft. The cooler suction refrigerant shows cooling effects on the electric motor as in the case of semi-hermetic compressors. The refrigerant is charged through the pinch off tube connected to the compressor body.

1.2.1. Efficiency of a Compressor

The overall efficiency of a compressor is a very important parameter when studying on a vapor compression refrigeration cycle from an energy saving point of view. There are many factors affecting a compressor's overall efficiency, which should be taken into account while choosing a correct and useful refrigeration capacity control method. In the following parts, the efficiency of a compressor is studied in detail for a better understanding of this thesis.

1.2.1.1. Isentropic Efficiency

Since the T-s diagram given in Figure 1.2 belongs to an ideal vapor compression refrigeration cycle, the compressor work between states 1 and 2 is indicated to be isentropic. In other words, entropy is the same at the compressor outlet as in the compressor inlet. However, this is not a real time scenario. Entropy cannot remain the same in the compressor due to the existence of the irreversibilities in the work of compression. The T-s diagram of an actual vapor compression refrigeration cycle is presented in Figure 1.9. In the figure, you will notice that there exist eight different states instead of four. The reason for this is that the piping losses are considered as well. The complete states can be seen on the schematic of the actual refrigeration cycle in Figure 1.10.

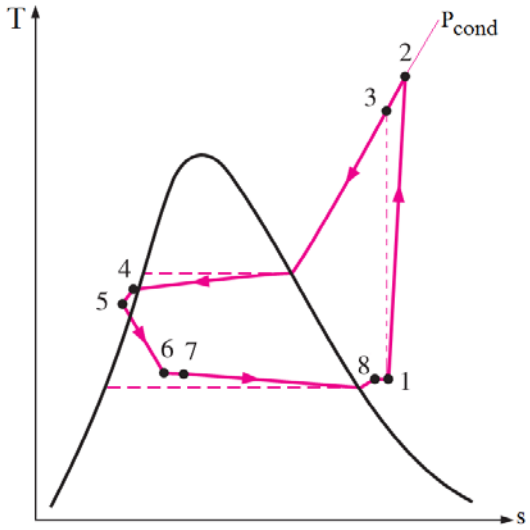

Figure 1.9. T-s diagram of an actual refrigeration cycle
(Source: Çengel & Boles, 2007).

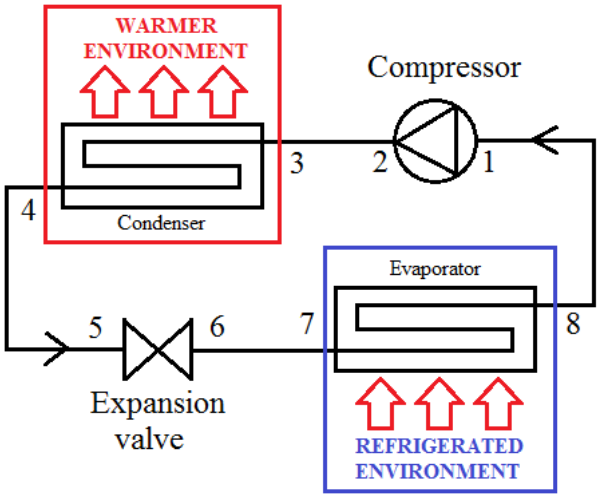

Figure 1.10. The schematic representation of the actual refrigeration cycle

The 3rd state in Figure 1.9 is the compressor outlet of the ideal vapor compression refrigeration cycle. However, in the actual vapor compression refrigeration cycle, the entropy of the compressor outlet (state 2) is higher than that of the compressor inlet (state 1). Since $P_{condensation}$ is already determined for the cycle to operate efficiently with respect to the design criteria, the compressor have to work with a higher power to increase the pressure of the refrigerant to the required level, increasing the compressor inlet power. This phenomenon leads to the definition of isentropic efficiency. Isentropic efficiency of a compressor is defined by Çengel and Boles (2007) as the ratio of the work input required to raise the pressure of a gas to a specified value in an isentropic manner to the actual work input.

$$\eta_{isen} = \frac{\text{Isentropic compressor work}}{\text{Actual compressor work}} = \frac{\dot{W}_{comp,\,isen}}{\dot{W}_{comp,\,actual}} \tag{1.7}$$

For the refrigeration cycle presented in Figure 1.10, isentropic efficiency of the compressor is written as

$$\eta_{isen} = \frac{\dot{W}_{comp,\,isen}}{\dot{W}_{comp,\,actual}} = \frac{h_3 - h_1}{h_2 - h_1} \tag{1.8}$$

It can be deduced from Eqn. (1.8 that if the discharge superheat of the compressor increases, the isentropic efficiency of a compressor decreases. The compressors of good design will have an approximately % 80 to % 90 isentropic efficiencies.

1.2.1.2. Volumetric Efficiency

The capacity of a compressor is a vital parameter since the refrigeration capacity is directly related to it. The capacity of a compressor is a function of the D_{piston}, L_{piston}, number of cylinders, and the compressor speed. The total cylinder volume swept through by the piston of a compressor is defined as the piston displacement, V_P, (Dossat, 1961) and it is defined as in Equation (1.9).

$$V_P = \frac{\pi\, D_{piston}^2\, L_{piston}\, N\, n}{240} \tag{1.9}$$

where “n” is the number of cylinders.

Even though the piston sweeps a total volume of V_P, this does not necessarily mean that the same amount of suction vapor will be compressed and pushed to the compressor head. Due to some certain reason, which will be discussed later, the real amount of suction vapor compressed is less than the piston displacement. The actual amount of suction vapor compressed is known as the actual piston displacement and is represented as V_A.

In this case, the total volumetric efficiency is given as

$$\eta_{vol\,total} = \frac{V_A}{V_P} \times 100 \tag{1.10}$$

There is no possible method to calculate the total volumetric efficiency theoretically. Because there are many factors that determine the total volumetric efficiency and they can be listed as follows:

- Compressor clearance
- Wiredrawing
- Cylinder heating
- Valve and piston leakage

All of these factors should be discussed separately to better understand their effects.

1.2.1.3. Compressor Clearance

A certain amount of distance is left between the top of the piston and the valve plate to prevent the piston from hitting to the valve plate during operation. Due to this clearance, a small amount of volume is left between the piston and the valve plate when the piston is at the top of its stroke. This volume is known as the clearance volume.

To understand the reason why the clearance volume decreases the volumetric efficiency, the working principle of a reciprocating compressor should be mentioned.

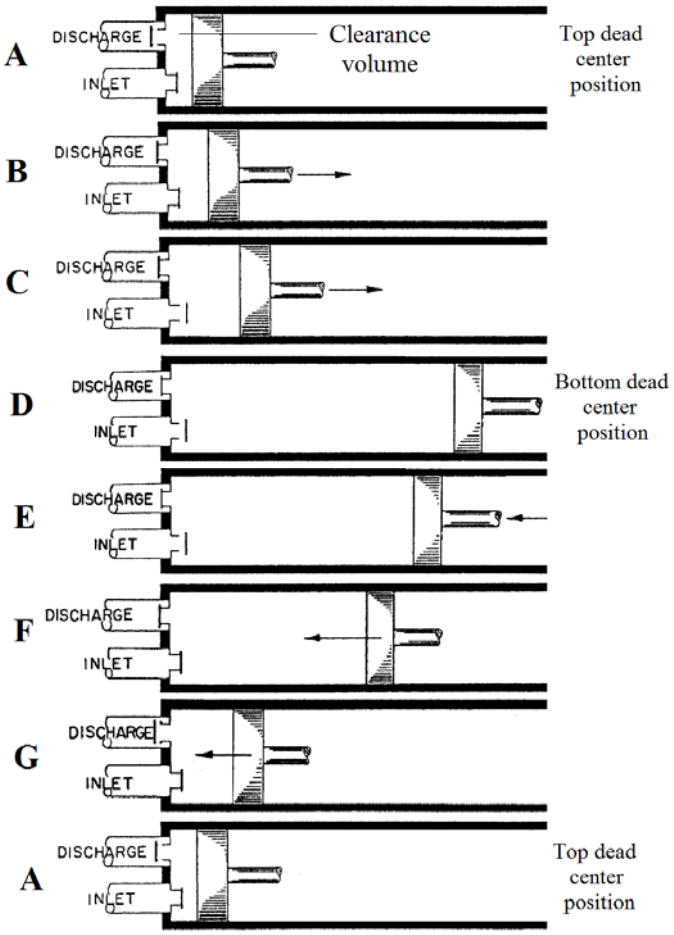

Figure 1.11. The stages of the compressor piston during operation (Source: Bloch, 2006)

In Figure 1.11, the details of the piston operation are presented schematically. At position A, the piston is at the top dead center position, leaving only the clearance volume in the cylinder. At this position, the pressure in the clearance volume, which is the pressure of the clearance vapor, is higher than the pressure of the compressor head. The discharge valve opens thanks to this pressure difference. As the piston starts to move back (position B), the clearance vapor pressure decreases and the discharge valve closes with the help of a light spring loading. However, for the inlet valve to open, the clearance vapor pressure should drop below the suction pressure which happens at the position C. The suction gas fills in the cylinder between position C and D and the piston reaches at the bottom dead center (position D). As the piston starts moving forward again, the pressure inside the cylinder increases slowly (position E). When the cylinder pressure exceeds the suction line pressure, the inlet valve closes with the help of a light spring loading (position F). When the compressed vapor pressure exceeds the pressure

of the compressor head, the discharge valve opens (position G) and the piston reaches at the top dead center.

The pressure vs. cylinder volume graph is presented in Figure 1.12.

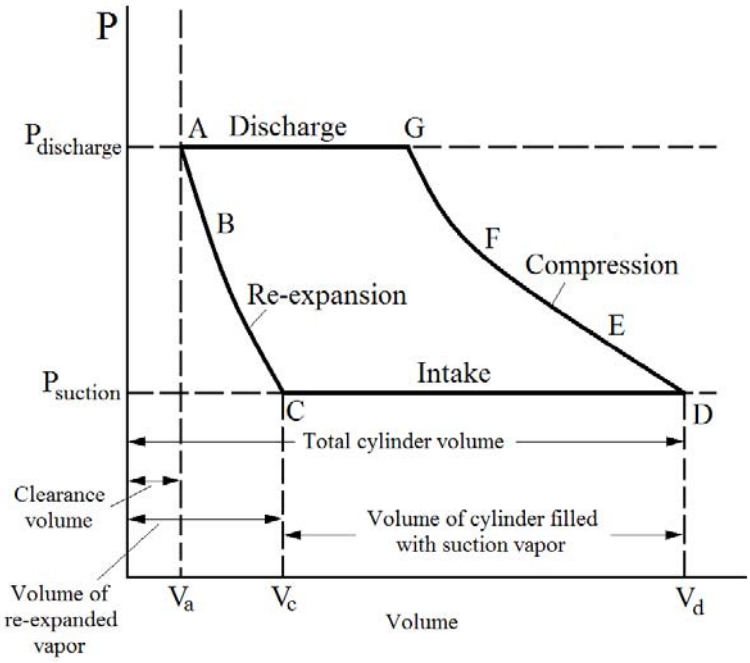

Figure 1.12. Pressure vs. cylinder volume during the compressor operation

Briefly, the delay in the opening of the suction valve due to the re-expansion of the clearance vapor results in a decrease in the amount of suction vapor taken in at stage C. This results in a decrease in the actual piston displacement, therefore the volumetric efficiency of the compressor.

The volumetric efficiency, which is calculated considering only the effect of the clearance volume, is known as the theoretical volumetric efficiency. Theoretical volumetric efficiency depends on the amount of the clearance, the suction pressure and the discharge pressure.

If the clearance volume is increased, the amount of re-expansion required will be higher for the cylinder to take suction vapor into the cylinder at stage C. Therefore increasing the clearance volume will decrease the theoretical volumetric efficiency. If the suction pressure is decreased, the same effect will be observed and the amount of re-expansion will increase. If the discharge pressure is increased, the pressure difference between the cylinder and the compressor head will increase. This will increase the required amount of re-expansion of the clearance vapor before the suction valve opens.

In simpler words, if the compression ratio is increased, the volumetric efficiency will decrease.

1.2.1.4. Wiredrawing Effect

Wiredrawing is the restriction of area for a flowing fluid, causing a loss in pressure by friction without the loss of heat or performance of work. To have a flow from the suction line to the cylinder, there must be a pressure differential across the suction valve to overcome the spring tension. This causes the suction vapor to experience a throttling expansion and a drop in its pressure as it flows through the suction valve. For this reason, the pressure of the suction vapor filling the compressor is always less than the suction line pressure. As a result, the volume of the suction vapor taken in from the suction line is less than if the vapor filling the cylinder was at the suction line pressure.

The same pressure differential is also required at the discharge valve. The pressure of the compressed vapor in the cylinder must exceed the compressor head pressure for the discharge valve to open. If there was no need for a pressure differential for the discharge valve to open, a higher cylinder pressure would not be required and the amount of re-expansion would decrease to take suction vapor into the cylinder.

Even though the speed of the refrigerant vapor across the suction and discharge valves depends on their design, if the speed of the compressor is increased, the vapor velocities through the suction and discharge valves, therefore the effect of wiredrawing increase. This causes the volumetric efficiency to decrease.

1.2.1.5. Cylinder Heating

Cylinder heating is the heating of the suction vapor in the cylinder of the compressors. The main reasons for this problem are the turbulence of the suction vapor coming in and the heat transfer from the piston to the suction vapor. When the vapor coming into the cylinder is heated up, the pressure of the cylinder increase and after some point, the high pressure does not allow more of suction vapor fill into the cylinder. This causes the volumetric efficiency to decrease.

If the compression ratio is increased, the work of compression and the discharge temperature increase. The temperatures of the pistons and the cylinder walls increase due to the increased environment temperature and their heating effect increase.

1.2.1.6. Valve and Piston Leakage

The back leakages from the suction and discharge valves and the piston decrease the volumetric efficiency.

At the beginning of the suction stroke (stage A to B) some of the vapor from the compressor head will leak back to the cylinder until the discharge valve closes. Similarly, some suction vapor will leak back to the suction line at the beginning of the compression stroke until the suction valve closes.

The compressor speed affects the amount of valve leakages directly. If the compressor speed is very high, the suction and discharge valves will immediately close before letting a high amount of vapor to leak back through the valves. If the compressor speed is very low, the pressure of the cylinder will change very slowly both in suction and compression; therefore it will take more time for the valves to close. In addition to this, the compression ratio has a negative effect on the valve and piston leakage, too. If the compression ratio increases, the amount of re-expansion in the suction stroke will increase and the amount of back leakage from the compressor head to the cylinder will increase due to a higher pressure differential.

The compressor valves are made out of lightweight materials and they are loaded with a small spring load to make them immediately close. However, if the spring load is increased for faster shut down, the flow area will contract and the wiredrawing effects will increase. For this reason, the spring load has to be adjusted very carefully.

1.2.1.7. The Total Volumetric Efficiency

The combined effects of the previous four factors vary with the refrigerant used, the design of the compressor and the operation conditions. That's why there is no possible way of calculating the total volumetric efficiency theoretically. The best method to calculate the total volumetric efficiency of a compressor is to test the compressor in a laboratory.

The results of such tests show that the volumetric efficiency of a compressor is mainly dependent on the compression ratio and for a given compression ratio, volumetric efficiency remains constant at any operation range. It is also deduced that similar compressors have similar volumetric efficiencies, regardless of their size. The relation between the volumetric efficiency versus compression ratio is given in Figure 1.13.

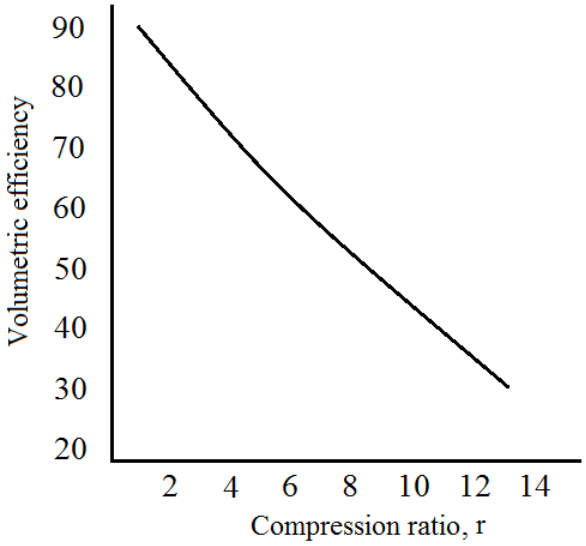

Figure 1.13. η_{vol} vs. the compression ratio, r
(Source: Dossat, 1961)

1.2.1.8. Mechanical Efficiency

Mechanical efficiency is about the effectiveness of the energy and power transformation. If the input to a device is equal to the output, then the device is said to be ideal one, having % 100 mechanical efficiency. However, in real life, there is no device working with maximum efficiency. Some portion of the work done is lost to friction –in the form of heat dissipation– or deformation.

In the case of the compressors, the mechanical friction is a function of the compressor rotational speed, but it does not depend on the operating conditions.

The total horsepower is the required total power to run the compressor and all of its components and it can be formulated as in Equation (1.11).

$$Total\ horsepower = Total\ break\ horsepower + Friction\ horsepower \quad (1.11)$$

Total break horsepower is the power required to set the compressor with all of its components in motion from a stop. The friction horsepower is the total power required to overcome the friction forces existing due to the design of the compressor. Taking the sum of these two horsepower components, the total horsepower is obtained.

It is not wrong to say that the friction horsepower depends only on the design of the compressor, but not the rotational speed. Therefore, as the load on the compressor increases, the total break horsepower and the total horsepower increases and the friction horsepower become a smaller and smaller percentage of the total horsepower. For this reason, tit can be deduced that the mechanical efficiency is highest when the compressor is fully loaded. A perfect design compressor could reach a mechanical efficiency above % 90.

1.3. Refrigeration Capacity Control

Since the inefficient use of electricity to power refrigeration compressors is considered as an indirect contributor to the emission of greenhouse gases to the atmosphere, the energy conversion efficiencies of these compressors has to be improved. Tassou and Qureshi (1998) stated the fact that the conventional refrigeration and air-conditioning systems were designed to operate at the maximum design capacity to be able to satisfy the maximum load. However, since the loading conditions vary continuously quite below the design criterion, these systems are exposed to part load conditions for most of their lifetime, still operating at maximum capacity. One method of reducing these emissions is the refrigeration capacity control, in other words, matching the refrigeration capacity instantly to the ever-changing system load. Controlling the refrigeration capacity reduces power requirement, therefore the energy consumption (EC), provides better dehumidification and decreases the starting load. As the compressor cycling reduces, the wearing problem is eliminated, too.

There are numerous commonly used refrigeration capacity control methods listed by Qureshi and Tassou (1996). These are known as

- On/off control,
- Hot gas bypass control,
- Evaporator temperature control,
- Clearance volume control,

- Multiple compressor control,
- Cylinder unloading,
- The variable speed control.

One of the most commonly used capacity control methods is the on/off control. In this type of control, the on/off cycles of the compressor is controlled with the signal coming from a temperature sensor, measuring the cold store temperature. When the cold store temperature exceeds a critical value, the compressor starts and when the temperature drops below a certain value, the compressor stops. There is a certain difference between these upper and lower temperature thresholds and it is known as the bandwidth. In Figure 1.14, the temperature variation of the cold store of a refrigerator can be seen. The desired cold store temperature is 4°C and the bandwidth is determined as 8°C.

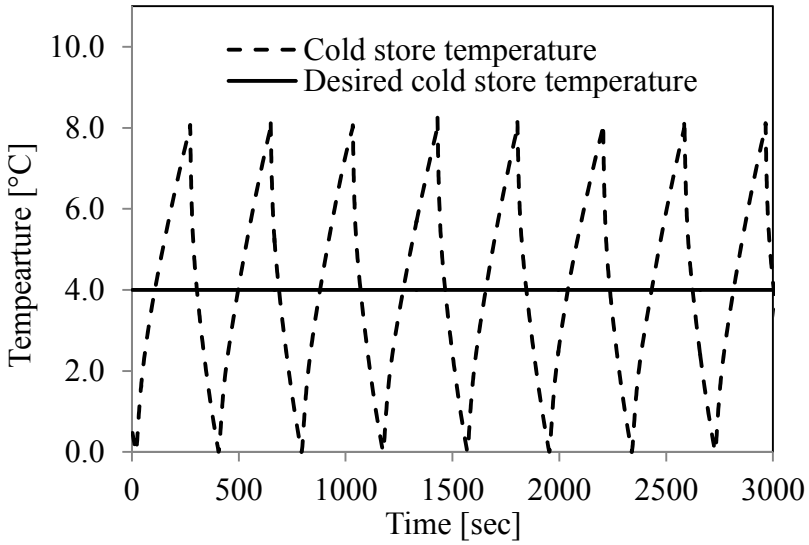

Figure 1.14. Desired cold store temperature and its oscillation bandwidth

The lower and upper temperature thresholds, therefore the bandwidth, should be determined carefully. If the lower threshold is too low, the compressor consumes too much electrical energy in vain, whereas if the upper threshold is too high, the food preserved in the cold store could be spoiled.

The hot gas by-pass is a refrigeration capacity control method in which there is a flow of hot refrigerant gas from the compressor head to the low-pressure side of the refrigeration system. This decreases the condensing unit's capacity to produce refrigeration because the portion of the gas that returns to the low-pressure side of the cycle does not produce useful cooling; instead it becomes an extra load on the

evaporator. The hot gas by-pass is done either to the compressor inlet or to the evaporator inlet. When the hot gas by-pass starts, the refrigeration cycle stabilizes at a higher than normal suction pressure and the refrigeration capacity lowers (The Trane Company, 2009).

When the load on the evaporator falls below the design point the refrigeration cycle moves outside of its stable operating range. In a situation such as this, the compressor and evaporator stabilize at lower pressures and temperatures. This results in the frosting of the evaporator coils. To enable a refrigeration system to operate over a wide range of conditions, still keeping the suction pressure and temperature high enough to avoid frosting of the evaporator coils, a hot gas by-pass system is used.

Clearance volume control is another useful capacity control method, suitable for reciprocating compressors. The clearance volume affects the volumetric efficiency of a compressor, as explained in detail in the previous section. While the volumetric efficiency is inversely proportional with the clearance volume, the capacity of a compressor is directly proportional with the volumetric efficiency. For this reason, by changing the clearance volume, the capacity of a compressor, therefore the power requirements could be decreased. The devices used to change the clearance volume are known as the "unloaders". When the clearance volume is increased, the capacity decreases and the compressor is unloaded. Opposite to this, when the clearance volume is decreased, the capacity of the compressor; therefore the power requirements increase (Shade & Doup, 2009).

Some refrigeration systems run on multiple compressors working in parallel to meet the cooling load requirement of a system. Usually, each compressor has its own control mechanism to adjust its capacity to meet the system load. Since the efficiency of a compressor changes as the load on it decreases, the partial load characteristics of the entire multiple compressor system change and unstable operation may begin. That's why, to prevent this, useful operating strategies are developed to obtain high energy conversion efficiencies for the compressors (Manske, Reindl, & Klein, 2000). When the cooling load is close to the design conditions, both of the compressors, of the same or different types, having similar or different capacities, share the total cooling load together. However, when the cooling load decreases, the decision-making procedure is automatically followed so that the efficiency of the whole system will be maximized. Either one of the compressors stops its operation, or one of the compressors decreases its capacity by half etc.

The cylinder unloading compressor capacity control mechanism is applied to reciprocating compressors having 4, 6 or 8 cylinders. The suction valves are controlled with a solenoid valve to keep them in closed position when the system loads decrease and some of the cylinders are determined to be unloaded (Lawrence, 1971).

Holdack-Janssen and Kruse (1984) investigated possible capacity control methods for reciprocating compressors. The purpose of their controlling process was to achieve the proper refrigerant mass flow rate, which would be sufficient to meet the refrigeration demand under the instantaneous operating conditions. They considered three different methods of changing refrigerant flow rate: varying the flow rate intermittently by interrupting the mass flow rate delivery occasionally, varying the flow rate in a stepwise manner and varying the flow rate continuously. For this purpose, they tried some of the refrigeration capacity control methods mentioned above such as

- Intermittently shutting the compressor on and off,
- Affecting the suction and discharge ports of the compressor by hot gas by-pass,
- Varying the amount of gas in the cylinder by controlling the suction valve,
- Varying the cylinder volume,
- Changing the compressor speed stepwise and continuously.

Speed control was declared to be the most economic method for varying the refrigerant mass flow rate of a reciprocating compressor since the frictional losses decreased proportionally with the flow rate. In addition, the decrease in the compressor speed meant a decrease in the gas velocities in the refrigeration system, decreasing the pressure losses. This resulted in a decrease in the power demand of the compressor more than the corresponding flow rate. However, changing the frequency required a frequency converter and the total energetic efficiency of a compressor equipped with a frequency converter at that time diminished the energy savings obtained from the compressor due to the losses in the driving unit. At the time, the application was not economically feasible even though the variable speed control proved itself to be a useful method.

Variable speed control means adjusting the compressor speed in such a way that the varying cooling load will be satisfied by the varying compressor capacity properly. Besides increasing the energy conversion efficiency of a refrigeration compressor, driving a compressor with such control logic increases the steady state efficiency of a

refrigeration cycle and provides better cold store temperature control (Tassou & Qureshi, 1998). Being controlled with a variable speed drive (VSD), a refrigeration compressor could handle climatic changes more efficiently, by adjusting its operation successfully at medium and very high outdoor temperatures.

Reviewing similar studies written from 70s to 90s, Qureshi and Tassou (1996) stated that the variable speed compressor control was the most energy efficient capacity control mechanism. They made a theoretical comparison of various capacity control methods at full and partial load (half-load) conditions, showing that the variable speed control to be the most energy efficient capacity control method (Figure 1.15).

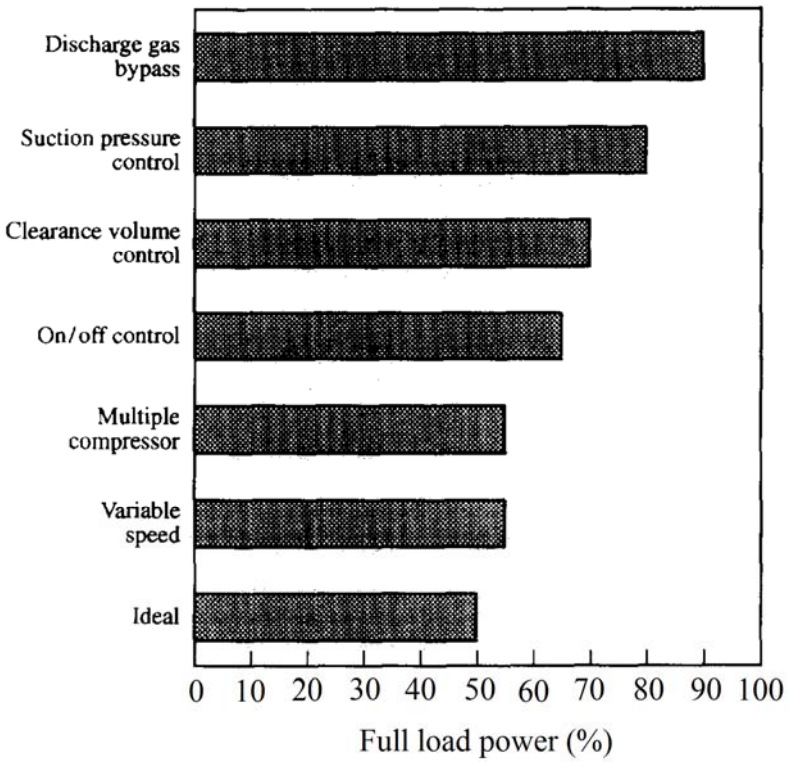

Figure 1.15. Comparison of capacity control methods at half load conditions (50%)

In Figure 1.15, the power requirements determined by each capacity control method are indicated at half load conditions. In the ideal case, when half reduces the cooling load, the compressor power requirement should also decrease by half. However, due to the losses occurring in the refrigeration cycle at low capacities, the power requirement could be decreased to a minimum of 55 % of the full load power utilizing the multi-compressor and the variable speed capacity control methods.

Qureshi and Tassou (1996) further commented about the problems impeding the successful implementation of the variable speed control to medium size refrigeration

systems. They mentioned the unsatisfactory development and integration of VSDs into the compressors and the relatively high cost and the unreliability of general-purpose VSDs. The insufficient information from the compressor manufacturers about the variable speed performance of their products was declared to be a problem at the time. They emphasized important consideration for the solution of these problems. They suggested that for a given application, the most suitable compressor and the most appropriate VSD had to be chosen so that lubrication, which is one of the most important problems for compressors which are supposed to work at lower speeds than optimum design speed, would not be a problem during operation with the integration of the most cost-effective control algorithm.

The authors' research revealed that the most common problems with the power inverters were gradually being solved. They stated that the price of the inverters had been decreasing for the last five years thanks to the reduction in the prices of the electronic equipment, increase in the production and the design improvements, which eventually increased the reliability of the power inverters.

Aprea, Mastrullo, and Renno (2009) tried to find the optimum operating conditions of a refrigeration compressor under different loading conditions. They defined the first step to accomplish this to find experimentally the performance parameters of a compressor in terms of refrigerant mass flow rate, compressor electric motor input power and cooling capacity at different frequencies. Fitting some curves on the gathered data, they obtained some polynomial functions for a compressor, giving the optimum operating frequency for a given cooling load. Having such a function made it possible to create very efficient continuous compressor control algorithms to use instead of the classical on/off (thermostatic) control, which could match the best compressor speed with a certain cooling load instantaneously.

The authors mentioned some restrictions while choosing the minimum available compressor speed. Certain vibration, noise and lubrication problems made it impossible to decrease the operating frequency of a compressor below a certain value. It is declared that for small to medium size refrigeration plants, it is not always necessary that a decrease in the compressor speed will result in a decrease in the energy consumption. Knowing the optimum frequency for each cooling load allows finding the optimum energy consumption when variable speed compressor control is utilized instead of the thermostatic control.

Aprea, Mastrullo, and Renno (2004) pointed out that in the applications of the VSC control, it is convenient to control the compressor at low speeds from an energy saving point of view. However, with such a control, the time required to reach the minimum set point temperatures may exceed the time required to reach the same temperature at the nominal frequency. Even though, the compressor runs on a lower power, the duty cycle might increase and the energy savings could be diminished. Therefore, the compressor speed should be selected carefully taking the system load into consideration and the duration for a certain compressor speed needs to be determined correctly.

The authors generated a control algorithm based on the fuzzy logic, which was able to select the most suitable compressor speed in function of the cold store air temperature.

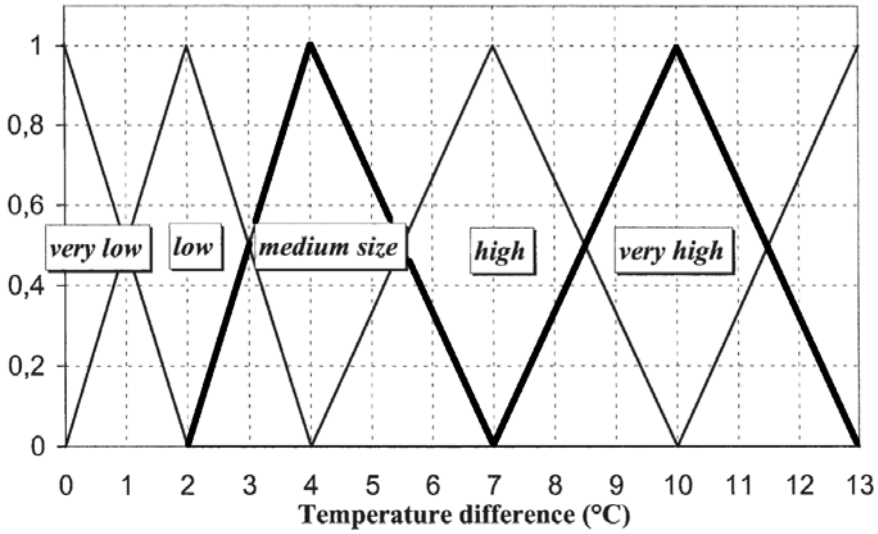

Figure 1.16. Triangular membership function
(Source: Aprea, Mastrullo, & Renno, 2004)

In Figure 1.16, the values of the triangular membership function, generated by the authors, are presented. The temperature difference values of the triangular membership function corresponding to “medium size” and “very high” compressor frequencies are indicated with bold lines for a better understanding. Each triangular part of the function has one center and two limits. According to the temperature difference, the compressor frequency is selected among the options ranging from “very low” to “very high”, corresponding to 30 to 50 Hz with 5 Hz increments. The second variable, which is the time rate of change of the temperature difference, accounts for the fast

variations of the temperature difference and increases or decreases the frequency by 5 Hz if the value of it is greater or smaller than a certain value, 0.007 K/sec.

Using electrical resistances, 200 kg of vegetables and the periodic opening of the cold store door as the cooling load, a maximum of 13 % of energy savings was achieved through the use of the mentioned control strategy with the refrigerant R407C compared to the classical thermostatic control.

Aprea, Mastrullo, and Renno (2006) performed an experimental study to evaluate the maximum energy savings performance of a variable speed scroll compressor. After performing experiments at different speeds to understand the performance characteristics of the scroll compressor, they rearranged the triangular membership function presented in the study by Aprea, Mastrullo, and Renno (2004). The authors strictly emphasized this because it was not a certain fact that a decrease in the compressor speed would mean a decrease in its energy consumption due to the unpredictable decrease in compressor and electric motor efficiencies at lower speeds. The authors obtained a maximum of 20% energy savings with the scroll compressor being driven with the variable speed controller.

An important observation is stated that decreasing the compressor speed decreases the refrigerant mass flow rate, therefore the evaporation and condensation powers. When the compressor speed decreases, the discharge temperature and the pressure decrease, whereas the evaporation pressure slightly increases. Particularly, the reason for obtaining the best energetic performance at lower speeds is due to the increase in the global efficiency of the refrigeration cycle and the reduced compression ratio.

Another observation the authors made is about the compressor operation. It is observed that the highest number of compressor stops occur when the compressor is controlled with on/off cycles with the use of a thermostat. When the compressor is controlled with the control algorithm, the duty cycle of the plant is longer than that of the thermostatic control.

Aprea, Mastrullo, Renno, and Vanoli (2004) studied on a semi-hermetic reciprocating compressor with different refrigerants: R22, R407C, R417A and R507. They stated that the maximum energy saving of about 12 % was obtained using R407C with variable speed control in comparison with the thermostatic control at the nominal frequency of 50 Hz. Among the problems impeding the use of a variable speed compressor put forward by Qureshi and Tassou (1996), some of the problems seem to

have been solved through the years. However, the authors still pointed out the fact that the relative cost of the power inverters was considerably high. This showed that the development in technology and the advances in the manufacturing processes decreased the prices of the refrigeration system components and the power inverters to manufacture VSDs, but still equipping a compressor with a power inverter to manufacture a high efficiency VSD was still expensive and the payback period was not short enough. The length of the payback period was declared to be inversely proportional with the size of the refrigeration system. Another important problem declared by the authors was the lubrication problem at lower speeds, which cause reliability issues. The last problem declared was about the correct working of the expansion devices. When the compressor was to be controlled with a thermostatic control, the expansion valve is designed to compensate the design conditions. However when the compressor is driven with a VSD, $P_{condensation}$ and the $P_{evaporation}$ changes and this affects the performance of the expansion valve. On decreasing the speed, $P_{condensation}$ decreases, whereas the $P_{evaporation}$ shows a small increase, resulting in that the compression ratio decreases. The most important reason for the energy savings at lower speeds is deduced to be an increase in the global efficiency of the compressor. Although the volumetric efficiency of the compressor is supposed to increase at lower speeds, it actually decreases due to the increasing valve leakages. In addition, the electric motor efficiency was considered to be decreasing for about 5% at lower speeds. However the global compressor efficiency is also a function of the isentropic and the mechanical efficiencies. The isentropic efficiency was greatly influenced by the speed reduction. Since the discharge superheat decreased considerably when the speed was lowered, the global efficiency of the compressor increased. Reducing the speed also decreased the frictional losses in the mechanical compression parts, again increasing the global compressor efficiency.

Most importantly the authors found an increase in the power requirements of the compressor at frequencies lower than 30 Hz. The induction motors showed very poor performance at such lower frequencies due to the fact that the inverter generates harmonics that caused the losses in the motor in comparison with the operation at the nominal frequency.

The authors finally pointed out the fact that operating even at 30 Hz; the thermostatic control interrupted the variable speed operation since the minimum

temperatures decreased below the lower thresholds and forced the compressor to stop. Even though the only cooling load is the heat transfer from the outer environment to the cold store, the refrigeration capacity generated at 30 Hz could be too high for continuous compressor operation.

Ekren, Celik, Noble, and Krauss (2012) extended the study of variable speed compressors to a new motor selection alternative: DC motors. They stated that although having similar compression parts, these compressors have brushless DC motors, which do not require power inverters for variable speed operation. Requiring low voltage such as 12-24 Volts and direct current, the DC compressors were found to be advantageous over their AC substitutes in terms energy efficiency and reliability thanks to the elimination of the need of using a power inverter, which increase the probability of failure and consume energy along with the compressor motor.

Their studies on variable speed DC compressors lead to the deduction that lowering the speed when the cooling load decreases results in a decrease in the compressor surface temperature. Showing a greater decrease in the surface temperature, the life of lubrication oil of the DC compressors could be substantially increased.

The literature review given above reveals the fact that there is a great potential in the VSC control for refrigeration capacity modulation. However, the problems regarding the VSD drives and the compressor utilized should be first solved to have an efficient system. Next, a refrigerator should be equipped with a special VSC control algorithm, which will be able to satisfy the refrigeration requirement of the refrigerator under issue with the lowest EC possible.

CHAPTER 2

THE HOUSEHOLD REFRIGERATOR

2.1. Types of Refrigerators

The simple refrigeration cycle, presented in section 1.1, is implemented into the household refrigerators in different ways. Even though the working principles of the refrigeration cycle remain the same, the mechanical design of the refrigerators and the location and the shapes of the refrigeration cycle components differ greatly from one design to another. In this section, two different types of refrigerators will be introduced; static refrigerators and no-frost refrigerators, which differ from each other due to the differences in the heat transfer mechanism and the evaporator design and its location.

In the conventional static refrigerators, the evaporator coil is wrapped around the body of the refrigerator so that the cooling process occurs directly from the refrigerator cabinet to the evaporator. As for the static refrigerators, having both a cold store and a freezer compartment, a longer portion of the evaporator coil is wrapped around the freezer, the temperature of which is supposed to be lower than that of the cold store. The remaining portion of the evaporator coil, which is much shorter than the remaining portion around the freezer, would be enough to satisfy the minimum temperature requirement of the cold store. A transparent view of a static refrigerator is presented in Figure 2.1 schematically.

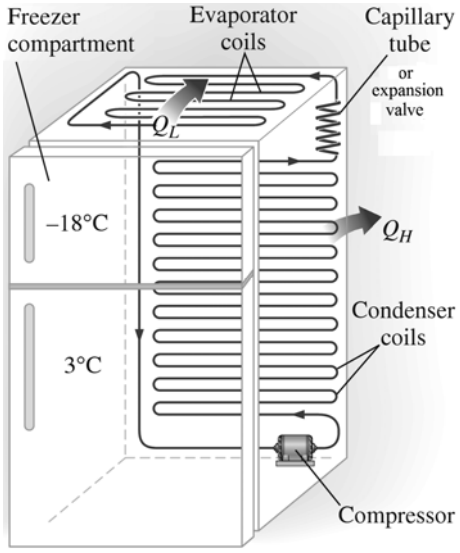

Figure 2.1. Schematic representation of a static refrigerator
(Source: Çengel & Boles, 2007)

This type of configuration of the evaporator is widely used by the manufacturers from all over the world. However such a design causes a certain problem. Since the temperature of the inner wall of the cold store compartment drops considerably due to the evaporator tubes, the moisture content of the air inside the cold store sticks to the wall and starts to crystallize. Throughout the daily usage, the door of the cold store cabinet is opened and closed very often that a large amount of moist air is taken into the cold store every single time. This moisture content of air forms a thin layer of ice on the inner wall of the cold store, around where the evaporator tubes are wrapped. Acting as an insulator, the layer of ice causes the refrigeration capacity to drop. Therefore some of these refrigerators are sold in the market with specially designed knives, made out of plastic, to remove the ice layer from the cold store inner wall.

The ice removal process was not a user-friendly application, which motivated the engineers to find a new way to solve the icing problem. The proposed solution to this problem is now globally known as the “no-frost” refrigerator. In this configuration, the evaporator coil is not wrapped around the body of the fridge; instead it is placed at the back of the refrigerator in a compact shape. The tubes are closely coiled together and to enhance the heat transfer rate, many thin fins are placed over the tubes. A schematic representation of a no-frost refrigerator is given in Figure 2.2.

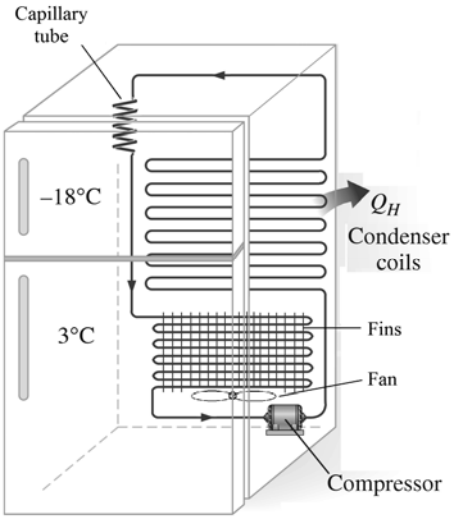

Figure 2.2. The schematic representation of a no-frost refrigerator

In the no-frost refrigerators, the heat transfer does not occur directly from the cabinet to the evaporator tubes, instead the air trapped inside the refrigerator is used to deliver the excessive heat energy to the evaporator. A small fan, placed at the back of the evaporator, draws the high temperature air from the freezer and the cold store, and then pushes it through the extremely cold evaporator tubes and fins. Heat transfer occurs from the air to the refrigerant and the air coming out of the evaporator, the temperature of which is very low at this point, is sent back to the refrigerator cabinets. The amount of air sent back to the freezer and cold store is adjusted in such a way that the desired temperature of each cabinet is reached and maintained.

It is inevitable that the icing problem will occur even in the no-frost refrigerators. The reason for this problem is that when the humid air comes across with a very cold surface, the moisture content in the air sticks to the cold surface and liquid droplets form. These droplets start to crystallize and finally, a thin layer of ice forms on the surfaces of the evaporator coils and the fins. The thin ice layer decreases the refrigerating capacity of the evaporator therefore the ice has to be removed from the evaporator occasionally. A small electrical resistance is utilized to perform this job and the process is known as the "defrost" process. The rate of the defrost operation is determined by the engineers so that once in a few days, a small amount of current is passed through the resistance. The broken pieces of ice are collected in a small container placed at the back of the refrigerator, which is generally used to decrease the compressor temperature. Due to the high operating temperatures of the compressors and the discharge superheat, the isentropic efficiency decreases (Qureshi & Tassou, 1996).

Decreasing the compressor surface temperature by the melting of the ice and the vaporization of the water, the efficiency of the compressor is increased.

The household refrigerator studied in this thesis is a no-frost refrigerator. The information given in this section will be useful in many ways for the understanding of the details of the rest of this study.

2.2. Standard Thermostatic (On/Off) Control of the Compressor

The thermostatic control is the most commonly used refrigeration capacity control method in the refrigeration industry. The details of this type of control are given at the beginning of the section 1.3. The household refrigerator under issue is originally designed to operate with the thermostatic control and in this section; the standard thermostatic control algorithm of the compressor is introduced.

The schematic view of the circulation of air inside the refrigerator under issue is presented in Figure 2.3. The freezer compartments, in general, are designed to be at the top of the refrigerators. In this design, however, it is placed at the bottom of the refrigerator since it is an undeniable fact that the door of the freezer compartment is not opened as often as that of the cold store in daily use. In this case, the user will not have to crouch down so often to use the cold store compartment. The fan, which is placed in front of the evaporator, draws the high temperature air from both of the cabinets, pushes it through the evaporator, then sends the low temperature air back to the cabinets.

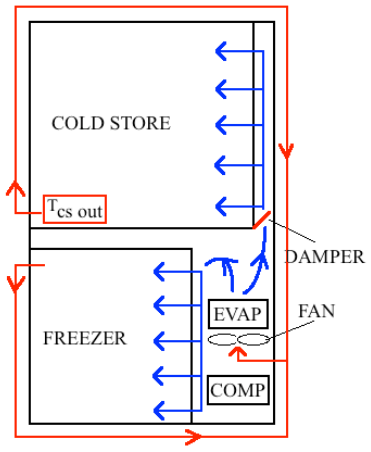

Figure 2.3. The schematic view of the circulation of air inside the refrigerator

In the standard compressor control algorithm, the compressor is programmed to answer the refrigeration requirements of the cabinets with 3000 RPM. The activating signal is taken from the temperature of the cold store only. A temperature sensor, placed at the air outlet of the cold store, measures the air temperature coming out of the cold store compartment, $T_{cs\,out}$, which is indicated in Figure 2.3. In this figure, the high and low temperature airflows are represented with red and blue lines, respectively.

The desired refrigerator cabinet temperatures are officially declared in the British Standard of Household Refrigerating Appliances (British Standards Institute, 2006). According to this standard, the refrigeration application should be able to simultaneously maintain the required temperatures in different compartments with the specialized temperature deviations. During the steady state operation, when the unique cooling load on the refrigerator is the heat transfer from the surroundings to the refrigerator cabinets,

- The air temperatures in the cold store have to be measured as $0°C \le T_{cs1}, T_{cs2}, T_{cs3} \le 8°C$ and $T_{cs\,mean} \le 4°C$,
- The temperature of the hottest thermal mass in the freezer has to be measured as $T_{th\,mass} \le -18°C$.

In the energy consumption (EC) calculation definition of this standard, the use of thermal masses in the freezer is an obligation. In the freezer compartment of the refrigerator under issue, a total of 92.25 kg of Tylose material packages are used and the package, having the highest temperature, is taken as the reference for the measurement of $T_{th\,mass}$. The details of the EC calculation are given later in this section.

The temperature sensor measures $T_{cs\,out}$ continuously. When $T_{cs\,out}$ is measured to be higher than 8°C, the control algorithm sends a signal to the compressor so that it starts its operation at 3000 RPM. At this instant the damper seen in Figure 2.3, which regulates the airflow from the evaporator to the cold store, is fully opened so that the low temperature air coming from the evaporator could flow not only to the freezer compartment but to the cold store, as well. When $T_{cs\,out}$ drops below 0°C, the control card sends a signal to the step motor of the damper so that it blocks the air flow to the cold store compartment. After that instant, the compressor continues its operation for exactly 300 seconds more only to decrease the freezer temperature. This time period of 300 seconds is known as the “fixed time” in this standard compressor control algorithm. Fixed time is a requirement for the refrigerator because without its implementation,

$T_{th\ mass}$ could not be decreased below -18°C. After 300 seconds, the compressor stops and does not start its operation until $T_{cs\ out}$ is measured to be higher than 8°C again.

In summary, the standard compressor control algorithm has only one input which is the $T_{cs\ out}$. This algorithm does not take the $T_{th\ mass}$ into consideration instantaneously, however it is experimentally adjusted in the design phase that the fixed time is capable of maintaining the $T_{th\ mass}$ below -18°C.

Table 2.1. Details of the standard control algorithm

Control method	On/Off
Compressor speed	0/3000 RPM
Fixed time	300 sec
$T_{cs\ out}$ **thresholds**	0°C< $T_{cs\ out}$ <8°C

As could be seen from Figure 2.5, $T_{cs\ out}$ is adjusted to oscillate between 0°C and 8°C with the damper operation. Every time $T_{cs\ out}$ exceeds 8°C, the compressor starts its operation. Whether or not the damper is switched off, $T_{f\ out}$ and $T_{th\ mass}$ continuously decreases as long as the compressor operation continues. However, when the damper switches off and blocks the air flow from the evaporator to the cold store, $T_{f\ out}$ and $T_{th\ mass}$ decreases at a higher rate until the compressor stops at the end of the fixed time due to the fact that all the refrigeration capacity of the refrigeration cycle is concentrated on the freezer compartment.

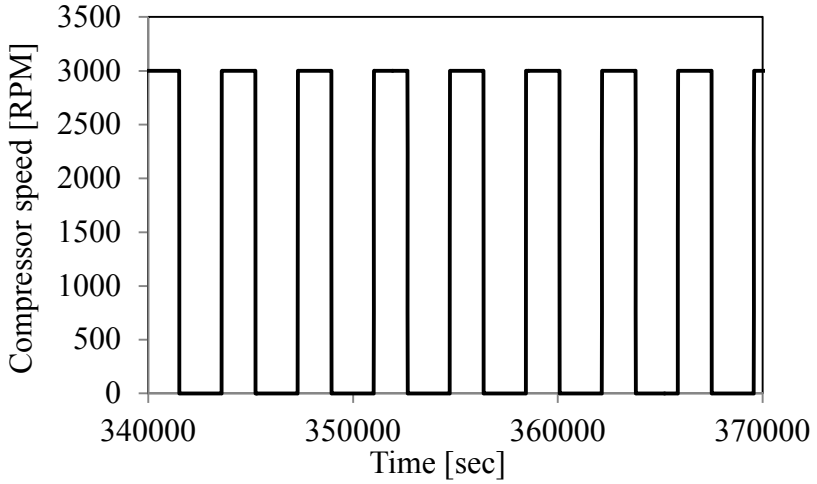

Figure 2.4. Compressor speed with the standard algorithm (simulation results)

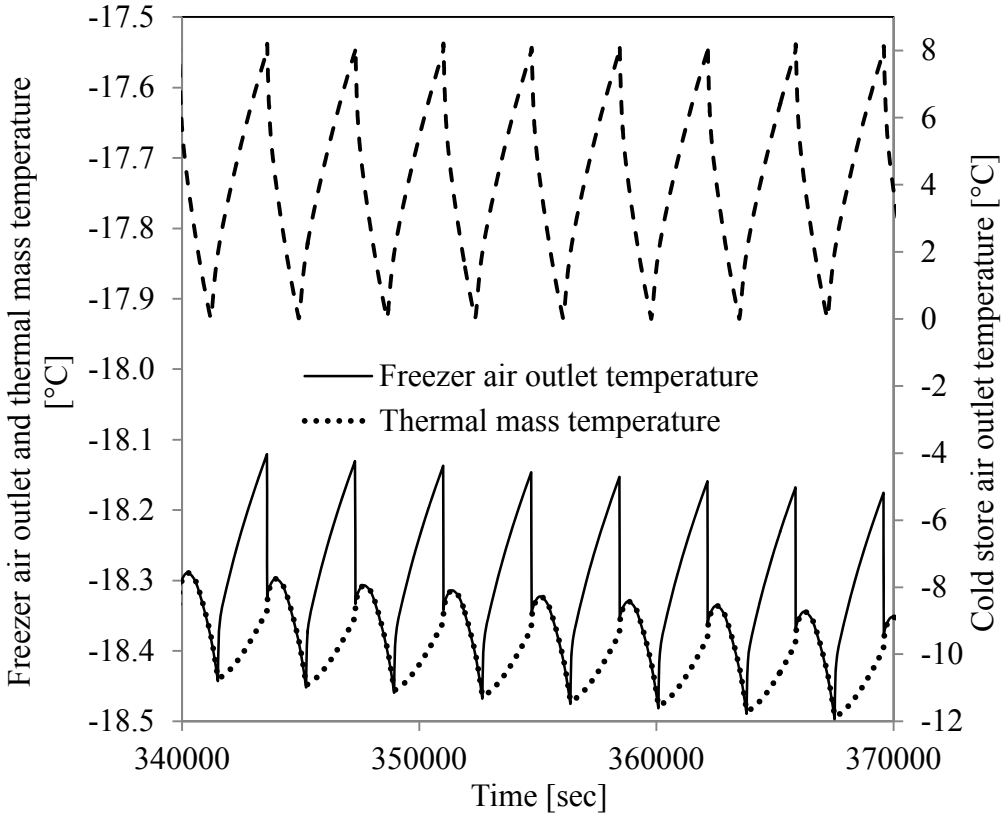

Figure 2.5. $T_{cs\,out}$, $T_{f\,out}$, $T_{th\,mass}$ with the standard algorithm (simulation results)

When the compressor stops at the end of the fixed time operation, the $T_{f\,out}$ and $T_{th\,mass}$ starts to increase. It can be observed from Figure 2.5 that the rate at which $T_{f\,out}$ increases is higher than that of the $T_{th\,mass}$. This occurs due to the fact that the fan operation is synchronized with the compressor operation. When the compressor stops at the end of the fixed time, the fan stops and the forced convection heat transfer is replaced with the natural convection in the refrigerator compartments. Since the heat transfer coefficient in the natural convection is much lower than that of the forced convection, the increasing T_f cannot increase $T_{th\,mass}$ at the rate at which T_f decreases $T_{th\,mass}$ when the fan is operating and the forced convection is dominant.

The method of energy calculation (EC) of the refrigerators is clearly standardized in the British Standard of Household Refrigerating Appliances (British Standards Institute, 2006). The EC calculation is performed in the steady state operation region of the compressor. The EC tests of the refrigerators are performed in special test chambers, in which the temperature and humidity conditions of a real environment are created. In such an environment, such as a kitchen, the temperature is about 25°C in the summer season. This experimental condition necessitates the initial cabinet

temperatures of the refrigerator to be very high, therefore after the refrigeration operation starts, sometime should be allowed so that the cabinet temperatures decrease to the desired levels and the temperature deviations become negligibly small.

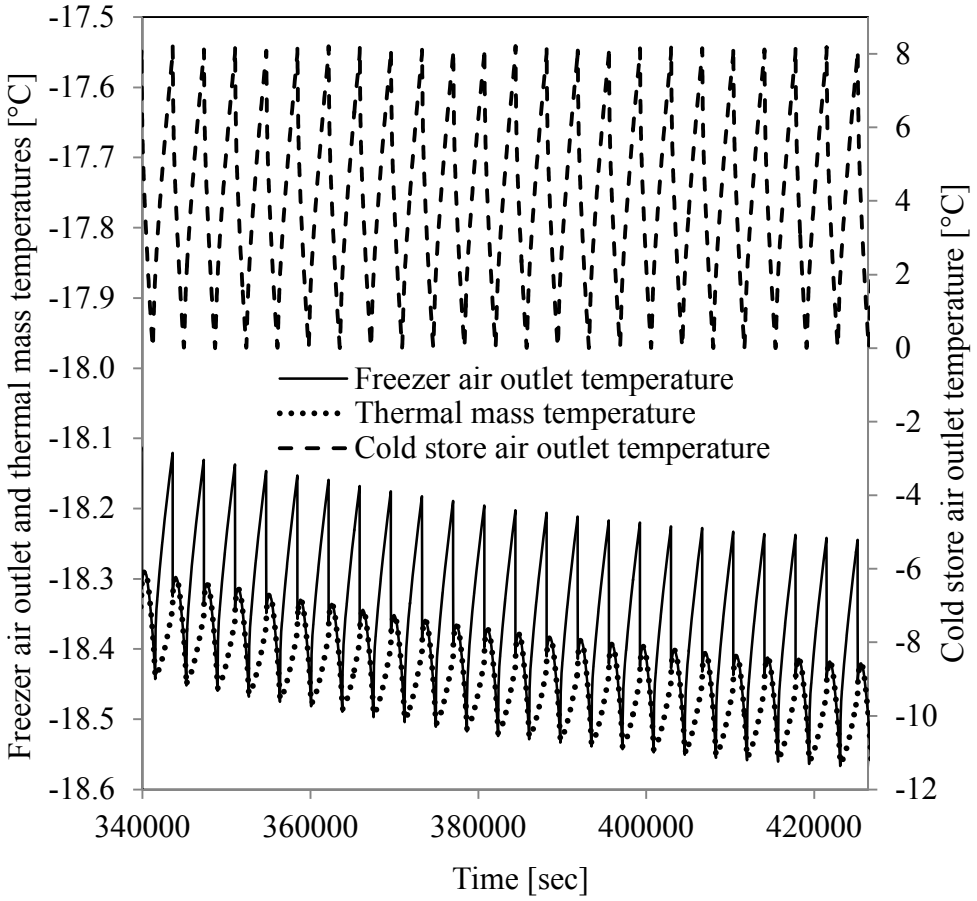

Figure 2.6. The 24-hour time interval for the EC calculation (simulation results)

In Figure 2.6, the temperature variations of the $T_{cs\,out}$, $T_{f\,out}$ and $T_{th\,mass}$ with respect to time are presented for a 24-hour period. $T_{cs\,out}$ oscillates within its bandwidth between the threshold properly, while the $T_{f\,out}$ and $T_{th\,mass}$ shows a decrease of only about 0.1°C in 24 hours. For this reason, the given interval could be taken as a reference to calculate the EC of the refrigerator. To calculate the EC, the instantaneous power requirement data of the compressor, which is presented in Figure 2.7, is recorded. The area under the curve, calculated using Equation (2.1), is equal to the total EC for the 24-hour period.

$$EC_{total} = \int_{24\,\text{hours}} \dot{W}_{comp}.\,dt \qquad (2.1)$$

In order to find the average instantaneous power requirement of the compressor, $\dot{W}_{comp\,inst\,avg}$, the EC value calculated using Equation (2.1) is divided by 86,400 sec (24h).

$$\dot{W}_{comp\,inst\,avg} = \frac{EC_{total}}{86,400\,\text{sec}} \tag{2.2}$$

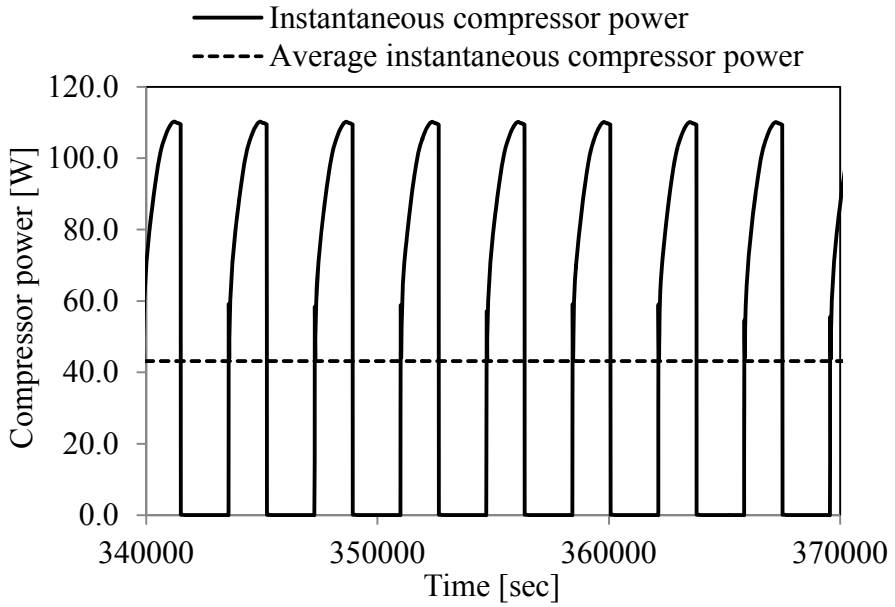

Figure 2.7. Power requirement of the compressor (simulation results)

According to the Directive 2010/30/EU energy labels standard adopted by the European Commission (2010), the refrigerators need to be labeled regarding to the level of their ECs. In this labeling system, their EC is expressed in the units of "kWh/24h". For instance, $\dot{W}_{comp\,inst\,avg}$ of the household refrigerator under issue with the standard control algorithm is calculated to be 43.15 W. To be able to express this in the units of kWh/24h, the following calculation is performed.

$$EC = 43.15\ \text{W} \times \frac{24\ \text{h}}{1000} = 1.036\ \text{kWh/24h} \tag{2.3}$$

1.036 kWh/24h energy consumption is rated with the energy label "A+" by the European Commission (2010). The energy level of a refrigerator is indicated with an energy window, an example of which is given in Figure 2.8.

Figure 2.8. The Directive 2010/30/EU energy window

On a standard energy window, the supplier's name and the model of the product takes place. The energy labels are listed on the left, whereas the real energy level is indicated with a white letter on a black background on the right. The total EC value is written annually instead of per day. Simply, the EC value calculated for a single day in Equation (2.3) is multiplied by the number of days in a year, 365, to find the total EC in the dimension of "kWh/annum". At the bottom of the window lies the total volume of all of the compartments, total volume of all frozen food compartments and the acoustical noise emission value in the dimension of decibel.

The selection of the energy label is performed considering the standards, determined and declared by the European Commission (2010), and the details are presented in Table 2.2. The energy efficiency classes given in Table 2.2 are declared to be valid until June 30th, 2014. From the beginning of July 1st, 2014, the upper EC limit for the A+ energy efficiency class and the lower EC limit for the A energy efficiency class will be lowered to 42 W. According to the energy efficiency classes, which will be valid until June 30th, 2014, the standard compressor control algorithm is labeled to be A+ energy efficiency class with 43.15 W instantaneous power requirements.

Table 2.2. Energy efficiency classes valid until June 30th, 2014
(Source: European Commission, 2010)

Energy efficiency class	Energy efficiency index
A+++ (most efficient)	EC<22
A++	22≤EC<33
A+	33≤EC<**44**
A	**44**≤EC<55
B	55≤EC<75
C	75≤EC<95
D	95≤EC<110
E	110≤EC<125
F	125≤EC<150
G (least efficient)	150≤EC

CHAPTER 3

1D MODELLING AND LMS AMESIM

1D model of a system is a mathematical representation, which could be utilized to understand the dynamic behavior of that system in the real world. In the most conventional sense, testing a phenomenon with an experiment is the best way to understand the physics behind a certain operation. When it comes to design process, however, the need of repetitive trials to find the perfect design becomes a burden to the engineers who work experimentally. The reason for this is that experimental work is expensive and it requires too much time and effort by nature. Thanks to the improvements in the computing systems and the numerical methods, the Computational Fluid Dynamics (CFD), which is one of the most useful design tools ever, has been created. Either writing a special code or using the commercial CFD codes, even extremely complicated heat transfer and fluid flow problems could be solved easily. Depending on the experience of the coder or the user, very precise results could be obtained. However, there is a certain drawback of the CFD tool that as the complexity of the problems under issue increases, the computer performance required to be able to perform calculations increases dramatically. The only way to solve this problem is to buy powerful computers, which could be very expensive. A complex problem could be simplified so that the required computing power could be decreased; however making too much simplification might affect the results and prevent the researcher from understanding the real insight of the phenomenon. The second drawback of the CFD analysis is the need of creating a mesh to be able to start a calculation. The CFD codes, written to solve fluid flow and heat transfer problems, solve the Navier-Stokes and the energy equations and the solver code is based on the finite volume method (FVM), which requires a mesh to calculate a solution. At this point, it is very important to know how to optimize the generated mesh. If a very fine mesh is used, the total run time and the computing requirements increase considerably. If a low quality mesh is generated, on the other hand, then the solution will not be reliable. The optimum point between the computing time and the quality of the solutions has to be found. This subject makes the meshing operation the most problematic part of the CFD analysis.

One of the most powerful design alternatives to the experimental measurements and CFD analysis is one dimensional modeling. It is performed either by writing a code or using commercial software. Each component, which is a part of the whole system, is added on one of another until all the details of the real system are modeled. Since 1D modeling is simply a mathematical representation of the phenomenon, it is possible to create a model including principles from different disciplines. As for the case of the household refrigerator under issue in this study, the 1D model of the refrigerator is created on the 1D simulation software LMS Amesim. LMS Amesim is user friendly, visual 1D modeling software, which enables the user to create complicated, multi-disciplinary models very easily. Using this commercial tool, it is also possible to perform both steady state and transient simulations to understand the dynamic behavior of a system. Since 1D simulations could eliminate the need for meshing, it is enough to change a couple of numbers and start new simulation immediately when a modification is required in the model during the design process. Besides, since there is no mesh requirement, the CPU and RAM usage is very low, which eliminates the need of powerful computers. From this aspect, 1D modeling and LMS Amesim saves a great deal of time and money during the design phase.

The 1D model of the household refrigerator is quite complicated. First of all, there is the heat transfer side of the problem, the components of which are taken from the “Thermal Library” of LMS Amesim. Second of all, single and two-phase flow of refrigerant occurs in the refrigeration cycle, which is introduced to the software with the components of the “Two-phase Flow Library”. The heat transfer interactions between the refrigeration cycle and the refrigerator cabinets are defined utilizing the proper components. The third library utilized is the “Signal Control Library” which serves the function of controlling the compressor with respect to the inlet parameters.

Besides the advantages, there are also some certain drawbacks of 1D modeling. Since there is no direct geometrical modeling as in the case of CFD analysis, it is inevitable to do some simplifications in the model. Therefore, the user has to be careful while determining the level of simplification not to miss the underlying phenomenon. As it was already mentioned in section 2.1, the refrigerator is a no-frost type refrigerator and the mode of heat transfer in the refrigerator cabinets is forced convection. Having forced convection heat transfer in the evaporator makes the modeling process very difficult since it requires an extremely detailed model of the evaporator. There are many correlations used in the components utilized to model the evaporator and the abundant

use of the correlations for every single detail decreases the accuracy of the simulation results. It takes too much effort to adjust the model so that the simulation results would be close to the experimental results and the model is reliable.

Another disadvantage of the 1D simulations is that some of the real time phenomena cannot be predicted correctly. For instance, the evaporator acts as a liquid tank to store the refrigerant during the off time of the compressor. However, the 1D model cannot predict the storage effect of the evaporator, which creates a difference between the simulation and the experimental results at the beginning of each compression cycle. However, being creative could still solve such modeling problems. Using an artificial liquid storage tank at the outlet of the evaporator, all the important parameters could be adjusted and a reliable 1D model of the no-frost refrigerator could still be generated.

3.1. The 1D Modeling Components of LMS

In this section, the mathematical details of the components used in the modeling of a household refrigerator will be introduced. In the 1D model of the refrigerator, a total of twenty-one different components are utilized, which are presented in Figure 3.1. Each and every one of these components will be introduced and the solved equations will be given.

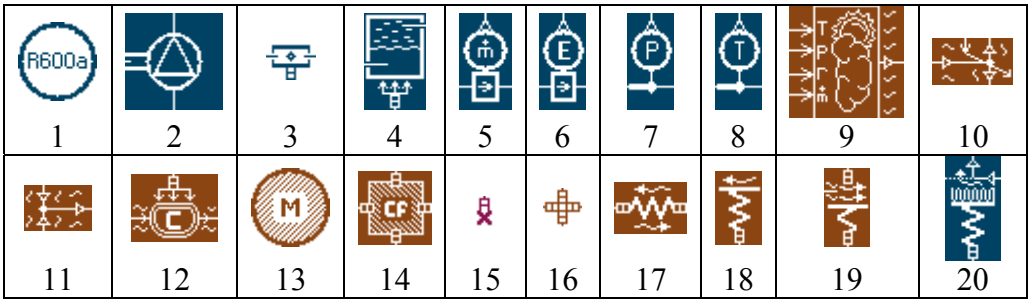

Figure 3.1. The utilized LMS components

3.1.1. Refrigerant Thermodynamic Properties

This component, #1 in Figure 3.1, is utilized to introduce the refrigerant thermodynamic properties to the 1D simulation model. The fluid properties of the selected refrigerant such as ρ, c_p, h, $\mu$and λ are computed instantaneously during the

simulations considering P_{fluid} and T_{fluid} at each component. The component #1 requires $m_{refrigerant}$ and $T_{refrigerant\ initial}$ as the inputs to the model. While making a steady state simulation, the value of $T_{refrigerant\ initial}$ does not make a difference, however for a transient simulation, it should be assigned correctly to be able to observe the real operating conditions of the refrigeration cycle with respect to time.

3.1.2. The Compressor

The component #2 in Figure 3.1 is the compressor with volumetric and isentropic efficiencies.

The compressor has a total of three ports: an inlet, an outlet and the rotary speed inlet port. $P_{refrigerant}$ and $\rho_{refrigerant}$ values are calculated in the adjacent pipe components and these values are taken as input at the compressor inlet and outlet ports, while the $h_{flow\ rate}$ and $\dot{m}_{refrigerant}$ are the calculated parameters. The rotary speed of the compressor, N, is input to the component at the third port.

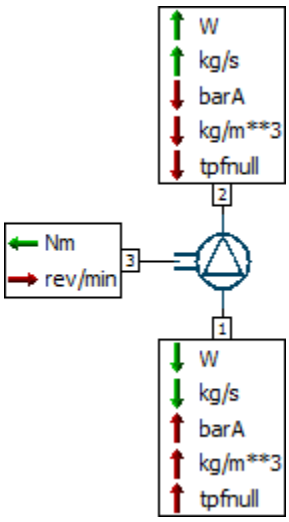

Figure 3.2. External variables of the compressor

Even though it is possible to introduce η_{vol} and η_{isen} as a function of "N" and "r" into the component, the nominal values of η_{vol} and η_{isen} at 3000 RPM are input to the component directly due to the lack of such information from the compressor manufacturer.

The mass flow rate through the compressor is calculated as in Equation (3.1), where the suction density of the refrigerant, $\rho_{refrigerant\ suc}$, is calculated automatically at $P_{comp\ suc}$ and $T_{comp\ suc}$.

$$\dot{m}_{refrigerant} = \eta_{vol}\ \rho_{refrigerant\ suc}\ N\ V_P \tag{3.1}$$

The enthalpy increase through the compressor, which is the difference between the discharge and the suction enthalpies, is calculated as

$$h_{inc} = h_{dis} - h_{suc} = \frac{h_{dis\ isen} - h_{suc}}{\eta_{isen}} \tag{3.2}$$

while the enthalpy flow rate increase is calculated as

$$h_{flow\ inc} = \dot{m}_{refrigerant}\ h_{inc} \tag{3.3}$$

The suction and discharge enthalpy flow rates, $h_{flowratesuc}$ and $h_{flowratedis}$, are calculated as in Equations (3.4) and (3.5), respectively.

$$h_{flow\ suc} = -\dot{m}_{refrigerant}\ h_{suc}(P_{suc},\ T_{suc}) \tag{3.4}$$

$$h_{flow\ dis} = h_{flow\ suc} + \dot{m}_{refrigerant}\ h_{inc} \tag{3.5}$$

The value of the $h_{flow\ inc}$ gives directly the compressor power since the effects of the η_{vol} and η_{isen} are taken into consideration during the calculations. The $h_{flow\ inc}$ data with respect to time is used in the EC calculation of the refrigerator in the simulations.

3.1.3. Pipe with Friction and Heat Exchange

The component #3 is a piping system element with friction and heat exchange. Using this component, it is possible to calculate not only the heat transfer from or to the pipe but the pressure drop along the pipe, as well.

The user has to first specify L_{pipe} and the cross sectional area of the pipe, $A_{cr\ pipe}$, along with the absolute surface roughness of the pipe material, e. Also the hydraulic diameter, D_H, of the pipe should be input to the component that different cross sectional areas such as rectangular or square could be tested.

This component has a total of three ports: pipe inlet, pipe outlet and the heat transfer port. At the pipe inlet, the h_{flow} and $\dot{m}_{refrigerant}$ are the input values, while the $P_{refrigerant}$ and $\rho_{refrigerant}$ are computed as output. At the pipe outlet, however, the inputs and outputs are replaced. At the heat transfer port, $T_{pipe\ wall}$ is the input for the calculation of the heat transfer as the output at this port.

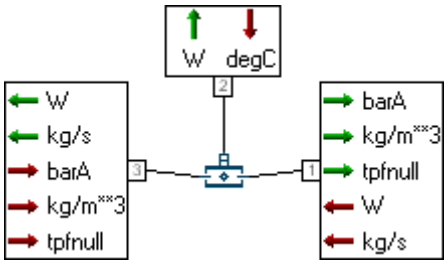

Figure 3.3. External variables of the pipe with friction and heat exchange

In this component, whatever the state of the fluid is, some parameters are observed. These are T_{fluid} and h_{fluid} in the pipe. Also the difference between T_{fluid} and the T_{sat} is continuously traced to observe the superheating or the subcooling of the fluid in the pipe.

If $T_{fluid} - T_{sat} < 0$, the refrigerant is assumed to be subcooled, while if $T_{fluid} - T_{sat} > 0$, the refrigerant is assumed to be superheated.

The pressure drop of the flow is calculated in this component depending on the flow regime and the relative roughness of the duct. If the flow is single phase, the Churchill correlation (Perry & Green, 2008), presented in (3.6), is used to compute the friction coefficient. This correlation is valid for all Re numbers, from laminar to turbulent regimes and e/D ratios.

$$f = 2\left(\left(\frac{8}{Re}\right)^{12} + (A+B)^{-1.5}\right)^{1/12}$$

where (3.6)

$$A = \left[2.457 \ln \frac{1}{(7/Re)^{0.9} + 0.27\, e/D}\right]^{16} \text{ and } B = \left(\frac{37{,}530}{Re}\right)^{16}$$

When the flow in the pipe is in two-phase, then the program allows the user to choose a friction coefficient correlation among McAdams, Cicchitti and Dukler correlations. For this calculation, homogeneous model McAdams correlation is selected. In a homogeneous model for two-phase flows, the vapor and liquid velocities are assumed to be the same. In the McAdams correlation, the viscosity of a homogeneous two-phase mixture is obtained as in Equation (3.7) (Ghiaasiaan, 2008).

$$\mu_{TP} = \left(\frac{x_{mixture}}{\mu_{vapor}} + \frac{1 - x_{mixture}}{\mu_{liquid}}\right)^{-1} \tag{3.7}$$

The density of the two-phase mixture is calculated n the same manner.

$$\rho_{TP} = \left(\frac{x_{mixture}}{\rho_{vapor}} + \frac{1 - x_{mixture}}{\rho_{liquid}}\right)^{-1} \tag{3.8}$$

The Re number is then equal to

$$Re_{TP} = \frac{\rho_{TP}\, V\, D_H}{\mu_{TP}} \tag{3.9}$$

Substituting these parameters into the Blasius's correlation, the friction coefficient is calculated as in Equation (3.10).

$$f = 0.079\, Re^{-0.25} \tag{3.10}$$

The convective heat flow rate from or to the pipe is calculated using Equation (3.11).

$$\dot{Q}_{conv,\,pipe} = \alpha\, A_{pipe\ inner\ surf}\ (T_{fluid} - T_{pipe\ wall}) \tag{3.11}$$

The inner surface area of the pipe, $A_{pipe\ inner\ surf}$, is calculated as in Equation (3.12). This calculation is compatible with all the pipes having both circular and rectangular cross sectional areas.

$$A_{pipe\ inner\ surf} = \frac{4\, A_{cr\ pipe}\, L_{pipe}}{D_H} \tag{3.12}$$

When the flow in the pipe is single-phase flow, the convective heat exchange coefficient, α, is determined according to the flow regime. If the flow is laminar, then the Nu is taken constant as 3.66 assuming that $T_{pipe\ wall}$ is constant. For the turbulent regime, Nu is defined by Gnielinski correlation, given in Equation (3.13) (Chemieingenieurwesen & Gesellschaft, 2010).

$$\mathrm{Nu} = \frac{(\zeta/8)(\mathrm{Re}-1000)\mathrm{Pr}}{1+12.7\sqrt{(\zeta/8)}(\mathrm{Pr}^{2/3}-1)} \tag{3.13}$$

where

$$\zeta = (1.8\ \log_{10}\mathrm{Re}\ -\ 1.5)^{-2}$$

This correlation is valid when $0.5 \le \mathrm{Pr} \le 2000$ and $3000 \le \mathrm{Re}_{\mathrm{D_H}} \le 5\times10^6$. All the fluid properties are calculated at the mean temperature, which is calculated as

$$T_{mean} = \frac{T_{pipewall} + T_{fluid}}{2} \tag{3.14}$$

In two-phase flow conditions, however, the program first checks for the condition of the flow whether boiling or condensation occurs. For this task, the program evaluates the value of $T_{fluid} - T_{pipewall}$. If the result is negative, then boiling is considered, whereas if the result is positive, condensation is considered.

For the case of boiling, the VDI for vertical tubes correlation (Bejan & Kraus, 2003) is utilized, which is given in Equation (3.15). This correlation is a corrected form of the Gnielinski correlation, which is for the single-phase flow case. To obtain the

convection coefficient for the boiling case, the convection coefficient for the single-phase liquid flow, α_{LO}, is multiplied with the two-phase flow correction factor, F_{TP}.

$$\alpha_{boiling} = \alpha_{LO}\, F_{TP}$$

where F_{TP} is defined as

$$F_{TP} = \frac{1}{\sqrt{A_1 + A_2}}$$

$$A_1 = \left[(1 - x_{mixture})^{1.5} + 1.9 x_{mixture}^{0.6} (1 - x_{mixture})^{0.01} \left(\frac{\rho_{liquid}}{\rho_{vapor}} \right)^{0.35} \right]^{-2.2} \qquad (3.15)$$

$$A_2 = \left[\left(\frac{\alpha_{VO}}{\alpha_{LO}} \right) x_{mixture}^{0.01} \left[1 + 8(1 - x_{mixture})^{0.7} \left(\frac{\rho_{liquid}}{\rho_{vapor}} \right)^{0.67} \right] \right]^{-2.0}$$

α_{VO} represents the convection coefficient for the single phase vapor flow.

As for the case of condensation, the Shah correlation is utilized, which is given in Equation (3.16) (Bejan & Kraus, 2003). Shah developed this correlation from his observation that the mechanisms of condensation and evaporation were very similar phenomenon in the absence of nucleate boiling. With this idea, he modified the convective component of his boiling flow correlation to use for condensation. The bracketed term is a two-phase multiplier, which properly approaches unity as $x_{mixture}$ approaches zero. In this case it predicts the convective heat transfer coefficient of the single-phase flow.

$$\mathrm{Nu} = 0.023 \mathrm{Re}_{\mathrm{L}}^{0.8} \mathrm{Pr}_{\mathrm{L}}^{0.4} \left[1 + \frac{3.8}{\mathrm{Pr}^{0.38}} \left(\frac{x_{mixture}}{1 - x_{mixture}} \right)^{0.76} \right] \qquad (3.16)$$

3.1.4. Stratified Chamber with Imposed Heat Flux

As it was mentioned at the beginning of this chapter, 1D modeling has some drawbacks in terms of modeling the real time phenomenon mathematically. As it will be mentioned in section 4.1, the refrigerant accumulation in the evaporator during the off time of the compressor in the form of liquid droplets is a proven fact. From this aspect, it is not wrong to say that the evaporator acts as a liquid refrigerant storage when the

compressor stops. However, it is not possible to model this phenomenon without using an artificial liquid storage tank in the 1D model. In some refrigerators, real vapor liquid separators are utilized to ensure that the refrigerant flowing to the inlet of the compressor is in vapor phase completely. However in this model, a stratified chamber is utilized not due to the fact that the refrigerator has one, but to be able to model the storage effect of the evaporator correctly.

When this component, #4 in Figure 3.1, is added to the model, the initial pressure, the volume and the initial percentage of the liquid volume are to be defined. Besides, since the component performs stratification process, the chamber height and the height of the inlet and outlet ports of the chamber should also be defined. The parameters observed during the simulations are $T_{chamber}$, the percentage of the liquid volume in the chamber and the refrigerant charge to the system. There is also a heat flow rate port of the component to model heat transfer to the chamber, however in this model, the port is insulated.

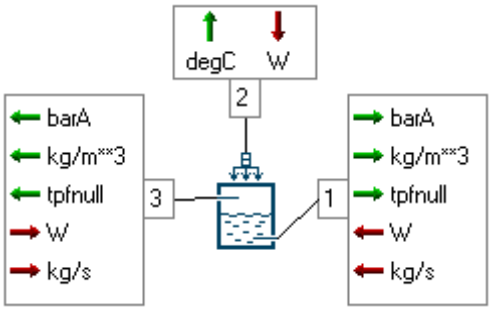

Figure 3.4. External variables of the stratified chamber with heat flux

The height of the liquid vapor interface, H_{VL}, is constantly observed during the simulations. The liquid volume percentage is multiplied with the height of the chamber. If H_{VL} level is higher than the outlet port, then the chamber charges liquid, while it charges vapor if the level is lower than the outlet port. In the simulations for the refrigerator, H_{VL} level never exceeds the height of the outlet port since it is undesirable to have liquid droplets of refrigerant in the compressor suction line since it damages the compressor. However, the use of this component makes it possible to model the refrigerant storage phenomenon of the evaporator successfully.

3.1.5. Sensors

The components #5 to #8 seen in Figure 3.1 are the sensors. These sensors could be placed at the proper locations in the model to be able to observe the values of the parameters instantaneously. The component #5 is a mass flow rate sensor, which directly gives the output in the dimension of kg/sec. If the user wants to make an instantaneous calculation, he can take this number, make an algebraic calculation and print the result instantly using this parameter. The components #6 is a power sensor, which gives $P_{refrigerant}$, $\rho_{refrigerant}$ and $h_{flow\ refrigerant}$ calculated in the previous component. Components #7 and #8 are for the instantaneous observation of the pressure and temperature measurements.

3.1.6. Moist Air Source

This component, #9 in Figure 3.1, is used as an airside boundary condition to heat exchangers, in this case, the evaporator. This component is from the thermal library. The imposed pressure at the inlet is duplicated without any modification at the outlet portion of the component. The gas mixture and the moist air libraries in the LMS Amesim are designed to model internal flow with pressure drops. However in the internal flow components pressure drop is not calculated since it does not use resistive elements. The only focus is on the evaluation of the convective heat transfer.

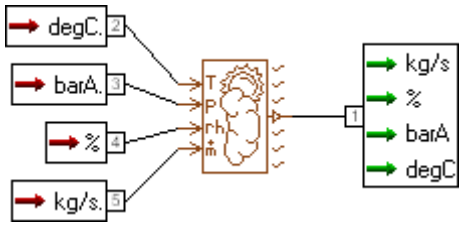

Figure 3.5. External variables of the moist air source

As could be seen from Figure 3.5, there are four inputs that should be made to the component. These are the temperature, pressure, relative humidity and the mass flow rate of the air, which is to be supplied to the system. Once these properties are attended properly, the absolute humidity and the specific enthalpy of the air is automatically calculated by the software.

3.1.7. Moist Air Splitter and Mixer

These two components, #10 to #11 in Figure 3.1, are utilized to control the moist airflow through the components.

When the air stream is to be divided into more than one stream, the component #10 is utilized. The amount of the percentage of the air stream, which is wanted to be separated, is directly input to the component. The temperature, pressure, relative humidity and the specific enthalpy of the separated air streams remain the same.

The mixer on the other hand could mix air streams of different properties. First of all, the summation of the mass flow rates of the two inlet ports is calculated to find the total mass flow rate of air mixed. Second, the absolute humidity, AH, of the output port is calculated from the absolute humidity values of the inlet ports and the conservation of mass equation as in

$$AH_{air\ outlet} = \frac{\frac{AH_{inlet\ 1}}{1+AH_{inlet\ 1}}\dot{m}_{air\ inlet\ 1} + \frac{AH_{inlet\ 2}}{1+AH_{inlet\ 2}}\dot{m}_{\text{air}\ inlet\ 2}}{\frac{\dot{m}_{air\ inlet\ 1}}{1+AH_{inlet\ 1}} + \frac{\dot{m}_{air\ inlet\ 2}}{1+AH_{inlet\ 2}}} \tag{3.17}$$

The temperature of the mixed air stream is computed from the specific enthalpy of the outlet port, which is computed as

$$h_{outlet} = \frac{\dot{m}_{air\ inlet\ 1}}{\dot{m}_{air\ inlet\ 1}+\dot{m}_{air\ inlet\ 2}} h_{inlet\ 1} + \frac{\dot{m}_{air\ inlet\ 2}}{\dot{m}_{air\ inlet\ 1}+\dot{m}_{air\ inlet\ 2}} h_{inlet\ 2} \tag{3.18}$$

The moist air properties could be monitored simultaneously with the simulations using the moist air properties generic sensor, the component #12.

3.1.8. The Moist Air Chamber with Heat Flux

This component, #12 in Figure 3.1, represents an air chamber with an air inlet, an air outlet and a heat transfer port to or from the chamber. This component is used to compute the temperature and the absolute humidity of air in an enclosed volume. In the

1D modeling of the refrigerator, this component is used two times to model the cold store cabinets.

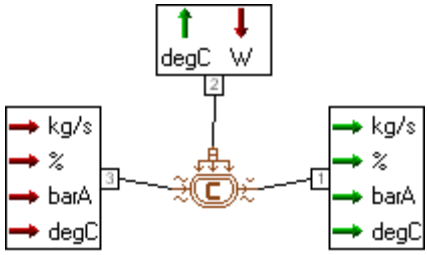

Figure 3.6. External variables of the moist air chamber with heat flux

When the component is first placed into the model, the program asks for the initial relative humidity of the air inside the chamber and the volume of the chamber. In addition to this, the initial values of $\dot{m}_{air\ outlet}$, $P_{air\ outlet}$ and $T_{chamber\ walls}$ are requested for the start of the simulations. The dry air mass flow rate at the inlet port is computed as in Equation (3.19).

$$\dot{m}_{dry\ air} = \frac{\dot{m}_{air\ inlet}}{1 + AH_{inlet}} \tag{3.19}$$

where AH_{inlet} is the absolute humidity in "kg vapor/kg dry air" at the chamber inlet.

The $\dot{m}_{air\ outlet}$ and the $P_{air\ outlet}$ are calculated from their derivatives as in Equation (3.20) and (3.21), respectively.

$$d\dot{m}_{air\ outlet} = \frac{\dot{m}_{dry\ air}(1 + AH_{outlet}) - \dot{m}_{air\ outlet}}{\tau} \tag{3.20}$$

$$dP_{outlet} = \frac{P_{inlet} - P_{outlet}}{\tau} \tag{3.21}$$

where τ is the time constant and it is equal to 0.01 sec.

The difference between $AH_{chamber}$ and AH_{outlet} corresponds to the condensate water. The condensate water mass flow rate is computed as in Equation (3.22).

$$\dot{m}_{water\ condensated} = \dot{m}_{dry\ air}(AH_{chamber} - AH_{outlet}) \tag{3.22}$$

3.1.9. Thermal Solid Properties and the Thermal Capacity

In order to define the solid masses into the 1D model, the thermal solid properties component, #13 in Figure 3.1, is to be used. If the desired solid material is already recorded in the LMS libraries, there is no need to attend the properties of the material manually. It is also possible to create some other materials that do not exist in the library and the entire thermal and mechanical solid properties could be input to the component. For each different material used, a new thermal solid properties component is to be added to the model. Each one of these components is created with its own solid type index.

The thermal capacity, component #14 in Figure 3.1, represents a certain mass of material. Therefore when the component is first put into the model, the program wants the user to input the mass, the initial temperature and the solid type index of the material. If more than one type of material is in use, each material will have its own solid type index and each thermal capacity should be input the proper index in order to be correctly introduced to the model.

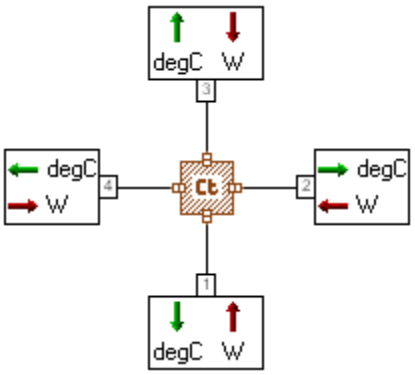

Figure 3.7. External variables of the thermal capacity

The thermal capacity has four thermal ports. The heat transfer occurs to or from the thermal capacity through these ports. The temperature of the thermal capacity is assumed to be homogeneous since the body is considered as a unique lumped body. This makes the temperature of each node the same. The temperature derivative of the thermal capacity is computed as in Equation (3.23).

$$\frac{dT}{dt} = \frac{\sum_{j=1}^{4} \dot{Q}_{in_j}}{m_{thermal\ capacity}\ c_p} \tag{3.23}$$

If the energy storage variable is to be observed, this option should first be activated. Then the program asks the user to enter the initial value of the stored energy for the start of the simulations. The derivative of the energy stored is defined as in Equation (3.24).

$$\frac{dE}{dt} = \sum_{j=1}^{4} \dot{Q}_{in_j} \tag{3.24}$$

If some of the ports of the thermal capacity are to be insulated, then the thermal plug, component #15 in Figure 3.1, should be utilized for zero heat flow. If, on the other hand, the number of ports on a thermal capacity component is to be increased, the thermal temperature and the heat flow node component, # 16, is utilized.

3.1.10. Linear Conductive Exchange

This component, component #17 in Figure 3.1, is utilized the model the conductive heat exchange between two temperature nodes. In the modeling of the refrigerator wall, for instance, there are three layers of materials that the heat energy needs to pass through. Each layer of material is modeled with a different thermal capacity and the linear conductive exchange component is placed between each pair of materials. The model of the refrigerator wall is presented in Figure 3.8. From left to right, the thermal capacities represent the steel, polyurethane and thermoform materials.

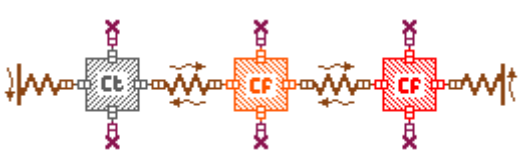

Figure 3.8. The 1D model of the refrigerator wall

When the component is placed into the model, the types of the materials connected to the each port should be defined to the program using the solid type

indexes. Next, the distances between the points of contact and the temperature points should be appropriately attended to both of the nodes. This information is required for the calculation of the conduction heat flow rate from one material to another. The next input parameter is the contact thermal resistance between the two different materials. In the modeling of the refrigerator, this number is found via trial and error. The last parameter to enter is the exchange area between the two different materials. Thus, all the parameters required to calculate the heat flow rate between the two nodes of the component would be input to use in the Equation (3.25).

$$\dot{Q}_{cnd} = \frac{\lambda A_{cnd\ exchange}}{L}(T_2 - T_1) \tag{3.25}$$

3.1.11. External Flow Free/Forced Convective Heat Exchange

This component, #18 in Figure 3.1, is utilized to model free or forced convection between a wall and its surroundings at constant temperature. The surroundings can be defined as a fluid or as an environmental moist air.

The component has only one port, which is to calculate the rate of heat transfer with respect to the temperature of the wall it is connected to.

Figure 3.9. External variables of the free/forced convective heat exchange

Initially, the type of fluid flowing over the wall is to be selected. In the case of the refrigerator, it is moist air for the outside of the refrigerator. The effective heat mode of transfer on the outside of the refrigerator is selected to be free convection heat transfer. Next, the convective heat exchange area and the characteristic length of the heat exchange are defined. For free convection, the inclination angle has to be input to the component. The temperature, the pressure and the moist air relative humidity are the other parameters required. Finally, the Nu number is defined as a function of Gr and Pr numbers.

In the case of the refrigerator, the free convection occurs on the vertical refrigerator walls. The average Nu for this case is recommended by Churchill and Chu (Incropera, 2007) as in Equation (3.26).

$$\mathrm{Nu}=\left\{0.825+\frac{0.387\mathrm{Ra}_{\mathrm{L}}^{1/6}}{\left[1+\left(0.492/\mathrm{Pr}\right)^{9/16}\right]^{8/27}}\right\}^{2} \tag{3.26}$$

where

$$\mathrm{Ra}_{\mathrm{L}}=\mathrm{Gr}_{\mathrm{L}}\ \mathrm{Pr}$$

This correlation is valid over the entire range of Ra numbers. The Gr number is defined as in Equation (3.27).

$$\mathrm{Gr}_{L}=\frac{g\beta(T_{pipewall}-T_{fluid})L_{characteristic}^{3}}{\nu^{2}} \tag{3.27}$$

where β is the bulk modulus of the fluid. When the free convection occurs on a vertical wall, the characteristic length is taken as the height of the plate.

The definition of the Pr number is

$$\mathrm{Pr}=\frac{c_{p}\ \mu}{\lambda} \tag{3.28}$$

The physical properties of the fluid flowing over the wall are calculated at the film temperature, which is defined as

$$T_{film}=\frac{T_{wall}+T_{fluid}}{2} \tag{3.29}$$

The convection coefficient on the vertical wall is calculated to be

$$\alpha=\frac{\mathrm{Nu}\ \lambda}{L_{characteristic}} \tag{3.30}$$

Finally, the convective heat flow rate is computed as

$$\dot{Q}_{conv} = \alpha\, A_{convection}(T_{fluid} - T_{pipe\ wall}) \tag{3.31}$$

3.1.12. Internal Mixed Convection

This component, #19 in Figure 3.1, is utilized to model free or forced convection between a wall and an internal environment moist air.

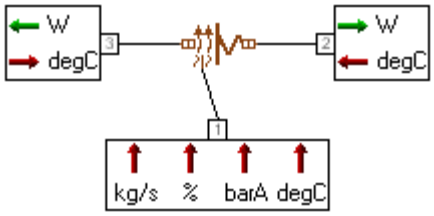

Figure 3.10. External variables of the internal mixed convection

Unlike the previous component, this one also has an airflow port in order to calculate the internal convective heat transfer. When the flow is external, the fluid temperature is assumed to be constant. However in an enclosed cabinet, the temperature always changes due to the heat transfer and this brings in a transient characteristic to the convective heat exchange. Therefore, this component is used for the inlet of the refrigerator cabinets.

The most general equations of this component regarding the free convection heat transfer are the same as that of the component #18.

Since the refrigerator under issue is a no-frost refrigerator, there is an air circulation in the refrigerator, which makes the type of the heat transfer inside the refrigerator cabinet forced convection during the simultaneous compressor and fan operation. The fan in front of the evaporator blows air at a volume flow rate of $50 m^3/h$ air. The flow is assumed to be turbulent and the Nu number for the forced convection (Incropera, 2007) is chosen as

$$\mathrm{Nu} = 0.037\mathrm{Re}^{0.8}\mathrm{Pr}^{0.33} \tag{3.32}$$

This Nu expression is actually for external flow. Even though, the forced convection heat transfer occurs inside the cabinets of a refrigerator, the heat transfer occurs on a wall. Therefore, a Nu number expression for external flow is selected for the forced convection heat transfer in an enclosed cabinet.

The Re number is defined as in Equation (3.33).

$$\mathrm{Re} = \frac{V\, L_{characteristic}}{\upsilon} \tag{3.33}$$

where the velocity is calculated as

$$V = \frac{\dot{m}_{air\ outlet}}{\rho_{air}\ \mathrm{A}_{cr}} \tag{3.34}$$

The software automatically calculates the Re number with respect to time and it shows that the Re number is on the order of 10^6. Since the Re number limit for turbulent flow on a plate is $5\text{x}10^5$, the turbulent flow assumption inside the refrigerator cabinets proved to be correct.

The convection coefficient on the inner surfaces of the refrigerator cabinets is calculated to be

$$\alpha_{forced} = k \times \frac{\mathrm{Nu}(\mathrm{Re},\mathrm{Pr})\,\lambda}{L_{characteristic}} \tag{3.35}$$

where the "k" is the gain of the forced convection heat transfer coefficient. This gain is a useful tool in matching the simulation results to the experimental data.

Since there is always a contribution of the free convection wherever there is a temperature gradient, the mixed convection coefficient, defined in Equation (3.36), has to be considered in calculating the convective heat transfer.

$$\alpha_{mixed} = \sqrt[3]{\alpha_{free}^3 + \alpha_{forced}^3} \tag{3.36}$$

Finally, the convective heat flow rate is computed as in Equation (3.37).

$$\dot{Q}_{conv} = \alpha_{mixed}\, A_{conv}\, (T_{wall} - T_{fluid}) \tag{3.37}$$

3.1.13. Thermal Convection Moist Air/Finned Wall

This component, #20 in Figure 3.1, is utilized to model the heat transfer in the evaporator from the air to the refrigerant. As it was already explained in section 2.2, there is a fan in front of the evaporator to suck the high temperature air from the cabinets and to blow it through the evaporator pipes and fins. This component is the one that is utilized to model the details of the fins.

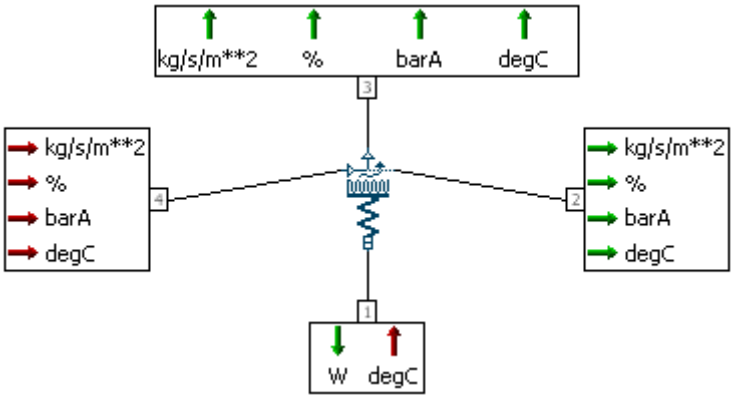

Figure 3.11. External variables of the thermal convection moist air/finned wall

This component has four ports. The convective heat flow rate is calculated on the thermal port to which the temperature is the input. The moist air properties are input to the air inlet port and they change at the outlet port due to the heat transfer. There is also a duplication of the air outlet port for the ease of modeling.

Using this model, it is possible to model convective heat exchange between moist air and part of the heat exchanger including fins since this model allows the user to define fin geometry instead of using global fin efficiency.

The fin geometry of the component is defined in the most general way as in Figure 3.12.

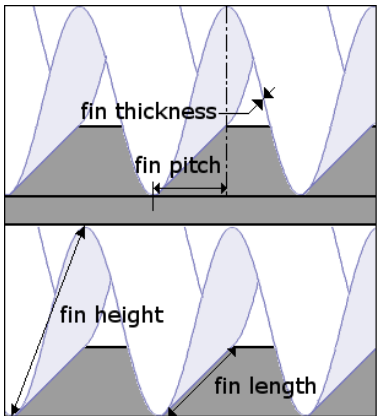

fti: fin thickness
fpi: fin pitch
fhe: fin height
fle:fin length

Figure 3.12. The fin geometry and the fin parameters

The complete model of the heat exchanger is presented in Figure 3.13. In this figure, W represents the width, H represents the height, D represents the depth (which is equal to fle) and L representes the distance between two refrigerant pipes of the heat exchanger.

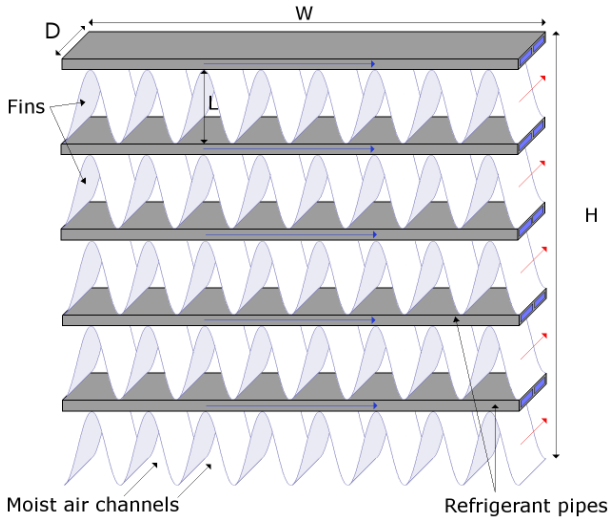

Figure 3.13. The fin geometry

The circulation area of the moist air is expressed as the cross sectional area and it is calculated as in Equation (3.38).

$$A_{cr} = (\mathrm{L} \times \mathrm{W} - \#\text{of fins} \times \mathrm{fti} \times \mathrm{fhe}) \times \#\text{of moist air channels} \qquad (3.38)$$

The number of fins in a row is computed as

$$\#\text{of fins} = \frac{\mathrm{W}}{\mathrm{fpi}} \qquad (3.39)$$

The total frontal area of the heat exchanger is equal to

$$A_{frontal} = W \times H \tag{3.40}$$

The open area ratio is computed as

$$Area\,ratio = \frac{A_{cr}}{A_{frontal}} \tag{3.41}$$

The total wet perimeter is first calculated as

$$Total\ wet\ perimeter = 2 \times (\mathrm{W} + \#\,\mathrm{of\ fins} \times \mathrm{fhe}) \times \#\,\mathrm{of\ moist\ air\ channels} \tag{3.42}$$

The convective exchange area represents the exchange area between the material and the moist airflow. It is found by multiplying the total wet perimeter by the depth of the fins.

$$A_{conv} = \mathrm{fle} \times \mathrm{Total\ wet\ perimeter} \tag{3.43}$$

In this kind of heat exchangers, the characteristic length of exchange is equal to the moist airside hydraulic diameter. In this case, it is calculated as

$$L_{characteristic} = \frac{4(\mathrm{fpi} \times \mathrm{L} - \mathrm{fti} \times \mathrm{fhe})}{\mathrm{Wet\ perimeter}} \tag{3.44}$$

where "*Wet perimeter*" is the length around one fin focusing on the moist air flow. Since there are two faces of each fin, it is equal to

$$\mathrm{Wet\ perimeter} = 2 \times (\mathrm{fpi} + \mathrm{fhe}) \tag{3.45}$$

Finally the relative finned area is defined by

$$\mathrm{rfa} = \frac{2 \times \mathrm{fhe}}{\mathrm{Wet\ perimeter}} \tag{3.46}$$

Then the global fin efficiency is calculated as

$$\eta_{fin\ global} = \frac{\lambda_{fin\ material}}{e^*} \tag{3.47}$$

where e* is defined as

$$e^* = 2\left(\frac{fti + fle}{fti \times fle}\right)\left(\frac{fhe}{2} - fti\right)^2 \tag{3.48}$$

The heat transfer between the wall and the moist air is calculated using these parameters.

This model is based on dry air mass flow rate conservation. The mass flow rate of the dry air is calculated as in Equation (3.49).

$$\dot{m}_{dry\ air} = \frac{\dot{m}_{air\ total}}{1 + AH_{inlet}} A_{frontal} \tag{3.49}$$

Finally the air mass flow rate per unit surface at the outlet is computed as in Equation (3.50).

$$\dot{m}_{air\ outlet} = \frac{\dot{m}_{dry\ air}}{A_{frontal}}(1 + AH_{outlet}) \tag{3.50}$$

CHAPTER 4

1D ANALYSIS OF COMPRESSOR CONTROL ALGORITHMS

Within the scope of this thesis, a 1D model of the household refrigerator under issue is utilized for the purpose of generating VSC control algorithms. In spite of the difficulties and impossibilities in 1D modeling, the most important parameters required for the evaluation of the performance of a household refrigerator are adjusted very well that the results of the 1D simulations could be taken as a reliable reference for the improvement of new VSC control algorithms. In this chapter, first, the simulation results of the standard on/off compressor control algorithm, which will henceforth be mentioned as the Algorithm #0, are presented and compared with those of the experiments to verify the validity of the 1D model. Next will be mentioned the importance of measuring the temperature of each and every one of the cabinets of a refrigerator simultaneously to control the compressor operation. The results of a simulation proving the advantages of such a control mechanism will be presented. The standard EC tests are performed considering the steady state part of the refrigeration operation. The definition of the phrase “steady state” in the current context is that the refrigerator will be uniquely exposed to a cooling load of heat transfer from the environment to the refrigerator cabinets. However, it was pointed out by Aprea, Mastrullo, and Renno (2004) that the real working conditions should be simulated especially for the performance evaluation of the VSC control algorithms since maintaining the minimum required temperatures in the cold storages is the main concern of the refrigeration process. For this reason, what will be introduced next is a transient cooling load algorithm, generated in the 1D modeling software to evaluate the VSC control algorithm performances under real operating conditions. In the transient loading scenario, the freezer compartment of the refrigerator will be exposed to a cyclic heating load, the effects of which will be evaluated both for the standard algorithm and for each and every one of the VSC control algorithms. Finally, the VSC control algorithms, Algorithm #1, #2 and #3, will be presented. The EC and the temperature management performances of each VSC control algorithm will be evaluated both for the

steady state operation and under the effects of the transient cooling loads. The algorithms will be evaluated in terms of maximum percentage energy savings they provide with respect to the Algorithm #0 and their temperature management capabilities will be questioned.

4.1. Algorithm #0: Standard On/Off Compressor Control Algorithm

Algorithm #0 is the design phase compressor control algorithm based on the on/off control at an operational speed of 3000 RPM, which is the most commonly used refrigeration capacity modulation method in the refrigeration industry. Since there is a single speed in this control method, there is no need for the use of a frequency converter. The activating signal is taken from the temperature sensor and if the upper temperature threshold is passed, the starting signal is sent to the compressor electric motor.

Since the standard algorithm, Algorithm #0, is explained in section 2.2 in great details, the results of the 1D simulations will be directly given in this section.

The refrigeration cycle is extensively complicated. For this reason, the 1D model is not supposed to predict every single pressure and temperature at every stage of the complete cycle correctly. However, to fulfill the requirements of this study, the calculated EC values and the cabinet temperatures should be predicted accurately.

First of all, the 1D simulation model should be able to predict $T_{th\ mass}$ precisely. Even though the Algorithm #0 does not involve a compressor control logic taking the $T_{f\ out}$ or the $T_{th\ mass}$ as the input, it is crucial that the $T_{th\ mass}$ is predicted accurately since the thermal mass packages represent a significant cooling load for the refrigerator. The $T_{th\ mass}$ data was not recorded with respect to time in the experimental measurements, but only the final values were recorded by the test chamber data acquisition system. The results of the 1D simulations are presented and compared with those of the experiments in Table 4.1. The percentage error of the simulation result to the actual value is calculated to be 0.55%.

Table 4.1. $T_{th\ mass}$ comparison with experimental data

	$T_{th\ mass}$ [°C]		
	Min	**Max**	**Average**
Experimental data	-18.4	-18.2	-18.3
1D simulation	-18.5	-18.3	-18.4

The second important parameter, which has to be predicted correctly, is the power requirement of the compressor since this data is used directly in the EC calculations. The comparison between the measured and calculated results is given in Figure 4.1.

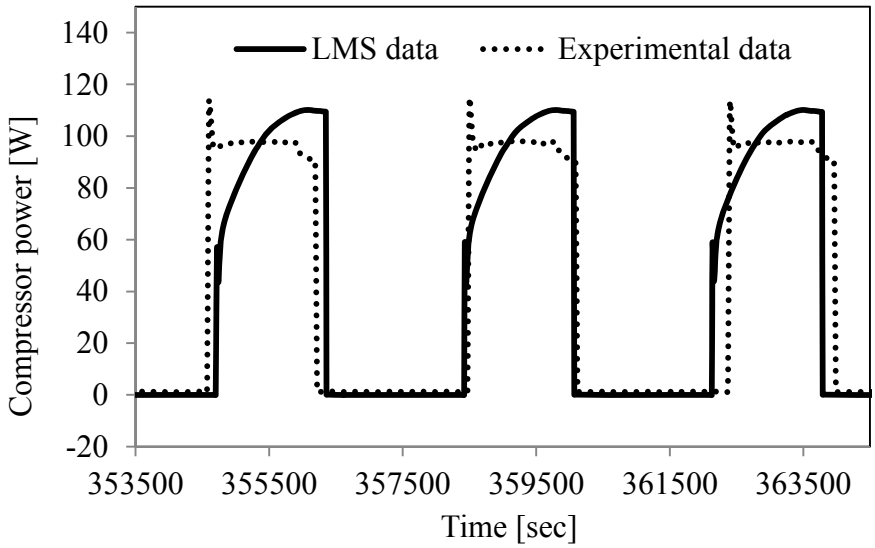

Figure 4.1. Compressor power comparison with the experimental data

The compressor requires a higher power at the beginning of its operation, after an off time period from the last stop. Researchers found out that the reason for this phenomenon was the refrigerant migration during the off time of the compressor. In the review study of Poggi, Macchi-Tejeda, Leducq, and Bontemps (2008), the main reason for the migration of the refrigerant during the off time is said to be the difference between $P_{condensation}$ and $P_{evaporation}$. As long as the compressor operates, $P_{evaporator}$ remains very low and the refrigerant evaporate absorbing heat from the refrigerator cabinets. However, when the compressor stops, the pressure difference results in the bulk movement of the refrigerant from the condenser to the evaporator through the expansion device. The increase in $P_{evaporator}$ results in an increase in $T_{sat\ ref}$ and when $T_{sat\ ref}$ reaches

$T_{evaporator}$, the refrigerant vapor starts condensing in the evaporator tubes. As the pressure difference between the condenser and evaporator decreases during the off period, a serious amount of liquid refrigerant accumulation in the evaporator is observed. It was experimentally measured and declared in one of the reviewed studies that the amount of the refrigerant in the evaporator would increase by nearly 50% during the off time compared to steady state operation. When the compressor starts again, it tries to suck refrigerant vapor from the evaporator, which is now filled with liquid refrigerant droplets. Having difficulty in decreasing the $P_{evaporator}$ to $P_{evaporation}$ of the steady state conditions, the compressor motor requires a higher power to operate until the refrigerant reaches its T_{sat} and starts vaporizing. The migration of the refrigerant causes a delay for the refrigeration system to reach back to its steady state operating conditions and this time period is called as the transition time.

Even though the compressor power cannot be predicted correctly, especially at the compressor start as could be seen from Figure 4.1, the total EC of the compressor is well predicted. EC is calculated by integrating the compressor power data and dividing the result of the integration by the length of the time interval using Equations (2.1) and (2.2). Thanks to the integration, the errors in the instantaneous compressor power prediction could not affect the accuracy of the EC considerably. The EC of the compressor is calculated experimentally to be 1.056 kWh/24h, while in the simulations it is calculated to be 1.036 kWh/24h, which yields a percentage error of 1.9%.

Taking a closer look at Figure 4.1, the time shift between the simulation results and the experimental data could be noticed. The reason for this is that the walls of the refrigerator are not modeled perfectly. Considering the direction of the shift, it can be deduced that in the 1D simulations, $T_{cs\ out}$ increases a little faster than the experiments, which shows that the refrigerator walls do not show enough resistance to heat transfer. That's why, the compressor starts earlier in the simulations than the experiments. However, there is always an optimum point to be found when modeling in 1D and in this case, the little time shift between the simulation results and the experimental data is neglected.

Another calculated parameter, verified in comparison with the experimental data, is the cooling capacity of the evaporator. The 1D simulation software calculates the refrigerant mass flow rate and the evaporator inlet and outlet enthalpies automatically. Therefore the cooling capacity is calculated easily using Equation (1.1).

In the experiments however, measuring the refrigerant mass flow rate is a little more complicated. Even though the refrigeration cycle is interrupted at some point and a mass flow meter is successfully placed in the middle, the device will create a certain pressure drop, which might change the operating conditions of the cycle and affect the accuracy of the results. For this reason, the refrigerant mass flow rate has to be calculated using a different method.

The piston displacement of a compressor, V_P, is defined in Equation (1.9). Multiplying V_P with the total volumetric efficiency of the compressor, $\eta_{vol\ total}$, which is supplied by the compressor manufacturer, the actual piston displacement of the compressor could be found using Equation (4.1).

$$V_A = V_P \times \eta_{vol\,total} \tag{4.1}$$

Measuring the refrigerant temperature and pressure at the inlet of the compressor, its density, $\rho_{refrigerant\ suc}$, could be read from property tables. Multiplying the V_A with $\rho_{refrigerant\ suc}$ the compressor inlet, $\dot{m}_{refrigerant}$ could be calculated as

$$\dot{m}_{refrigerant} = \rho_{refrigerant\ suc} \times V_A \tag{4.2}$$

From the measurements of $P_{evap\ in}$, $P_{evap\ out}$, $T_{evap\ in}$ and $T_{evap\ out}$, the evaporator inlet and outlet enthalpies of the refrigerant are determined from the property tables. Utilizing Equation (1.1), the cooling capacity is calculated experimentally and the difference between the simulation and the experimental results is presented in Figure 4.2. It could be observed that the cooling capacity is estimated as good as the compressor power.

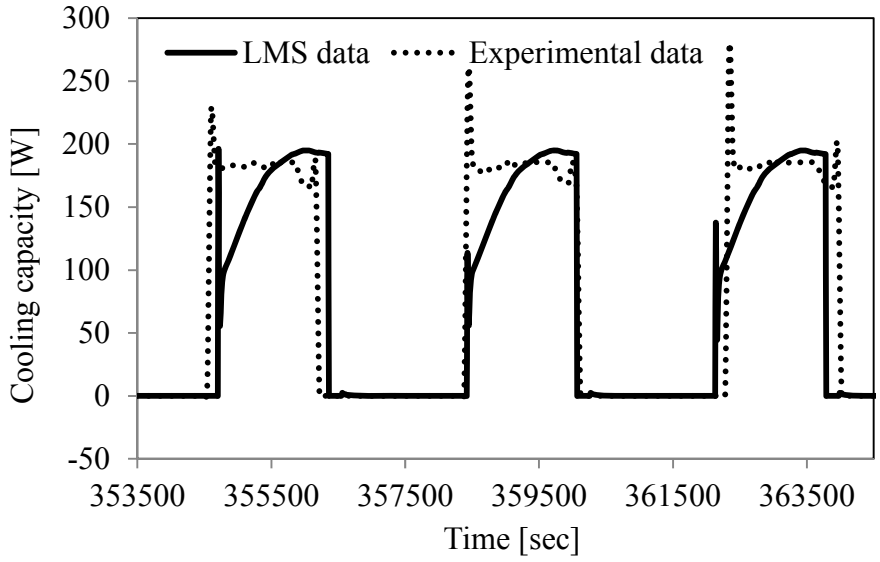

Figure 4.2. Cooling capacity comparison with the experimental data

The last parameter compared for the verification of the 1D model is the COP of the refrigeration cycle, the definition of which is given in Equation (1.6). The comparison of the simulation results with the experimental data is presented in Figure 4.3. In the experimental data, the COP values show a small increase through the end of each compressor duty cycle. The reason for this is the damper operation to adjust T_{cs}. When the damper shuts down to create a blockage to the air flow from the evaporator to the cold store, the air inlet temperature to the evaporator decreases since the high temperature air flow from the cold store cabinet to the evaporator stops. Due to the decrease in the average air temperature flowing across the evaporator tubes, the refrigerant temperature at the outlet of the evaporator decreases with an accompanying increase in the $\rho_{refrigerant\ suc}$. For the last 300 seconds of the fixed time operation, $\dot{m}_{refrigerant}$, therefore the refrigeration capacity increases. Being able to compress a higher amount suction vapor, the volumetric efficiency of the compressor increases with an accompanying decrease in the power requirement. Even though the 1D simulations underestimate the COP of the refrigeration cycle and cannot predict the COP increase during the fixed time operation, the results are still in an acceptable range, which indicates that this model could be utilized for improving VSC control algorithms.

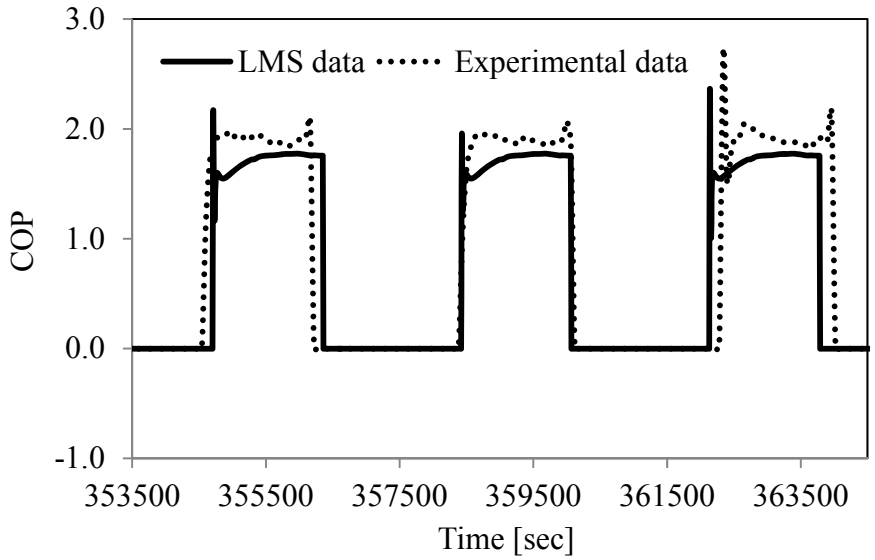

Figure 4.3. COP comparison with the experimental data

4.2. Algorithm #0.1: Eliminating the Fixed Time Operation

VSC control is a method to modulate the refrigeration capacity, which eventually controls the cabinet temperatures of a refrigerator. As long as the cabinet temperatures are maintained in the desired interval easily, the refrigeration capacity could be kept low to save energy. For this reason, it is not logical to control the compressor with the information coming from a single temperature sensor only, measuring $T_{cs\,out}$. In this compressor control algorithm, which is not yet a VSC algorithm, a second temperature sensor is added to measure the temperature of the air being drawn from the freezer compartment, $T_{f\,out}$, and this algorithm, the details of which are given in Table 4.2, is implemented on the 1D model of the refrigerator to evaluate the EC and the temperature management performances.

Table 4.2. The details of Algorithm #0.1

Control method	On/Off
Compressor speed	0/3000 RPM
Fixed time (300 sec)	NONE
$T_{cs\,out}$ **thresholds**	0°C< $T_{cs\,out}$ <8°C (Controlled with the damper)
$T_{f\,out}$ **thresholds**	-18.5°C< $T_{f\,out}$ <-18°C

The difference between the Algorithms #0.1 and #0, mentioned in section 2.2, is that the fixed time operation is eliminated in this case. The algorithm continuously measures the $T_{cs\,out}$ and $T_{f\,out}$ to start or stop the compressor operation. When the $T_{cs\,out}$ exceeds 8°C and/or when the $T_{f\,out}$ exceeds -18°C, the compressor starts its operation at 3000 RPM. The compressor does not stop until both of the temperature sensors measure the lower temperature threshold values for $T_{cs\,out}$ and $T_{f\,out}$.

It should be noted at this point that the compressor operates between these temperature thresholds only in the direction of decreasing temperatures. When $T_{cs\,out}$ or $T_{f\,out}$ reaches the upper threshold, the compressor starts to work. When $T_{cs\,out}$ or $T_{f\,out}$ reaches the lower threshold, the compressor stops and waits until either one of the temperatures reaches its upper thresholds again.

Another operational condition is observed when the refrigeration demands of the two compartments occur simultaneously. Suppose that both $T_{cs\,out}$ and $T_{f\,out}$ reaches their upper temperature thresholds and the compressor starts its operation. At first the damper switches to the on condition so that the low temperature air coming from the evaporator could flow into the cold store cabinet to decrease its temperature. But after some time, the $T_{cs\,out}$ reaches its lower threshold, 0°C, before $T_{f\,out}$ reaches -18.5°C. In this case, the damper switches to off condition, blocking the airflow from the evaporator to the cold store and the compressor continues its operation until $T_{f\,out}$ reaches -18.5°C.

In Figure 4.4, the changes in $T_{th\,mass}$ with respect to time are presented both with and without the fixed time operation. It should be noted that both of the simulations started with an initial cabinet temperature of 25°C, as in the case of the experiments. The freezer compartment is full of with Tylose material, the initial temperature of which is also 25°C. When the $T_{f\,out}$ is controlled with a separate sensor with the Algorithm #0.1, it takes a much shorter time for $T_{th\,mass}$ to reach -18.5°C. With the Algorithm #0, on the other hand, it takes more than three days for $T_{th\,mass}$ to reach its lower threshold. Besides reducing the time required to reach the desired temperatures, Algorithm #0.1 is also capable of managing T_f better than the Algorithm #0. Especially under the effects of transient cooling loads, controlling the compressor with respect to $T_{f\,out}$ will greatly improve the temperature management capabilities. As could be seen from the figure,

$T_{th\ mass}$ of the Algorithm #0.1 oscillates in its bandwidth, keeping the food in the freezer compartment safe.

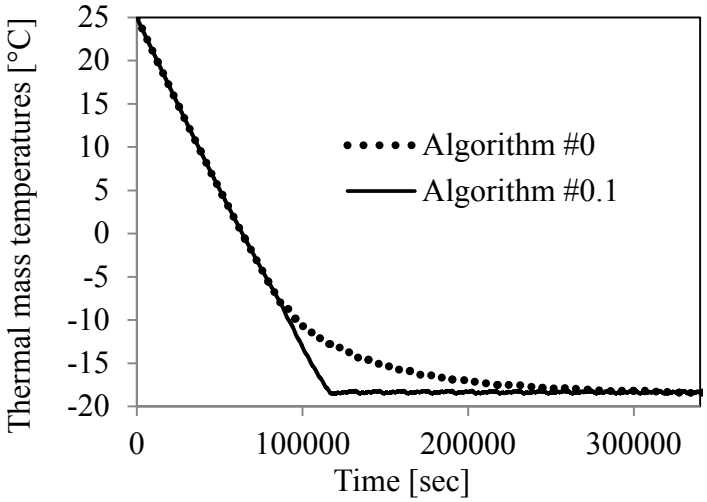

Figure 4.4. $T_{th\ mass}$ with and without the fixed time operation

Taking a closer look at $T_{th\ mass}$ and $T_{cs\ out}$ in Figure 4.5, the synchronized oscillations of both of the temperatures could be observed easily. The freezer compartment's refrigeration requirement with the given temperature bandwidth is not as frequent as the cold store. For every oscillation of $T_{th\ mass}$, $T_{cs\ out}$ oscillates for four times, which can also be observed in Figure 4.6, which compares the compressor operation of the two algorithms.

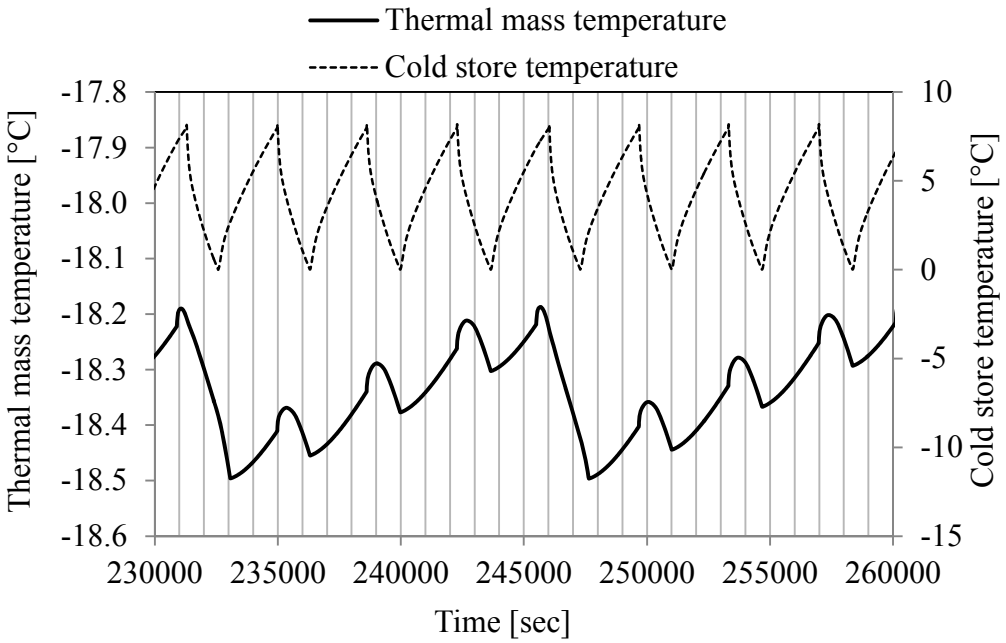

Figure 4.5. $T_{th\ mass}$ and $T_{cs\ out}$ with Algorithm #0.1

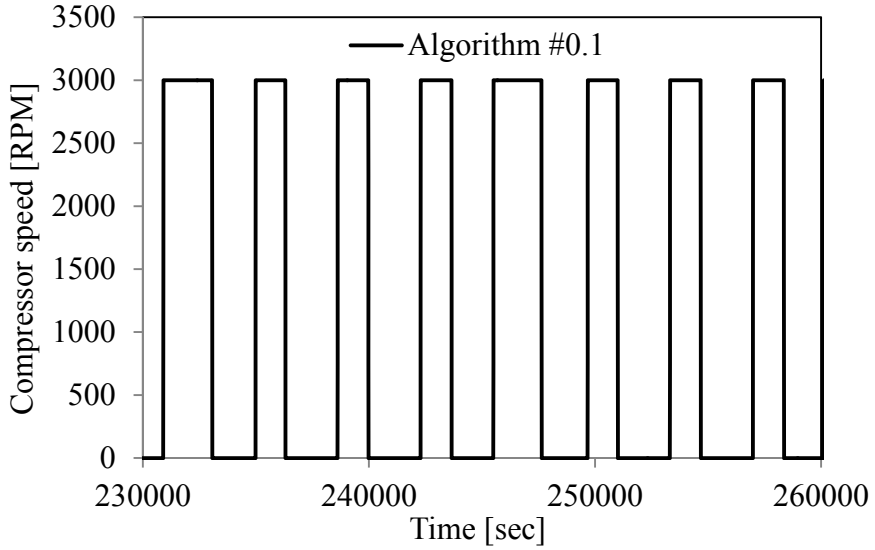

Figure 4.6. Compressor speed without the fixed time operation

In Algorithm #0, the time duration between the on/off cycles are equal to each other (Figure 2.4), whereas in Algorithm #0.1 both the on and off time of the compressor vary. Looking at the compressor operation of Algorithm #0.1, it could be observed that the compressor operates for a longer time period once every four cycles in the steady-state conditions. During the longer cycle, both of the cabinets are refrigerated, while during the shorter cycles the cold store compartment is refrigerated only. Therefore, for the Algorithm #0.1, it can be said that the 75% of the fixed time operations are eliminated with the use of a second temperature sensor. The validity of

this comment is also proved by the EC of the refrigerator, when the compressor is controlled with the Algorithm #0.1. The EC decreases from 1.036 kWh/24h to 0.966 kWh/24h, which yields an energy saving of 6.8% just by eliminating the fixed time operation and installing a second sensor without any VSC algorithm improvements.

4.3. The Effects of the Transient Cooling Loads

The method of the calculation of the EC is clearly defined in the British Standard of Household Refrigerating Appliances (British Standards Institute, 2006), which was explained in detail in section 2.2. However, this method of EC calculation does not consider the effects of the transient cooling loads, to which a real refrigerator could be exposed to in real life use. Aprea, Mastrullo, and Renno (2004) pointed out the importance of the investigation of changing cooling loads on refrigerators for VSC control applications. In the literature, generally three different experimental methods were utilized to observe the effects of time dependent cooling loads.

- Opening and closing of the refrigerator doors occasionally,
- Placing a certain amount of fruits and vegetables to the refrigerator cabinet after reaching the steady state operating conditions,
- Assembling electrical resistances into the refrigerator cabinets and passing current through them in a controlled manner.

It is deduced that the third option is the most reliable method since the amount of heat generated in the resistances could be easily determined and it is the most easily repeatable method. In addition, this was the easiest and most reliable method to apply both in the 1D simulations and the real time experiments. For this reason a simple algorithm is created to expose the freezer cabinet to a standard time dependent cooling load to evaluate the performances of different VSC control algorithms under real life operating conditions. The details of the transient cooling load algorithm are given in Table 4.3.

Table 4.3. The details of the standard transient cooling load algorithm

Time interval [sec]	The heating power [W]
150000-158000	100
200000-208000	150
250000-258000	100
300000-308000	150
350000-358000	100
400000-408000	150

At each row on the left column, a time interval is given, in which the heating power in the adjacent column on the right is applied to the thermal mass in the freezer compartment. Once the cooling load is applied, the VSC control algorithm measures a higher temperature than the one measured in the steady state conditions and adjusts the compressor speed accordingly.

The total amount of heat energy transferred to the thermal mass in the freezer compartment can be found as

$$3\times\left(8000\text{sec}\times\frac{100\text{Joules}}{\text{sec}}\right)+3\times\left(8000\text{sec}\times\frac{150\text{Joules}}{\text{sec}}\right)=6\text{ MJ}$$

6 MJ of energy is capable of increasing the temperature of 92.25 kg of Tylose material by about 32°C. However, such a temperature increase is not supposed to be observed in the simulation results since refrigeration continues simultaneously with the heat transfer to the thermal masses.

4.3.1. Performance of the Algorithm #0 Under the Effects of the Transient Cooling Loads

Before introducing and evaluating the performances of the VSC control algorithms under the effects of the transient cooling loads, the performance of the standard control algorithm should be evaluated when the cooling load on the refrigerator is unusually high. For this reason, the Algorithm #0 is simulated with the transient cooling load algorithm and the results are presented below.

The speed of the compressor with respect to time is the same as presented in Figure 2.4. Since Algorithm #0 controls the compressor with the $T_{cs\ out}$ measurement, the compressor cannot take any action on the additional cooling loads on the freezer compartment, the evidence of which is given in Figure 4.7.

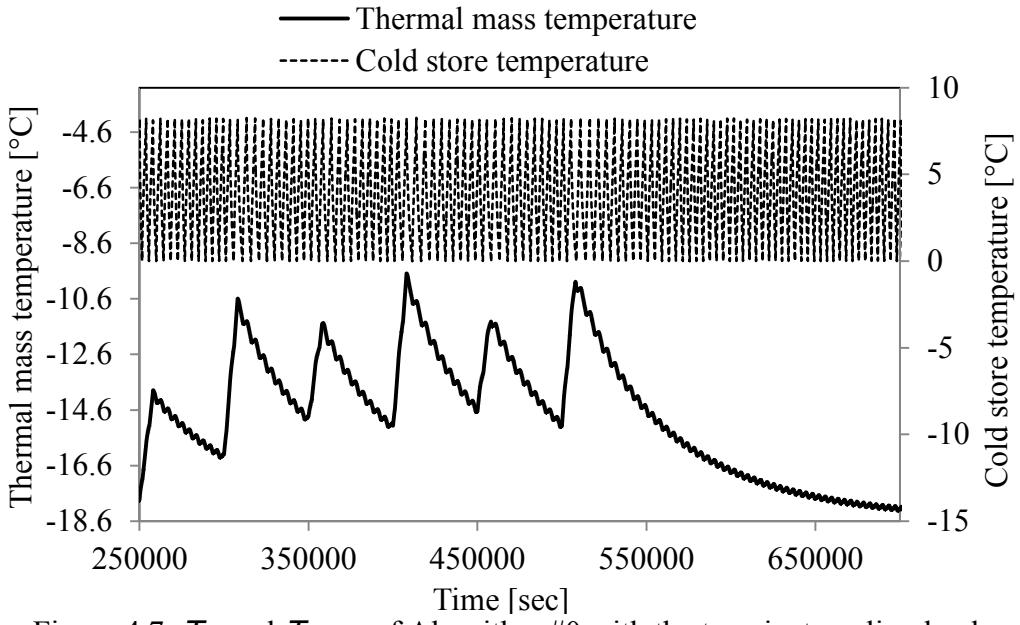

Figure 4.7. T_{cs} and $T_{th\ mass}$ of Algorithm #0 with the transient cooling loads

Even though T_{cs} oscillates regularly within its thresholds, $T_{th\ mass}$ cannot reach back to the minimum desired temperatures for a long period of time, once the transient cooling loads start affecting the freezer compartment. This unsuccessful temperature management profile proves that the Algorithm #0 is not a reliable compressor control algorithm when it comes to manage T_f.

There is no regulation for the EC calculation of a refrigerator, which is exposed to transient cooling loads in the British Standard of Household Refrigerating Appliances (British Standards Institute, 2006). Therefore, for the sake of comparability of different results, the time interval for the EC calculation is determined to be from the beginning of the first application of the heat flux to the final instant, when the $T_{th\ mass}$ is decreased back to -18.5°C after the last heat flux period is finished. In Figure 4.7, the results are presented in this time interval.

Using Equations (2.1) to (2.3) –by taking the aforementioned time interval instead of 86,400 sec in Equation (2.2)– the refrigerator is calculated to consume 1.507 kWh/24h of energy without performing a successful temperature management.

4.3.2. Performance of the Algorithm #0.1 Under the Effects of the Transient Cooling Loads

For the purpose of improving Algorithm #0, eliminating the fixed time operation and installing a second temperature sensor to measure the $T_{f\ out}$ and control the compressor operation accordingly has proved itself to be useful by decreasing the EC of the refrigerator and performing a better temperature management in the freezer compartment. However, the performance of the Algorithm #0.1 should also be questioned under the effects of the transient cooling loads. For this reason, the Algorithm #0.1 is simulated with the transient cooling load algorithm and the results are presented in this section.

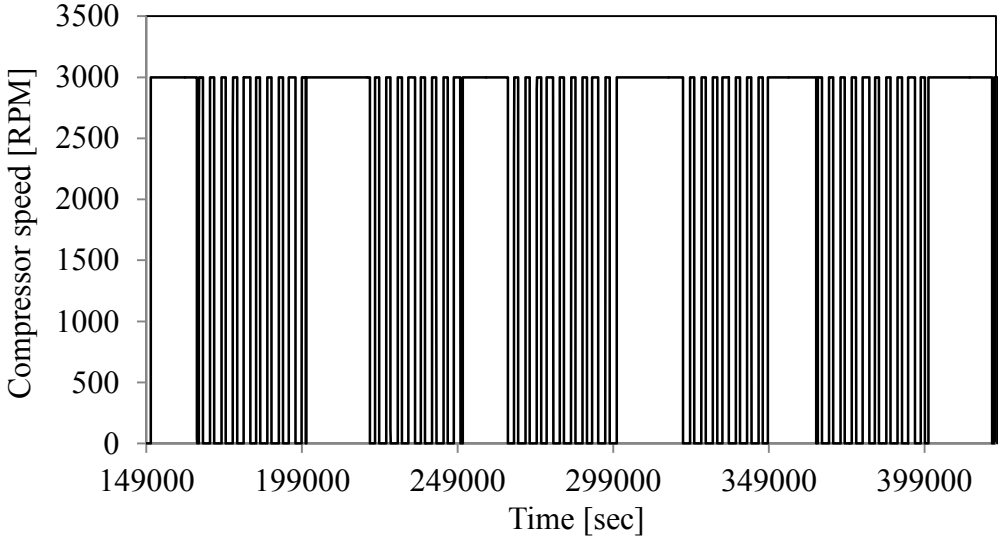

Figure 4.8. Compressor speed of Algorithm #0.1 at the transient cooling loads

The speed of the compressor with respect to time is presented in Figure 4.8. Since Algorithm #0.1 controls the compressor both with the $T_{cs\ out}$ and $T_{f\ out}$ measurements, the compressor is capable of taking actions when the $T_{th\ mass}$ increases due to the heat transfer. In order to decrease the increasing $T_{th\ mass}$, the compressor increases its duty cycle to overcome the cooling load. T_{cs}, on the other hand, is continuously controlled with the damper operation therefore it continuously oscillates between its thresholds. The cabinet temperatures with respect to time are presented in Figure 4.9.

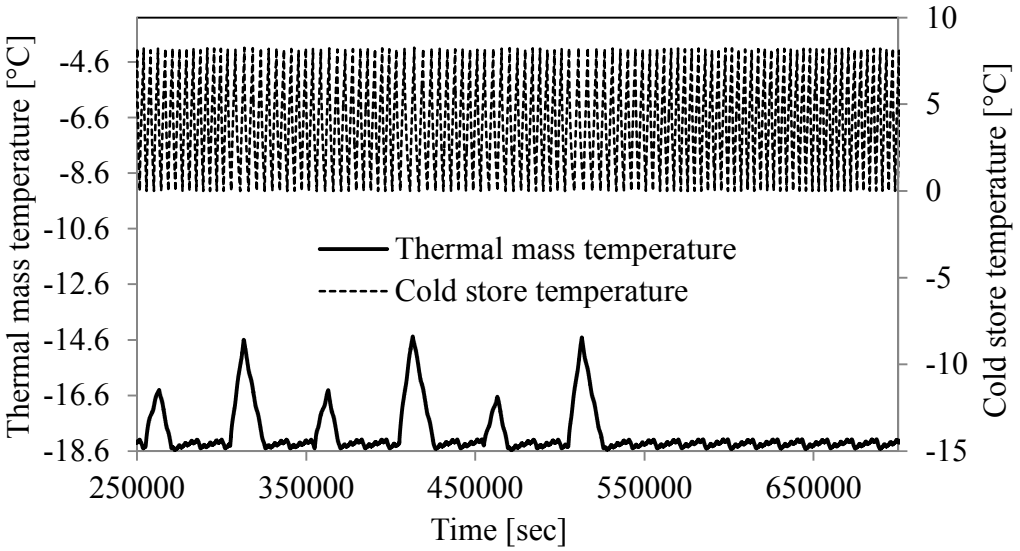

Figure 4.9. Cabinet temperatures of Algorithm #0.1 with the transient cooling loads

Since the compressor increases the cooling capacity by increasing the duty cycle, $T_{th\ mass}$ is decreased to the desired levels immediately once each heating cycle ends. Despite the fact that the Algorithm #0.1 provided an energy savings of 6.8% in comparison with the Algorithm #0 under steady state conditions, the refrigerator consumes 1.607 kWh/24h of energy in the transient cooling load period, which is around 6% higher than that of the Algorithm #0. However, it should be mentioned that Algorithm #0.1 is capable of performing a very successful temperature management to fulfill the food safety requirements in the freezer compartment. For this reason, the temperature management and EC performance of the Algorithm #0.1 will be taken a reference to compare those of the VSC control algorithms.

4.4. VSC Control Algorithms

As it was already explained in the introduction part of chapter 4, three different VSC control algorithms are generated within the scope of this thesis and they will be introduced in this section. The performance of each VSC control algorithm will be evaluated at steady state operating conditions and under the effects of the transient cooling loads. After all the algorithms and their results are presented, the EC and temperature management performances of the algorithms will be briefly compared and commented.

4.4.1. Algorithm #1: Stepwise Speed Selection from $T_{f\,out}$

The VSC control algorithm #1 is inspired by the study of Aprea, Mastrullo, and Renno (2004). As it was already explained in the literature survey, section 1.3, the authors pointed out that the compressors should be controlled from an energy saving point of view in the VSC control applications and a certain cooling load should be compensated with the lowest possible compressor speed. However, with such control logic, the time period required to reach the minimum set point temperatures would exceed the time required to reach the same temperatures at the nominal on/off frequency of 50 Hz. Regardless of the low power requirement of the compressor, the increased duty cycle might diminish all the energy savings. Due to this, the authors suggested that the compressor speed should be selected carefully to take the instantaneous system load into consideration.

The VSC control algorithm, generated by Aprea, Mastrullo, and Renno (2004), is modified in this thesis regarding the requirements of the household refrigerator under issue. For instance, the authors studied on a refrigerator having only a cold storage but not a freezer compartment, whereas the purpose of this thesis is to investigate the performance of different VSC control algorithms on a double door refrigerator, having both a cold store and a freezer compartment.

Aprea, Mastrullo, and Renno (2004) defined a parameter which gave the difference between the instantaneous and the desired temperature of the cold storage in order to use the value of this parameter as an input to the VSC control algorithm which selected the best compressor speed instantaneously. A similar function is defined for the VSC Algorithm #1 taking the $T_{f\,out}$ as the reference and it is given in Equation (4.3).

$$\Delta T = T_{f\,out} - T_{f\,out\,desired} \tag{4.3}$$

where $T_{f\,out\,desired}$ is taken as -18.5°C.

It is worth to remember at this point that the control signal of the compressor in the Algorithm #0 was the $T_{cs\,out}$. The reason for taking the $T_{f\,out}$ instead of the $T_{cs\,out}$ as the reference temperature in the Algorithm #1 is that managing T_f is much more difficult and important than managing T_{cs} since the desired T_f value is much lower than

the desired T_{cs} (section 2.2). The reason for taking $T_{f\ out\ desired}$ as -18.5°C is to ensure that the refrigerator will operate in accordance with the temperature regulations declared in the British Standard of Household Refrigerating Appliances (British Standards Institute, 2006). In this standard the $T_{th\ mass}$, which is the temperature of the warmest thermal mass package in the freezer compartment, is supposed to be measured lower than -18°C. Therefore taking the minimum threshold of $T_{f\ out}$ as -18°C would not be enough to decrease the $T_{th\ mass}$ below of -18°C.

The algorithm selects a suitable compressor speed with respect to the value of the ΔT. In Figure 4.10, the pre-determined compressor speeds corresponding to certain ΔT intervals are presented.

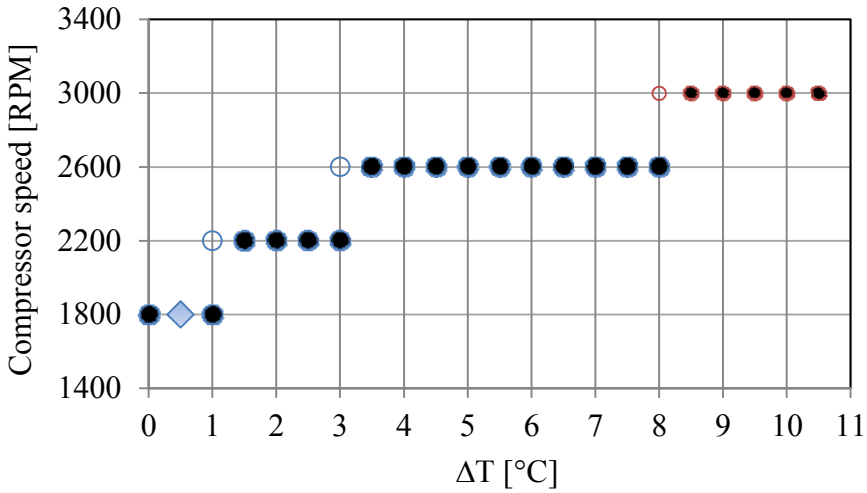

Figure 4.10. The selected compressor speeds with Algorithm #1

For a better understanding of the compressor speed selection of the Algorithm #1, it is useful to study Figure 4.10 along with Table 4.4, which samples random $T_{f\ out}$ values from each temperature interval corresponding to a different compressor speed. Assuming the initial temperature of the refrigerator to be 25°C, which is generally the real case scenario at the first start of the compressor; the temperature difference function determines the value of ΔT as 43.5°C. Since ΔT is calculated to be higher than 8°C, the control algorithm selects 3000 RPM as the starting speed. As long as the compressor operation continues and $T_{f\ out}$ decreases, the VSC control algorithm decreases the compressor speed accordingly.

Table 4.4. The compressor speeds corresponding to certain ΔT intervals

$T_{f\ out}$ [°C]	$T_{f\ out\ desired}$ [°C]	ΔT [°C]	ΔT intervals [°C]	RPM
-10	-18.5	8.5	8 < ΔT	3000
25	-18.5	43.5		
-14.5	-18.5	4.0	3 < ΔT < 8	2600
-17.4	-18.5	1.1	1 < ΔT < 3	2200
-18.1	-18.5	0.4	0 < ΔT < 0.5	1800

The point ΔT=0.5°C in Figure 4.10 is indicated with a different symbol than the others since it represents the freezer temperature upper threshold for the compressor operation to start. In more clear words, Algorithm #1 runs the compressor until $T_{f\ out}$ is decreased to -18.5°C, which gives a value of ΔT=0°C. After the compressor stops, T_f starts to increase and when ΔT=0.5°C, the compressor starts its operation at 1800 RPM. If the user opens the door of the freezer compartment, loads some warm food and ΔT is increased to 0.9°C for instance, the compressor continues its operation again at 1800 RPM. The compressor speed increases to 2200 RPM only when the ΔT increases over 1°C. Briefly, under the steady state operating conditions, the $T_{f\ out}$ oscillates between -18.5°C and -18°C, responding to the refrigeration requirement of the freezer compartment with 1800 RPM.

In this function, the minimum compressor speed is determined to be 1800 RPM, which is considered to be a reasonable value in order to keep the power consumption as low as possible when the cooling load is at minimum. In addition to this, the minimum speed at which the compressor should operate is declared to be 1600 RPM in the manufacturer's catalogue. Below this speed, the efficiencies of the compressor and its electric motor might substantially decrease, which would cause a considerable increase in the EC. For this reason, selecting the minimum compressor speed as 1800 RPM eliminates the risk of operating in the low efficiency region.

Table 4.5. The details of Algorithm #1

Control method	VSC
Compressor speed limits [RPM]	0-3000
Compressor speed	Selected according to Table 4.4
$T_{cs\ out}$ **thresholds**	0°C< $T_{cs\ out}$ <8°C (Controlled with the damper)
$T_{f\ out}$ **thresholds**	-18.5°C< $T_{f\ out}$ <-18°C

Even though T_{cs} does not independently control the compressor operation in Algorithm #1, it is controlled thanks to the damper operation as in the case of Algorithm #0. Whenever T_{cs} increases to its upper threshold, 8°C, the damper switches to the on position to let the low temperature air coming from the evaporator flow to the cold store compartment. When T_{cs} decreases to its lower threshold, 0°C, the damper switches to the off position. If the compressor is already operating to decrease T_f, the damper switches to the on and off positions sequentially to maintain the desired T_{cs}. If the compressor is not operating to decrease T_f and suddenly $T_{cs\ out}$ passes the upper threshold, this time the compressor starts its operation at 1800 RPM to decrease T_{cs} with the damper in the on position. The compressor operates with a speed of 1800 RPM if the requirement belongs to the cold store only. However, both of the compartments are refrigerated in this case since it is impossible to refrigerate the cold store compartment alone. But if both of the cabinets require to be refrigerated, the damper switches on and compressor speed is selected with respect to the value of ΔT. These operational details could be better understood by analyzing Figure 4.11 and Figure 4.12.

The compressor speed with respect to time, under the control of the Algorithm #1, is presented in Figure 4.11. Since the initial temperature of the refrigerator and the $T_{th\ mass}$ is 25°C, compressor starts its operation at 3000 RPM and continues its operation for a long period of time at 3000 RPM until ΔT drops below 8°C, at 2600 RPM until ΔT drops below 3°C and 2200 RPM until ΔT drops below 1°C. When ΔT drops below 1°C, the control algorithm selects 1800 RPM for the rest of its operation. Since there is no transient cooling load on the refrigerator but the steady state heat transfer from the environment to the refrigerator cabinets, ΔT never exceeds 1°C. No matter how low the

compressor speed is, should the compressor operate with the additional help of the on/off capacity control method not to decrease cabinet temperatures extremely.

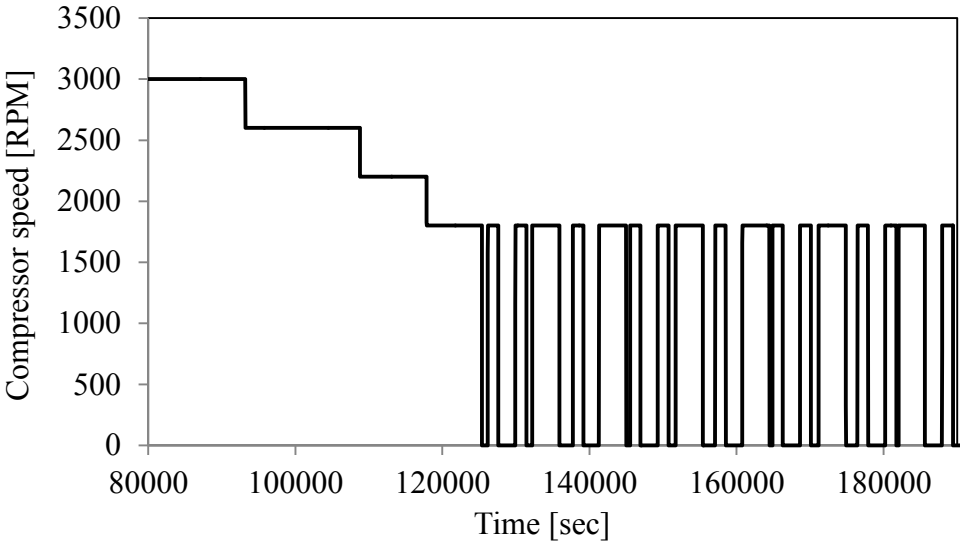

Figure 4.11. Compressor speed with Algorithm #1

The shorter cycles, seen in Figure 4.11, are to decrease to T_{cs} only, while the longer cycles are to decrease both T_{cs} and T_f. This could be observed better looking at Figure 4.12, the predicted cabinet temperatures by the simulations. The shorter compressor cycles, which decrease $T_{cs\,out}$ from 8°C to 0°C, decrease the rate of increment of the $T_{f\,out}$ but $T_{f\,out}$ shows a considerable decrease only when the compressor duty cycle increases. Since there is no thermal mass in the cold store compartment, the determined $T_{cs\,out}$ thresholds are directly observed on the T_{cs}. However, $T_{th\,mass}$ remains below the upper $T_{f\,out}$ threshold since it takes more time for the thermal mass temperature to increase than for the air inside the freezer compartment. The cabinet temperatures presented in Figure 4.12 represent a successful temperature management.

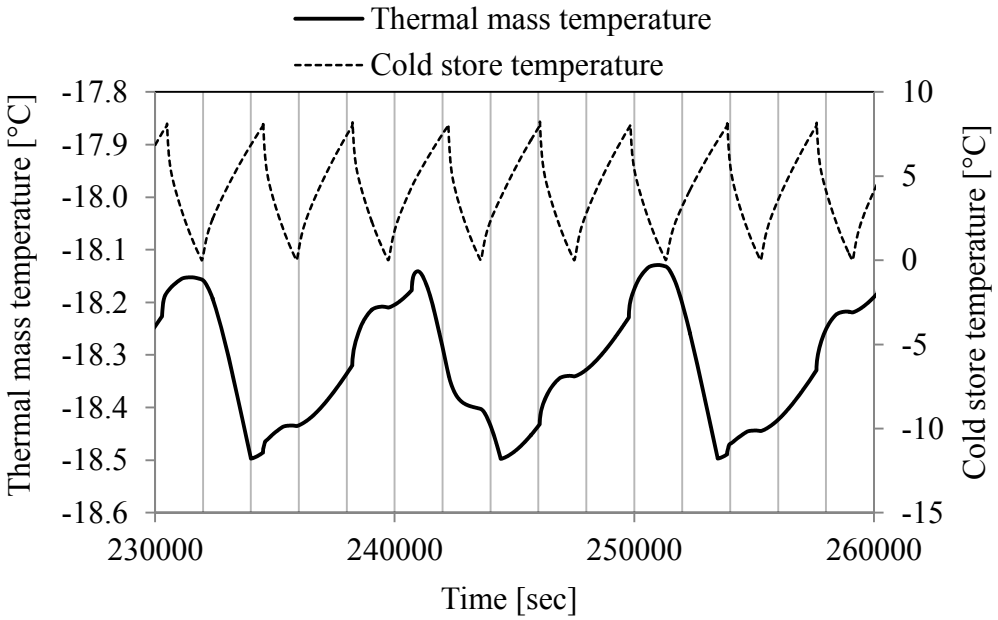

Figure 4.12. T_{cs} and $T_{th\ mass}$ with Algorithm #1

Using the VSC control Algorithm #1, the EC of the refrigerator is calculated to be 0.864 kWh/24h. In comparison with the Algorithm #0, the energy savings provided by the Algorithm #1 is 16.6%, which is a remarkable improvement of the energy conversion efficiency of the refrigerator.

4.4.1.1. Performance of the Algorithm #1 Under the Effects of the Transient Cooling Loads

Even though the Algorithm #1 does not look like a VSC control algorithm since it operates with on/off control method after reaching the steady state operating conditions, it should be remembered that this case does not take the effects of the transient cooling loads into consideration. In daily use, when the cabinet doors are opened and closed periodically while at the same time high temperature masses are added to the cabinets regularly, the compressor speed will vary appropriately by measuring the $T_{f\ out}$ instantaneously. In this section, this phenomenon will be investigated.

The transient cooling load algorithm, the details of which are given in Table 4.3, is implemented in the simulation model. Since $T_{th\ mass}$ increases due to the heat transfer, the air temperature inside the freezer compartment increases, too. Therefore, the

Algorithm #1 selects different compressor speeds for the higher values of ΔT. The speed of the compressor with respect to time is presented in Figure 4.13.

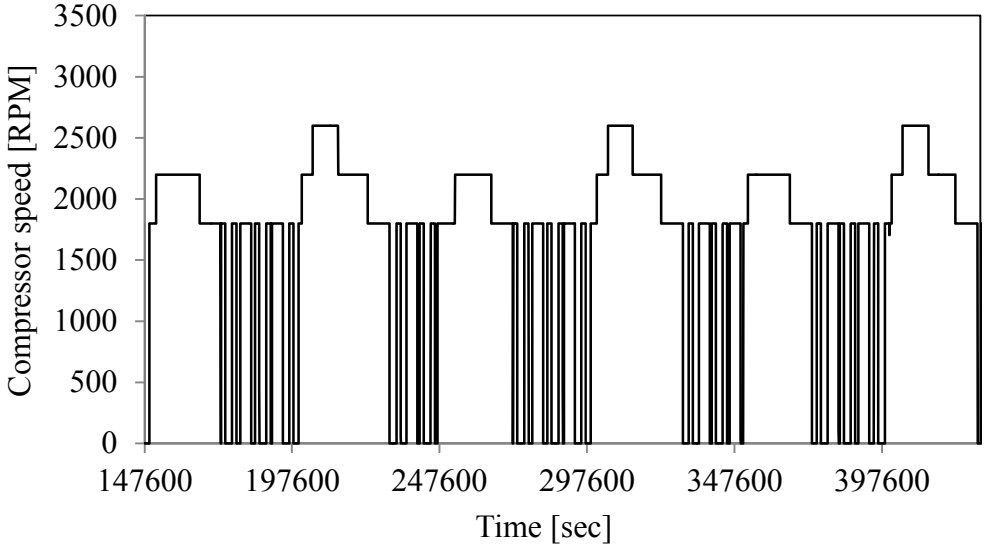

Figure 4.13. Compressor speed with Algorithm #1 at the transient loading conditions

Since the transient cooling load algorithm has two different heat flux values imposed one after another, the Algorithm #1 responds each one of them with a different speed selection. When the thermal masses in the freezer compartment are exposed to 100W of heating power for 8000 seconds at the beginning of the first loading cycle, ΔT increases for about 2.5°C (Figure 4.14) and the algorithm selects 2200 RPM to overcome this load. When the heating power is increased to 150W, ΔT increases for more than 4°C that the algorithm increases the compressor speed to 2600 RPM. As the ΔT decreases at the end of the loading cycles, the compressor speed decreases step by step and then finally the compressor comes to a stop.

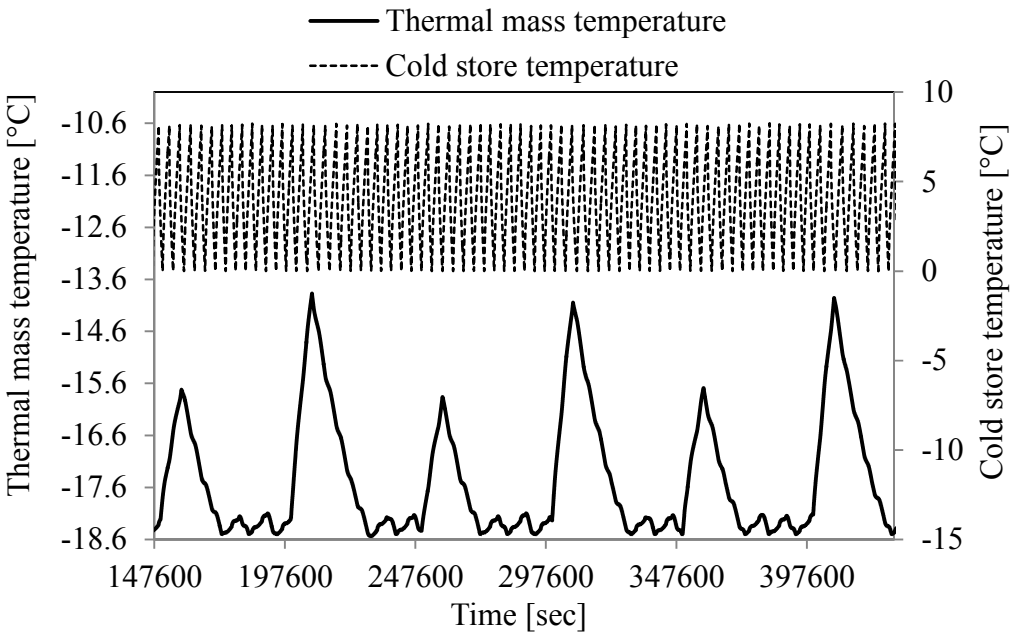

Figure 4.14. T_{cs} and $T_{th\ mass}$ with Algorithm #1 with the transient loading conditions

The change of $T_{th\ mass}$ with respect to time, presented in Figure 4.14, shows that Algorithm #1 is capable of performing successful temperature management even under the effects of transient cooling loads. In between the heating cycles, Algorithm #1 could decrease $T_{th\ mass}$ to the desired values, whereas the Algorithm #0 could not manage to maintain the desired $T_{th\ mass}$ for a considerably long period of time (Figure 4.7). T_{cs}, on the other hand, continuously oscillates between its thresholds, 0°C and 8°C since it is controlled with the damper operation.

With the use of the VSC control Algorithm #1, the refrigerator consumes 1.433 kWh/24h of energy under the effects of the transient cooling loads with performing a successful temperature management. This means 10.8% of energy savings in comparison with the Algorithm #0.1.

4.4.2. Algorithm #2: Continuous Speed Selection from $T_{f\ out}$

This VSC control algorithm #2 is inspired by the study of Aprea et al. (2009). As it was explained in the literature survey, the authors first determined the performance parameters of the compressor experimentally in terms of $\dot{m}_{refrigerant}$, compressor power and the cooling capacity at different compressor speeds. Curve fitting some polynomial functions on the gathered data, the authors generated a function

which determines the optimum speed of a compressor for an instantaneous cooling load. Having such a function made it possible to generate a control algorithm, which could match the best compressor speed to the cooling load instantaneously.

In the scope of the studies for this thesis, it was not possible to perform experiments on the compressor at many different speeds to determine the actual performance parameters of the compressor. 1D simulations to obtain such performance parameters at different speeds would not be reliable since the compressor efficiency could decrease at lower speeds, which cannot be predicted by the simulations. However, a random function, which could be manipulated easily to evaluate its EC and temperature management performances, could be generated which will run the compressor with the same logic. For this reason, the compressor speed function, presented in Equation (4.4), is generated.

$$N = k \times \Delta T + 1800 \tag{4.4}$$

The speed adjustment with respect to the increasing cooling load, on the other hand, is performed with the $k \times \Delta T$ term. The definition of the ΔT term in Equation (4.4) is the same as the definition given in Equation (4.3) that the main control parameter of the Algorithm #2 is T_f. The ΔT term is multiplied with a gain "k" and the result of the multiplication is added to the minimum allowed compressor speed. Eventually, the sum gives the instantaneous speed of the compressor. The operational details of the Algorithm #2 are briefly summarized in Table 4.6.

Table 4.6. The details of Algorithm #2

Control method	VSC
Compressor speed limits [RPM]	0-3000
Compressor speed	$N = k \times \Delta T + 1800$
$T_{cs\ out}$ **thresholds**	0°C< $T_{cs\ out}$ <8°C (Controlled with the damper)
$T_{f\ out}$ **thresholds**	-18.5°C< $T_{f\ out}$ <-18°C

In order to manipulate the compressor speed selection function, the value of the gain is changed to observe the changes in the EC and the temperature management

performances of the control algorithm. The compressor speeds with respect to ΔT and the different values of the gain "k" are presented in Figure 4.15.

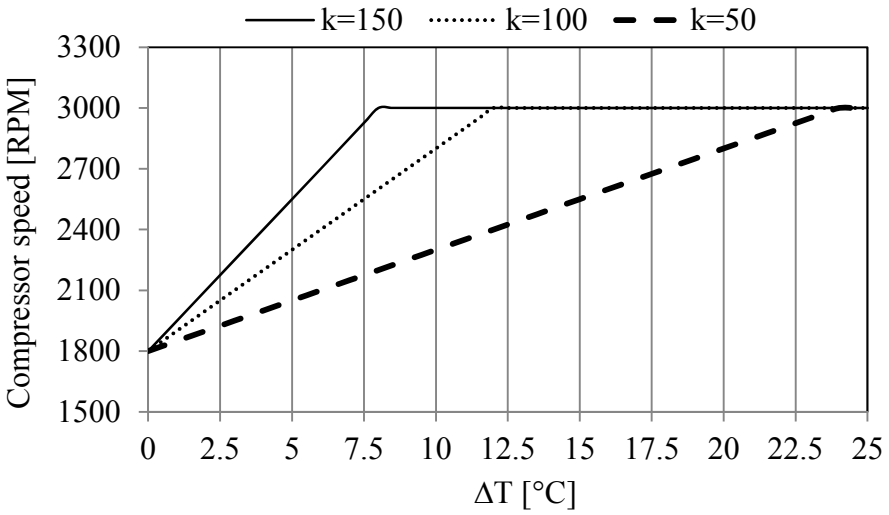

Figure 4.15. Compressor speeds selected for the different values of "k"

As could be seen from Table 4.6 and Figure 4.15, the compressor speed is limited in Algorithm #2 with 3000 RPM to prevent the compressor from wasting energy in vain since it has already been proved that a compressor speed of 3000 RPM is more than enough even in on/off control to maintain the desired T_{cs} and T_f. T_{cs} is maintained in the desired temperature interval with the same thresholds of the $T_{cs\,out}$ as in the Algorithm #1. As the gain decreases, the speed response of the compressor for a given ΔT decreases. Giving a response to a certain cooling load with a lower speed is supposed to decrease the EC of the refrigerator, while it increases the time period required to reach the minimum desired cold store temperatures.

The compressor speed with respect to time, under the control of the Algorithm #2, is presented in Figure 4.16. Since the initial temperatures of the refrigerator cabinets and the $T_{th\,mass}$ are 25°C, as in the case of Algorithm #1, compressor starts and continues its operation at 3000 RPM and continues for a while until ΔT drops below 8°C. After this point, the compressor speed is started to be calculated using Equation (4.4). At the instant when the compressor is calculated to be 1800 RPM, the compressor stops for whatever the value of the gain "k" is since this compressor speed means that $T_{f\,out}$ is decreased to -18.5°C.

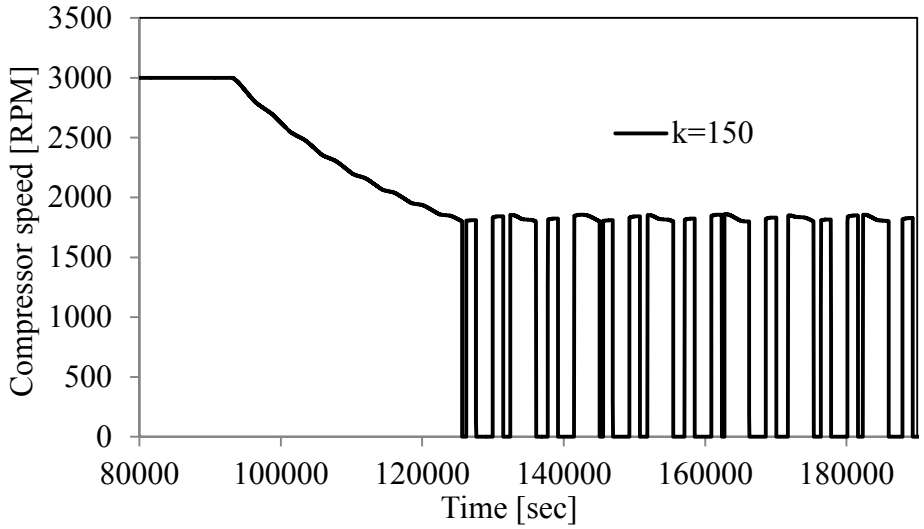

Figure 4.16. Compressor speed with Algorithm #2

The shorter cycles of the compressor in Figure 4.16 are to decrease T_{cs} only, while the longer cycles are to decrease both T_{cs} and T_f. This could be better observed looking at Figure 4.17. The shorter compressor cycles, which decrease $T_{cs\,out}$ from 8°C to 0°C, decrease the rate of increment of the $T_{th\,mass}$ but $T_{th\,mass}$ shows a considerable decrease only when the compressor duty cycle increases due to the signal coming from $T_{f\,out}$ measurement.

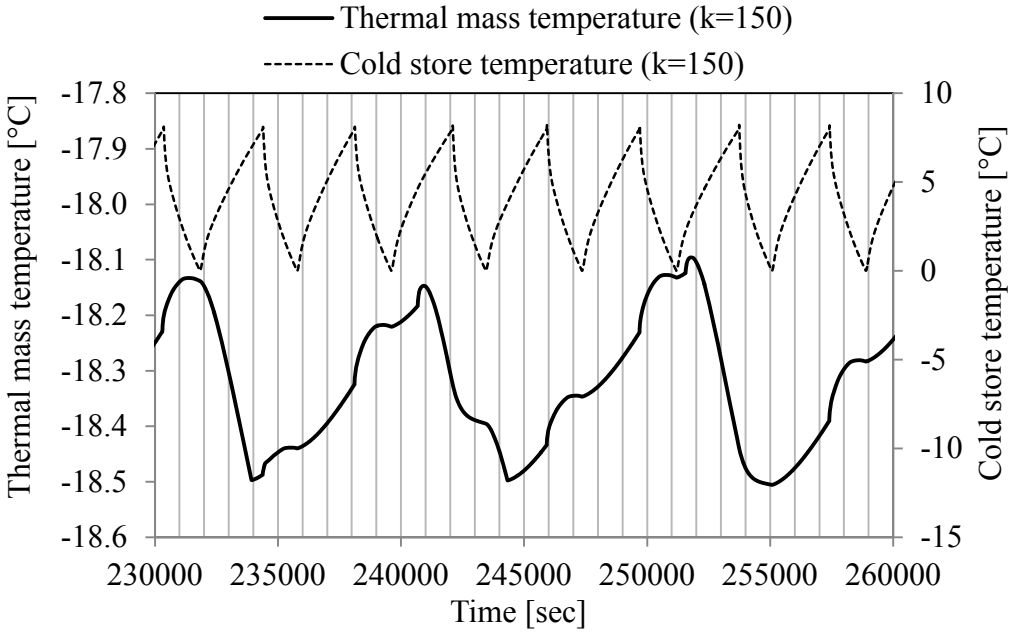

Figure 4.17. T_{cs} and $T_{th\,mass}$ with Algorithm #2

The cabinet temperatures, predicted by the simulations, are presented in Figure 4.17. As always, T_{cs} is easily managed within its bandwidth, while at the same time $T_{th\ mass}$ is kept below its upper limit, -18°C, successfully.

Using the VSC control Algorithm #2, the EC of the refrigerator is calculated to be 0.866 kWh/24h. In comparison with the Algorithm #0, the energy savings provided by the Algorithm #2 is 16.4%, which is a remarkable improvement of the energy conversion efficiency of the refrigerator. Comparing the EC of the Algorithm #2 with that of #1, it is observed that they are almost the same, differing from each other only by 0.2%.

Two more simulations are performed for the Algorithm #2 with the varying values of the gain "k". The simulation results show that the calculated EC does not change more than 1%. As the gain decreases, the compressor speeds selected by the control algorithm become closer and closer to the Algorithm #1 as expected (1800 RPM). Because in this simulation, there is no effect of the transient cooling loads but just the heat transfer from the surroundings to the refrigerator cabinet. The compressor starts operating when ΔT increases to 0.5°C at a speed of 1875 RPM when the gain is 150 and even at a lower speed when a lower gain is selected.

There are some certain results that as the gain decreases, the time required to reach the minimum desired cabinet temperatures increase considerably. In Figure 4.18, the compressor speeds with respect to time are presented for three different values of the gain in the compressor speed selection function. As the gain decreases, the operation time of the compressor increases for the first pull-down cycle to decrease $T_{f\ out}$ to -18.5°C. When the deep-frozen food safety is a matter of concern in industrial applications or cold chain refrigeration processes, this topic phenomenon should be paid enough attention.

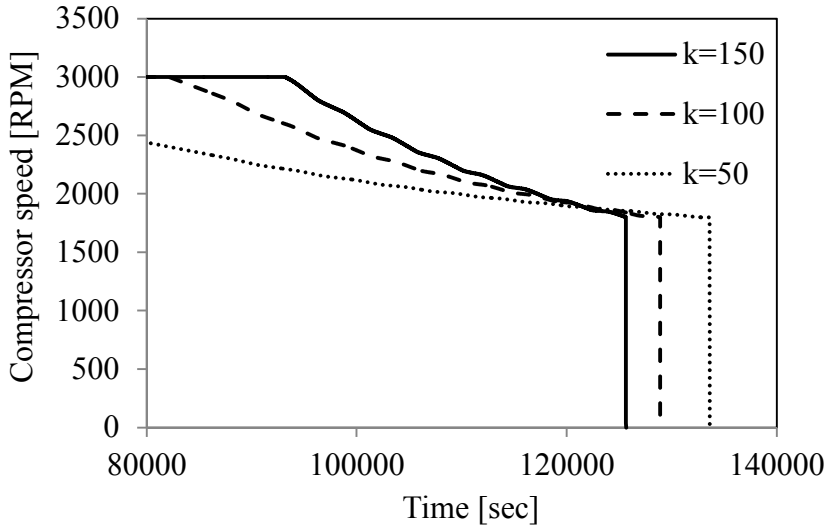

Figure 4.18. The first pull-down cycles for the different values of the gain "k"

Without the effects of the transient cooling loads, the Algorithm #2 gave similar results with the Algorithm #1 since the compressor speeds selected are very close to each other. For this reason, the performance evaluation of the Algorithm #2 should be carefully done with the transient cooling load algorithm.

4.4.2.1. Performance of the Algorithm #2 Under the Effects of the Transient Cooling Loads

The transient cooling load algorithm, the details of which are given in Table 4.3, is implemented in the 1D model of the refrigerator. The compressor speeds with respect to time are presented in Figure 4.19, for the different values of the gain in the compressor speed function (Equation (4.4)).

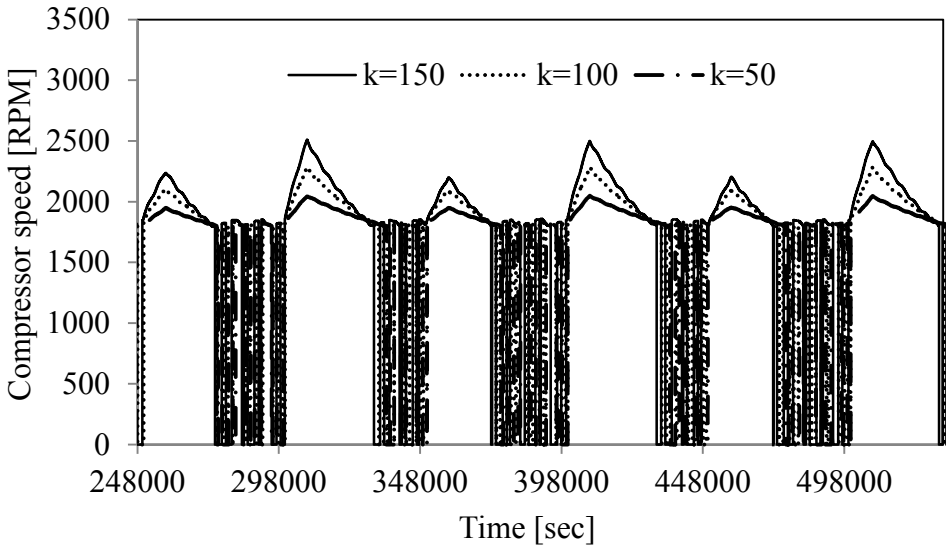

Figure 4.19. Compressor speed with Algorithm #2 at the transient loading conditions

Once the transient cooling load algorithm starts affecting $T_{th\ mass}$ in the freezer compartment, $T_{f\ out}$, ΔT starts increasing with an accompanying increase in the compressor speed. Even though, changing the value of the gain does not create a considerable change in the compressor speed during the steady state operating conditions, the change in the compressor speed during the transient cooling load period is obvious. The effects of the differences in the selected compressor speeds with different gains can be better observed from $T_{th\ mass}$, presented in Figure 4.20.

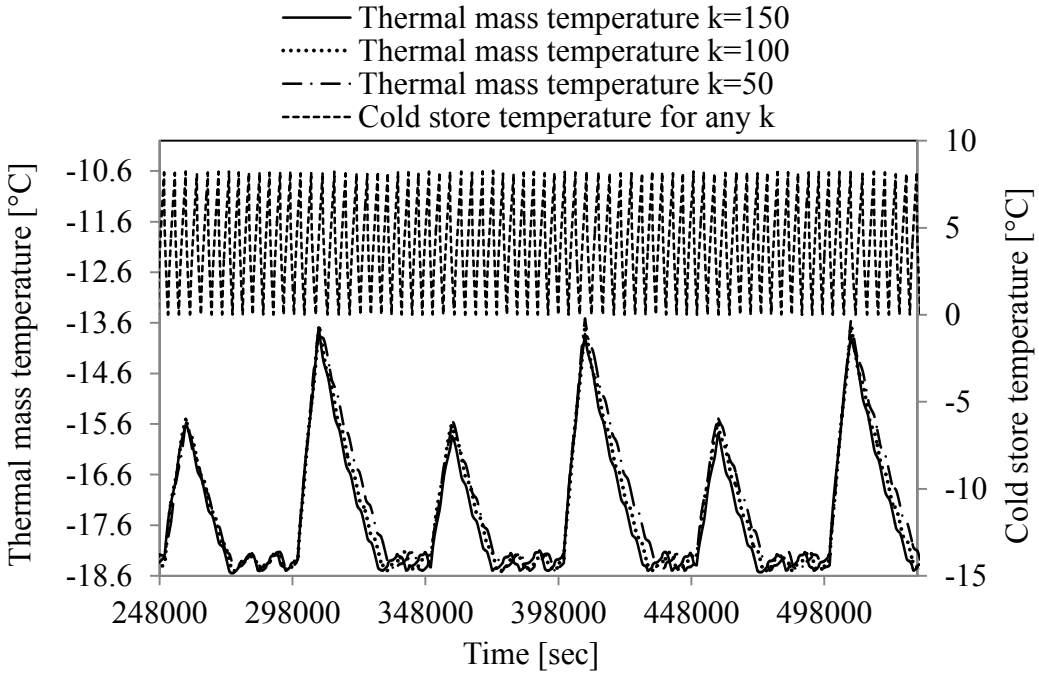

Figure 4.20. T_{cs} and $T_{th\ mass}$ with Algorithm #2

The change in $T_{th\ mass}$ with respect to time shows that the temperature management capability of the Algorithm #2 is satisfactory for each value of the gain. The compressor speeds selected by the Algorithm #2 are capable of decreasing $T_{th\ mass}$ back to the desired levels before another loading cycles starts. It takes about 72 minutes more time for the Algorithm #2 to compensate for the large loading cycle and decrease $T_{th\ mass}$ back to -18.5°C when the gain is 50 than when it is 150. However, the performance is still acceptable, especially once the ECs are compared for the three values of the gain. The refrigerator consumes 1.528, 1.497 and 1.480 kWh/24h of energy during the transient loading cycles when the gains are 150, 100 and 50, respectively. Taking the gain as 50, Algorithm #2 consumes 7.9% less energy than the Algorithm #0.1, providing a successful temperature management. However, the EC of the Algorithm #2 with the gain taken as 50 is still higher than that of the Algorithm #1 for the transient loading cycles since this algorithm selects higher compressor speeds than the Algorithm #1 due to the $k \times \Delta T$ term. Algorithm #2 consumes 3.2% more energy than the Algorithm #1 during the transient loading cycles.

4.4.3. Algorithm #3: Variable Compressor Speed Response to the Refrigeration Demand of Refrigerator Cabinets

This VSC control algorithm is created considering the operational details of the household refrigerator under issue. In the algorithms #1 and #2, the minimum compressor speeds in response to the refrigeration requirement of the cold store and the freezer compartments were selected to be the same. However, the cooling load of the cold store is much less than that of the freezer compartment. For this reason the refrigeration requirement of the cold store compartment is responded with the possible minimum compressor speed. In addition to this, the temperature bandwidth of $T_{cs\ out}$ has always been the same in the previous algorithms. For the improvement of the Algorithm #3, different temperature thresholds are implemented for the $T_{cs\ out}$ and their effects on the EC are investigated. The details of the Algorithm #3 are given in Table 4.7.

Table 4.7. The details of Algorithm #3

	Temperature interval	**Compressor speed [RPM]**
$T_{cs\ out}$ **thresholds** (Controlled with the damper)	0°C < $T_{cs\ out}$ < 8°C	1600
	1°C < $T_{cs\ out}$ < 7°C	
	2°C < $T_{cs\ out}$ < 6°C	
	3°C < $T_{cs\ out}$ < 5°C	
	2°C < $T_{cs\ out}$ < 8°C	
$T_{f\ out}$ **thresholds**	-18.5°C < $T_{f\ out}$ < -18°C	1800
	-17.5°C < $T_{f\ out}$	Speed selection according to Table 4.4

In the Algorithm #3, the refrigeration requirements of the cold store and the freezer compartments are responded with different speeds. The compressor speed is selected to be the minimum possible value, declared by the compressor manufacturer, since the refrigeration cycle could easily overcome the cooling load of the cold store compartment. When it comes to the freezer compartment, on the other hand, the control algorithm operates similar to the Algorithm #1. When the only cooling load on the refrigerator is the steady state heat transfer from the environment to the refrigerator cabinets, the compressor operates at 1800 and 1600 RPM in response to the cooling requirements of the freezer and the cold store compartments, respectively. If the refrigeration requirements of the two compartments coincide, then T_{cs} is controlled in the determined temperature interval with the use of the damper with a compressor speed of 1800 RPM. The compressor speed with respect to time under the control of the Algorithm #3 is presented in Figure 4.21.

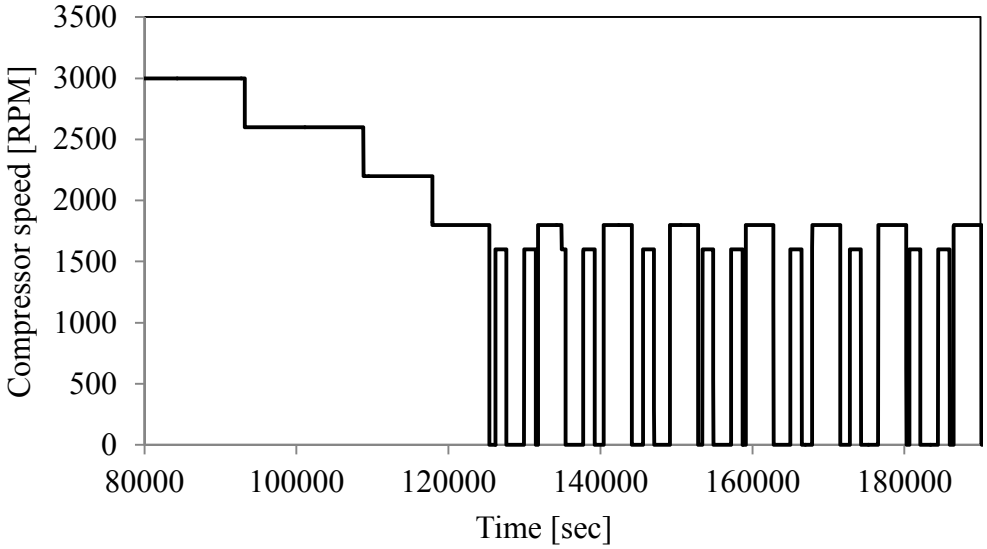

Figure 4.21. Compressor speed with Algorithm #3

As this is the case in every simulation, the initial cabinet and thermal mass temperatures are 25°C, which makes a pull-down initialization of the compressor at 3000 RPM. As the ΔT decreases, the compressor decreases its speed and finally when ΔT is equal to 0, the compressor stops. After that instant, the compressor starts its operation either at 1600 RPM or at 1800 RPM depending on the refrigeration requirements of the cabinets. If $T_{cs\ out}$ increases to the above of its upper threshold, the compressor starts at 1600 RPM with the damper switched on to decrease T_{cs} to the minimum desired temperature. During this time period, as could be seen from Figure 4.22, the increase rate of $T_{th\ mass}$ decreases since both of the compartments are refrigerated at the same time. However $T_{th\ mass}$ decreases at a faster rate only when the compressor increases its duty cycle at the speed of 1800 RPM.

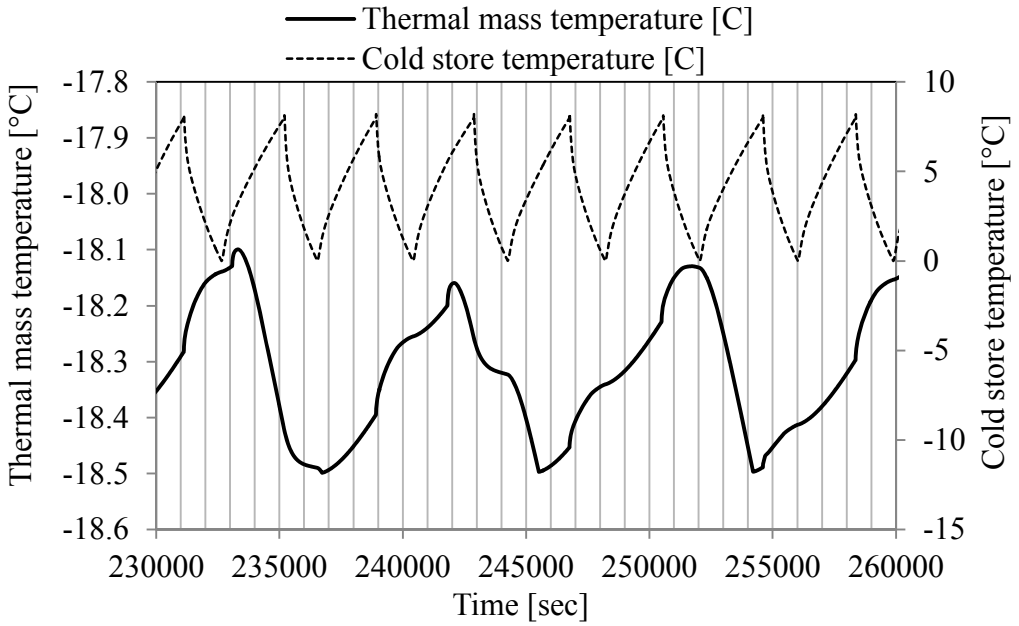

Figure 4.22. T_{cs} and $T_{th\ mass}$ with Algorithm #3

The Algorithm #3 is capable of performing a successful temperature management. Using this algorithm with the cold store air outlet temperature thresholds of 0°C< $T_{cs\ out}$ <8°C results in an EC of 0.857 kWh/24h under the steady state operating conditions. This means 17.3% of energy savings in comparison with the Algorithm #0 with a more successful temperature management.

In the simulations performed for the improvement of the VSC control algorithm #3, different values of the $T_{cs\ out}$ thresholds are implemented into the control algorithm to see their effect on the EC.

As the bandwidth of $T_{cs\ out}$ is changed by increasing and decreasing the lower and upper thresholds, respectively, the frequency of the on/off compressor operation changes. For instance, when the thresholds are taken as 0°C< $T_{cs\ out}$ <8°C, the compressor performs either one or two 1600 RPM cycles between two 1800 RPM cycles as could be seen from Figure 4.21. However, when the bandwidth of the $T_{cs\ out}$ is decreased, the number of 1600 RPM on/off cycles increases, while the duty cycle of each on/off cycle decreases. Shorter duty cycles provide a lower EC of the compressor due to the decreased bandwidth. However, if the bandwidth is decreased too much, then the compressor has many on/off cycles and the EC starts increasing. The EC of the compressor for different values of the $T_{cs\ out}$ thresholds are given in Table 4.8.

Table 4.8. Change in the EC of the compressor w.r.t. $T_{cs\ out}$ bandwidth

$T_{cs\ out}$ **bandwidth**	**EC of the compressor [kWh/24h]**
0°C < $T_{cs\ out}$ < 8°C	0.857
1°C < $T_{cs\ out}$ < 7°C	0.843
2°C < $T_{cs\ out}$ < 6°C	**0.833**
3°C < $T_{cs\ out}$ < 5°C	0.839
2°C < $T_{cs\ out}$ < 8°C	**0.823**

As the bandwidth of the $T_{cs\ out}$ is decreased, the EC decreases until 2°C< $T_{cs\ out}$ <6°C operation conditions are implemented. Under these conditions, the compressor has three 1600 RPM cycles between two 1800 RPM cycles and this is the minimum bandwidth applicable to obtain the minimum compressor EC. Because when the 3°C< $T_{cs\ out}$ <5°C temperature thresholds are chosen, the EC starts increasing as could be seen in Table 4.8 since the compressor has around nine 1600 RPM cycles in a row. Starting and stopping of the compressor frequently diminishes the energy savings obtained.

In the last simulation, the lower threshold of the $T_{cs\ out}$ is increased to 2°C in order to decrease the duty cycle of the compressor. The lowest compressor EC is obtained in this configuration as 0.833 kWh/24h, which means an energy savings of 19.6% in comparison with the Algorithm #0 with a successful temperature management. When the thresholds of $T_{cs\ out}$ are taken as 0 and 8°C as in the standard case, the EC of the refrigerator is calculated to be 0.857 kWh/24h, which yields an energy saving of 17.3%.

4.4.3.1. Performance of the Algorithm #2 Under the Effects of the Transient Cooling Loads

The Algorithm #3 proved itself to be useful under steady state operating conditions and its performance under the transient cooling loads has to be evaluated. The transient cooling load algorithm is implemented into this simulation and the results are evaluated in this section.

The compressor speed with respect to time is presented in Figure 4.23.

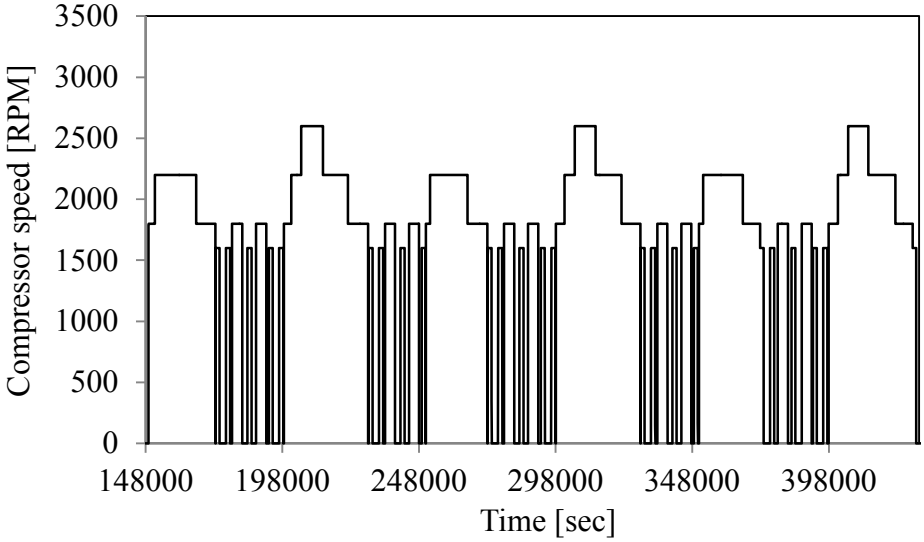

Figure 4.23. Compressor speed with Algorithm #3 at the transient loading conditions

As could be seen from Figure 4.23, the compressor operates at 1600 and 1800 RPM when the transient cooling loads are not affective. When $T_{th\ mass}$ increases due to the heat transfer, the control algorithm starts selecting higher speeds to overcome the cooling load. The change in $T_{th\ mass}$ and the T_{cs} temperatures with respect to time are presented in Figure 4.24.

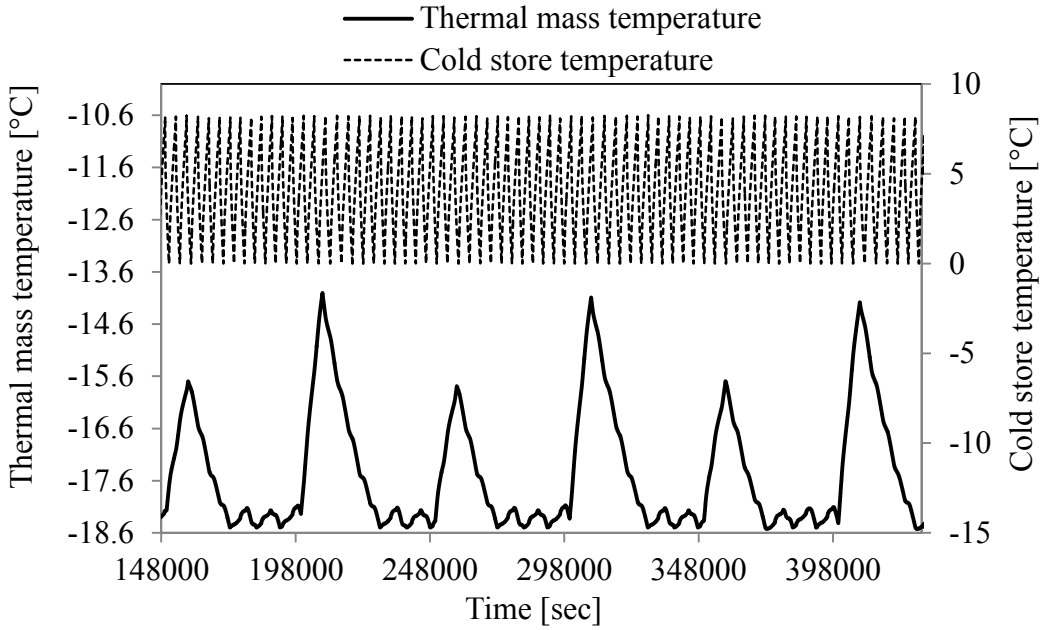

Figure 4.24. T_{cs} and $T_{th\ mass}$ with Algorithm #3 at transient loading conditions

Similar to the Algorithm #1, Algorithm #3 is capable of performing a successful temperature management under the effects of the transient cooling loads. $T_{cs\,out}$ oscillates between 0°C and 8°C thanks to the damper operation and the EC of the compressor in the given time interval is calculated to be 1.429 kWh/24h, which means a 11.1% increase in the energy conversion efficiency of the refrigerator in comparison with the Algorithm #0.1.

4.5. Comparison of the Results

In this section, the simulation results presented in this chapter are summarized in Table 4.9 for a better understanding.

The temperature management capabilities of the Algorithm #0 both for steady state and transient loading operating conditions are considered to be unsuccessful since the this algorithm takes only $T_{cs\,out}$ into consideration to adjust the compressor speed. The other four control algorithms, on the other hand, measure both $T_{cs\,out}$ and $T_{f\,out}$ to modulate the refrigeration capacity instantaneously. Therefore, they can manage the cabinet temperatures successfully under not only steady state but also transient loading operating conditions.

The EC of the Algorithm #0 is taken as the reference for the energy labeling of the refrigerator according to the standards declared by European Commission (2010). Since the value of the $\dot{W}_{comp\,inst\,avg}$ is less than 44 W under the steady state operating conditions, the refrigerator is labeled with "A+" energy label operating with the Algorithm #0 and the EC performances of each VSC control algorithm are compared with this algorithm.

Eliminating the fixed time operation and installing a second temperature sensor in the Algorithm #0.1 made it possible to control the freezer temperature, too, while at the same time decreasing the EC of the refrigerator by 6.8%. Besides, Algorithm #0.1 provided a very successful temperature management under the effects of the transient cooling loads with an EC of 1.607 kWh/24h that was calculated for the time interval during which the effects of the cooling load was observed. The EC and temperature management performances of the Algorithm #0.1 under the effects of the transient

cooling loads are also taken as a reference to compare those of the VSC control algorithms.

The Algorithm #1 is inspired by the study of Aprea, Mastrullo, and Renno (2004). Depending on the value of ΔT, the corresponding compressor speed is selected by the control algorithm. Even though the corresponding compressor speeds are determined experimentally in the aforementioned study, they were determined intuitively in the improvement of the Algorithm #1 since such experiments were not possible. The algorithm decreased the steady state EC of the compressor to 0.864 kWh/24h, which yielded a 16.6% energy savings in comparison with the Algorithm #0. Under the effects of the transient cooling loads, the Algorithm #1 proved itself to be very successful in managing the cabinet temperatures with an EC of 1.433 kWh/24h, which corresponds to 10.8% energy savings with respect to the Algorithm #0.1.

Under the steady state operating conditions, the Algorithm #1 drove the compressor with on/off control method at a speed of 1800 RPM. Without the effects of the transient cooling loads, the algorithm looked like an ordinary on/off control algorithm. For this reason, the Algorithm #2 is generated being inspired by the study of Aprea et al. (2009). Fitting some curves on the experimental data, the authors generated a function, which determined the best compressor speed instantaneously as a function of ΔT and yielded the maximum energy savings. Similarly, a compressor speed determination function, which is easily manipulable, is generated and implemented on the 1D model. The algorithm not only proved itself to be a useful one in terms of low EC and good temperature management, but also proved that the compressor speeds selected in Algorithm #1 were so proper that both of the algorithms required almost the same EC under the steady state operating conditions. As the value of the gain is decreased and increased from its optimum value k=150, an increase in the EC is observed. Under the effects of the transient loading conditions, however, the EC of the compressor decreased as the gain is decreased since lowering the speed has a direct effect on the EC. This leaded to a conclusion that the gain in the compressor speed selection function could be adjusted by the user in a way that there could be two modes of operation such as a holiday mode and daily use mode. In the holiday mode, the function chooses the optimum value of the gain since the refrigerator door will not be opened and the only cooling load will be the heat transfer from the environment to the refrigerator cabinets. On the daily use mode, however, the function chooses a lower value for the gain to keep the compressor speed as low as possible while compensating

for the additional cooling loads by increasing the duty cycle. In this way, both the cabinet temperatures could be maintained successfully and the EC would be kept low under any operating conditions.

Actually, there is a problem with the application of the Algorithm #2 that it requires a very sensitive temperature sensor, which is not frequently used in the industry. Even though such a control algorithm cold be applied in laboratory with high precision thermocouples easily, the precision of the commercial sensors is generally on the order of 0.5°C, which makes it impossible the proper use of the Algorithm #2 in mass production refrigerators.

The difference between the Algorithms #3 and #1 is that the minimum compressor speed, 1600 RPM, is selected to respond the refrigeration requirement of the cold store cabinet. Even though, this compressor speed is not experimentally verified for this study whether it provides useful cooling with a low EC or not, it was officially declared by the compressor manufacturer that such a low speed operation was possible. The simulation results showed that the algorithm is capable of maintaining the desired temperatures in both of the cabinets and requiring the lowest EC among all the algorithms studied; 0.857 kWh/24h, which meant 17.3% energy savings with respect to the Algorithm #0. Under the effect of the transient cooling loads, the EC is calculated to be 1.429 kWh/24h with a successful temperature management and this meant 11.1% energy savings with respect to Algorithm #0.1.

In all the simulations performed until this point, the temperature thresholds of $T_{cs\,out}$ were taken as 0 and 8°C. For this algorithm, shorter temperature intervals are simulated for $T_{cs\,out}$ to see their effect on the EC performance. It was proved that decreasing the bandwidth until some point would decrease the EC of the compressor but after some point, the compressor starts wasting energy due to the high number of on/off cycles of the compressor. It was proved that the temperature thresholds of $T_{cs\,out}$, giving the lowest EC, were 2 and 8°C. Even though the lowest EC is obtained with these values of $T_{cs\,out}$ in the simulations, these results should be verified experimentally before implementation of the algorithm in the commercial refrigerators in order to be sure that the minimum desired temperature will be reached with these thresholds in the cold store compartment.

Table 4.9. Summary of the simulation results

<table>
<tr><th rowspan="3">Algorithm</th><th rowspan="3">Fixed time</th><th colspan="4">Temperature thresholds [°C]</th><th colspan="2" rowspan="2">Compressor speed response [RPM]</th><th rowspan="3">Transient loading</th><th colspan="2" rowspan="3">EC [kWh/24h]</th></tr>
<tr><th colspan="2">$T_{cs\ out}$</th><th colspan="2">$T_{f\ out}$</th></tr>
<tr><th>Min</th><th>Max</th><th>Min</th><th>Max</th><th>Cold store</th><th>Freezer</th></tr>
<tr><td>#0</td><td>300 sec</td><td>0</td><td>8</td><td>-</td><td>-</td><td>3000</td><td>3000</td><td>-</td><td colspan="2">1.036*</td></tr>
<tr><td></td><td></td><td></td><td></td><td></td><td></td><td></td><td></td><td>+</td><td colspan="2">1.507</td></tr>
<tr><td>#0.1</td><td>-</td><td>0</td><td>8</td><td>-18.5</td><td>-18</td><td>3000</td><td>3000</td><td>-</td><td colspan="2">0.966</td></tr>
<tr><td></td><td></td><td></td><td></td><td></td><td></td><td></td><td></td><td>+</td><td colspan="2">1.607**</td></tr>
<tr><td rowspan="2">#1</td><td rowspan="2">-</td><td rowspan="2">0</td><td rowspan="2">8</td><td rowspan="2">-18.5</td><td rowspan="2">-18</td><td rowspan="2">1800</td><td rowspan="2">0<ΔT<0.5 | 1800
1<ΔT<3 | 2200
3<ΔT<8 | 2600
8<ΔT | 3000</td><td>-</td><td colspan="2">0.864</td></tr>
<tr><td>+</td><td colspan="2">1.433</td></tr>
<tr><td rowspan="6">#2</td><td rowspan="6">-</td><td rowspan="6">0</td><td rowspan="6">8</td><td rowspan="6">-18.5</td><td rowspan="6">-18</td><td rowspan="6">1800</td><td rowspan="6">$k \times \Delta T + 1800$
(when ΔT>0.5)</td><td rowspan="5">-</td><td>k</td><td>EC</td></tr>
<tr><td>50</td><td>0.870</td></tr>
<tr><td>100</td><td>0.867</td></tr>
<tr><td>150</td><td>0.866</td></tr>
<tr><td>200</td><td>0.870</td></tr>
<tr><td>250</td><td>0.872</td></tr>
<tr><td rowspan="4">+</td><td>k</td><td>EC</td></tr>
<tr><td>50</td><td>1.480</td></tr>
<tr><td>100</td><td>1.497</td></tr>
<tr><td>150</td><td>1.528</td></tr>
<tr><td rowspan="9">#3</td><td rowspan="9">-</td><td>0</td><td>8</td><td rowspan="9">-18.5</td><td rowspan="9">-18</td><td rowspan="9">1600</td><td rowspan="9">0<ΔT<0.5 | 1800
1<ΔT<3 | 2200
3<ΔT<8 | 2600
8<ΔT | 3000</td><td rowspan="7">-</td><td colspan="2">0.857</td></tr>
<tr><td>1</td><td>7</td><td colspan="2">0.843</td></tr>
<tr><td>2</td><td>6</td><td colspan="2">0.833</td></tr>
<tr><td>3</td><td>5</td><td colspan="2">0.839</td></tr>
<tr><td>2</td><td>8</td><td colspan="2">0.823</td></tr>
<tr><td>0</td><td>8</td><td rowspan="2">+</td><td colspan="2">1.429</td></tr>
<tr><td>2</td><td>8</td><td colspan="2">1.396</td></tr>
</table>

*Reference result for EC under steady state operating conditions.
**Reference result for EC under transient operating conditions.

CHAPTER 5

CONCLUSION

The on/off control of the compressors has been the most commonly used method of refrigeration capacity control in the refrigeration industry. The researchers from the academia and the industry have always tried to find better methods to modulate the refrigeration capacity. Among numerous methods proposed, the VSC control was found to be one of the most useful one in the literature. In this study, the effectiveness of the VSC capacity control method was investigated. Due to the difficulties in experimental studies and the CFD analysis, a 1D simulation tool, LMS Amesim was used to model the household refrigerator under issue. The model was simulated for the on/off control of the refrigerator so that the existing experimental results and the simulation results could be compared. Once the model was verified to be a reliable one, the VSC control algorithms were started being analyzed.

The performance evaluation of the VSC control algorithms was performed in terms of their EC and their temperature management performances. From this aspect, all of the VSC control algorithms presented managed to do a successful temperature management since the algorithm takes $T_{f\ out}$ into consideration as an input. In this study, it is proven that measuring the instantaneous cabinet temperatures to control the compressor is the only method to perform a successful temperature management with the least amount of energy usage.

The algorithms proved that they could manage the cabinet temperatures not only during steady state conditions, but also under the effects of the transient loading. Transient loads should be taken into account regarding the food safety issues. A refrigerator could both be able to maintain the minimum desired cabinet temperatures and compensate for the high cooling loads, which increase the food temperatures in the refrigerator compartments.

The 1D modeling is the first step of the design process. The results obtained from these simulations should be experimented on the refrigerator under issue to observe the performance of the VSC control algorithms in real life. The off the shelf variable speed drives are known to have some compatibility issues with the

compressors. To be able to get the maximum efficiency out of a VSC control system, the VSD components should be selected very carefully or they need to be specially designed for a certain compressor in order to utilize VSC refrigeration capacity control method in the most efficient manner.

REFERENCES

Aircon. (2013). *Reciprocating piston compressors.* Retrieved April 16, 2013, from http://www.china-aircon.com/detail-10001895/masterclass-compressors-part-5.html

Aprea, C., Mastrullo, R., & Renno, C. (2004). Fuzzy control of the compressor speed in a refrigeration plant. *International Journal of Refrigeration, 27*(6), 639-648. doi: 10.1016/J.Ijrefrig.2004.02.004

Aprea, C., Mastrullo, R., & Renno, C. (2006). Experimental analysis of the scroll compressor performances varying its speed. *Applied Thermal Engineering, 26*(10), 983-992. doi: 10.1016/J.Applthermaleng.2005.10.023

Aprea, C., Mastrullo, R., & Renno, C. (2009). Determination of the compressor optimal working conditions. *Applied Thermal Engineering, 29*(10), 1991-1997. doi: 10.1016/J.Applthermaleng.2008.10.002

Aprea, C., Mastrullo, R., Renno, C., & Vanoli, G. P. (2004). An evaluation of R22 substitutes performances regulating continuously the compressor refrigeration capacity. *Applied Thermal Engineering, 24*(1), 127-139. doi: 10.1016/S1359-4311(03)00187-X

Bejan, A., & Kraus, A. D. (2003). *Heat transfer handbook*: John Wiley.

Bloch, H. P. (2006). *A Practical Guide to Compressor Technology*: John Wiley.

British Standards Institute. (2006). BS EN ISO 15502:2005 *Household refrigerating appliances. Characteristics and test methods.* London.

Çengel, Y. A., & Boles, M. A. (2007). *Thermodynamics: an engineering approach*: McGraw-Hill Higher Education.

Charney, J. G., Arakawa, A., Baker, D. J., Bolin, B., Dickinson, R. E., Goody, R. M., . . . Wunsch, C. I. (1979). Carbon dioxide and climate: a scientific assessment. *National Academy of Sciences Press*.

Chemieingenieurwesen, V.-G. V. u., & Gesellschaft, V. (2010). *VDI Heat Atlas*: Springer.

Dossat, R. J. (1961). *Principles of refrigeration*: John Wiley.

Ekren, O., Celik, S., Noble, B., & Krauss, R. (2012). Performance Evaluation of a Variable Speed DC Compressor. *International Journal of Refrigeration*. doi: 10.1016/j.bbr.2011.03.031

European Commission. (2010). Directive 2010/30/EU of the European Parliament and of the Council of 19 May 2010 on the indication by labelling and standard product information of the consumption of energy and other resources be energy-related products. *Official Journal of the European Union*.

Ghiaasiaan, S. M. (2008). *Two-Phase Flow, Boiling, and Condensation: In Conventional and Miniature Systems*: Cambridge University Press.

Giampaolo, T. (2010). *Compressor Handbook: Principles and Practices*: Taylor & Francis.

Hanlon, P. C. (2001). *Compressor handbook*: McGraw-Hill.

HVAC: Systems and Equipment. (2000). Ashrae Handbook: Inch-Pound. ASHRAE.

Holdack-Janssen, H., & Kruse, H. (1984). Continuous and discontinuous capacity control for high speed refrigeration compressors.

Incropera, F. P. (2007). *Fundamentals of heat and mass transfer*: John Wiley.

Lawrence, W. C. (1971). United States Patent No. US 2010/0040484 A1.

Lerner, K. L., & Lerner, B. W. (2004). *The Gale Encyclopedia of Science: Factor-Kuru*: Gale.

Liyang. (2013). *Hermetic compressor.* Retrieved April 16, 2013, from http://www.liyangcompressor.com/r600a-compressor/13.html

Manske, K. A., Reindl, D., & Klein, S. (2000). Load sharing strategies in multiple compressor refrigeration systems.

Perry, R. H., & Green, D. W. (2008). *Perry's Chemical Engineers' Handbook*: McGraw-Hill Professional Publishing.

Poggi, F., Macchi-Tejeda, H., Leducq, D., & Bontemps, A. (2008). Refrigerant charge in refrigerating systems and strategies of charge reduction. *International Journal of Refrigeration, 31*(3), 353-370. doi: 10.1016/J.Ijrefrig.2007.05.014

Qureshi, T. Q., & Tassou, S. A. (1996). Variable-speed capacity control in refrigeration systems. *Applied Thermal Engineering, 16*(2), 103-113. doi: 10.1016/1359-4311(95)00051-E

Shade, N., & Doup, R. (2009). United States Patent No. US 2010/0040484 A1.

Tassou, S. A., & Qureshi, T. Q. (1994). *Investigation into alternative compressor technologies for variable speed refrigeration applications.* Paper presented at the International Compressor Engineering Conference.

Tassou, S. A., & Qureshi, T. Q. (1998). Comparative performance evaluation of positive displacement compressors in variable-speed refrigeration applications. *International Journal of Refrigeration, 21*(1), 29-41. doi: 10.1016/S0140-7007(97)00082-0

The Trane Company. (2009). Applications Engineering Manual: Hot Gas Bypass Control. Trane Air Conditioning.

Twidell, J., & Weir, T. (2006). *Renewable Energy Resources*: Taylor & Francis.